PERFORMANCE ANALAYSIS OF A PROPOSED HYBRID OPTICAL NETWORK

by

Natthapong Liamcharoen

B.Eng. (Electrical Engineering), Kasetsart University, 1998

M.S. (Electrical Engineering), Washington University in St.Louis, 2003

Submitted to the Graduate Faculty of

School of Information Sciences in partial fulfillment

of the requirements for the degree of Doctor of Philosophy

University of Pittsburgh

2016

UNIVERSITY OF PITTSBURGH

SCHOOL OF INFORMATION SCIENCES

This dissertation proposal was presented

by

Natthapong Liamcharoen

It was defended on

April 2015

and approved by

Dr. David Tipper, Associate Professor, Telecommunications Program

Dr. Martin B.H. Weiss, Associate Professor, Telecommunications Program

Dr. Prashant Krishnamurthy, Associate Professor, Telecommunications Program

Dr. Chunming Qiao, Professor, Computer Science and Engineering, University at Buffalo

Dissertation Advisor: Dr. Richard A. Thompson, Professor, Telecommunications Program

PERFORMANCE ANALAYSIS OF A PROPOSED HYBRID OPTICAL NETWORK

Natthapong Liamcharoen, PhD Candidate

University of Pittsburgh, 2015

This dissertation discusses a novel Hybrid Optical Network (HON) that can provide service differentiation based on traffic characteristics (i.e., packet, burst, and long-lived flow) with QoS guarantee not only in network layer, but also in physical layer. The DHON consists of sophisticated edge-nodes, which can classify, monitor, and dynamically adjust optical channels in the core layer as traffic variation. The edge nodes aggregate traffic, identifying end-to-end delay by ingress queuing delay or burst timeout. The network can estimate number of channels by arriving traffic intensity and distribution with estimated upper-bound delay. The core layer employs two parallel optical switches (OCS, OBS) in the same platform. Thanks to the overflow system, the proposed network enhances utilization with fewer long distance premium channels. The premium channel can quickly handle burst traffic without new channel assignment. With less overprovisioning capacity design, the premium channel enhances utilization and decrease number of costly premium channels. This research also proposes mathematic models to represent particular DHON channels (i.e., circuit, packet, and burst). We employ method of moments based on overflow theory to forecast irregular traffic pattern from circuit-based channel (i.e., M/M/c/c) to overflow channel, in which G/G/1 model based on Ph/Ph/1 matrix can represent the overflow channel. Moreover, secondary channel supports packet-based traffic over wavelength channel with two service classes: Class I based on delay sensitive traffic (i.e., long flow) and

Class II for non-delay sensitive traffic (e.g., best effort). In addition, mixture of traffic in the wavelength channels is investigated based on M/G/1 and M/G/2 with specific service time distribution for particular class. Finally, we show our DHON based on (O-O-O) switching paradigm has improved the performance over typical (O-E-O) switching network architecture based on NSF topology.

TABLE OF CONTENTS

LIST OF TABLES

LIST OF FIGURES

1.0 INTRODUCTION

Innovations of optical components and switching fabrics have significantly contributed to the telecommunication industry. Regarding the optical access network, Fiber-to-the-Home (FTTH) can provide much faster broadband access compared to xDSL or coaxial cables. As a result, high-speed services can be provided to customers without bottlenecks. For core networks, a single fiber is able to deliver several Terabits/sec data when using dense wavelength division multiplexing (DWDM), which couples multiple colors of light in a single optical fiber. Therefore, network providers can optimize optical resources including transponders, fibers, and amplifiers. Typically, IP/DWDM network is based on point-to-point connection, which requires electronic switches (i.e., routers) to perform routing and aggregating functions. Consequently, every single node requires O-E-O converters between O-E interfaces, causing the bottlenecks due to relatively slow electronic processing, compared to the light travel speed. In this research area, variations of optical switches have been discussed for future optical switching architectures; for instances, OXC, OPS, OBS, and OPLS. However, a particular switch has some advantages and drawbacks over the others.

On the other hands, Hybrid Optical Networks (HONs) eliminate some drawbacks and maintain existing advantages for each switching type so that overall network performance is improved. In this dissertation, we propose a new paradigm of HON, called the Dynamic Hybrid

Optical Network (DHON), which is able to: (i) support various types of traffic depending on traffic characteristics and (ii) provide a QoS channel while optical resources are efficiently utilized.

The rest of this chapter is organized as follows: Section 1.1 discusses some reasons why we need a new optical transport system for backbone networks. Section 1.2 provides a brief explanation of the HONs. Section 1.3 investigates some challenging issues, which affect the existing HONs, and then addresses research questions. Section 1.4 explains key steps that we have contributed to the research study. Section 1.5 discusses some methodologies we used to conduct the research. Section 6 outlines some assumptions we have made throughout the research.

1.1 MOTIVATION

In this section, we discuss some weaknesses of the existing optical transport systems deployed in backbone networks. In addition, some threats to current network infrastructure are mentioned, and we explain why the transmission system is not compatible with future traffic environment. Then, we discuss several promising optical switches for future backbone network.

The section is divided into two subsections: weaknesses and threats to current backbone networks discussed in subsection 1.1.1. Strengths and opportunities with optical networks in subsection 1.1.2.

1.1.1 Weaknesses Threats & to Existing Backbone Networks

In the past, web service applications were the majority of internet traffic. However, the rapid growth of multimedia communication has stimulated broadband service demands (e.g., video-on-demand, HDTV steaming, and cloud computing) which will exponentially increase traffic volume on backbone networks. Cisco's traffic forecast [1] shows that global IP traffic will surpass zettabyte (1.4 zettabytes) by the end of 2017, in which video traffic will be 69 percent of all Internet traffic. As a result, the future backbone network should be more powerful, flexible, and scalable in order to handle such dynamic traffic environment. An existing network like IP or MPLS is able to support various traffic types differentiated by virtual channels.

However, the network bundles those virtual channels and transport them on integrated and transported over the same optical switching infrastructure. In fact, each type of traffic has its own characteristic, which is compatible with particular type of optical switching infrastructure. In addition, IP/MPLS backbone networks deploy DWDM system for their optical transport system (i.e., IP over DWDM [2, 3]), in which each IP node performs switching, grooming and restoration. Since IP/DWDM is based on point-to-point connection (i.e., hop-by-hop routing), the traffic will always be converted between electrical and optical domains (O-E-O) at every IP node. The above reasons bring about the following drawbacks: high end-to-end delay (e.g., processing and queuing), traffic congestion in the core nodes, and high network cost due to large number of converters, and lack of data transparency in the core layer [3].

In fact, O-E-O conversion is required mainly for routing purpose, in which the routing is processed in IP layer (i.e., electronic domain). Therefore, the IP packet transmitted in the form of optical signal consists of a header and a payload. Specially, each optical payload needs to wait in

the buffer whereas the packet header is being processed. In practice, data transmission rates according to optical domain range from 10 Gigabit/s to Terabit/s; while electronic rate is approximately two Gigabit/s. Therefore, mismatch of the rates can cause network bottlenecks, which allow overall throughput lower than optical line rate. Moreover; under a network-congested circumstance, additional queuing delay will accumulate at all nodes in the network, and definitely contribute to end-to-end delay. Specifically, when source and destination nodes are far apart, packets travelling via a number of intermediate nodes have high end-to-end delays, exceeding upper bounds of certain applications. Lastly, data may be lost during a transmission under traffic-congested environment.

1.1.2 Strengths, Opportunities with Optical Transport Networks

Currently, there are several variations of optical switching architectures proposed for future optical transport networks. Examples include Optical transport network (OTN), Optical burst switch network (OBSN), and Optical packet switch network (OPSN). However, there are strengths and drawbacks with respect to each type of optical switching networks as discussed below:

An OTN, consisting of optical cross connects (OXCs) and DWDM multiplexers can be employed as a long haul transport network for Telco and internet service providers (ISPs) due to its fast restoration and economic feasibility [2, 3]. Many providers have modified their optical transport systems from ring topology using SONET add/drop multiplexer to mesh topology with OXC [4]. However, the OTN is based on circuit switching, in which the entire capacity of individual wavelength channel is dedicated to a particular demand. For channel reservation, it

needs to allocate adequate bandwidth for each traffic demand based on over-provisioning capacity in order to handle fluctuated traffic during peak hours. Therefore, the OTN requires large numbers of connections due to mesh topology [2], and its channels are not efficiently utilized.

In this research area, there are other types of optical switches, which have different switching schemes. An alternative is the OBSN [5-11], in which the switching fabrics are configured according to bursts. Mainly, OBS edge nodes perform traffic aggregation and burst assembly. Regarding the burst assembly, the edge switches accumulate several packets and bundle the packets in a burst format. The OBS edge nodes send out a header prior to the burst in order to configure intermediate nodes along a path to the destination, referred to burst reservation protocol JET [8]. The advantage for the OBS is that optical channels are efficiently utilized, especially under fluctuated traffic environment. However, there is additional delay (i.e. offset time) according to assembly process, and burst drop at intermediate switches in highly congested environment. On the other hand, the OPSN [12-16] consists of a group of OPS edges and core switches which route the traffic based on packets. The edge node is able to aggregate the traffic; but there is no burst assembly and no advanced channel reservation through the core switches. The OPS core switches reserve switching fabric on the fly according to packet headers. As a result, the OPS network requires fiber delay lines (FDLs) and synchronizer at individual switches to delay packets while the controller processes the packet header, resulting in high channel utilization and low packet drop in the core switches. However, the OPS network yields relatively high end to end delay due to the accumulation of processing and queuing delays in every intermediate node.

In conclusion, OBS and OPS are based on connectionless scheme, which enables to perform several virtual channels over a connection. As a result, they both can improve channel utilization through the traffic aggregation or assembly in the buffer. However, they are //comparatively sophisticated switches, which require faster setup times and advance control signaling. Moreover, the end-to-end delay issue mentioned above will affect certain traffic types if the delay is greater than upper bound of particular applications.

1.2 HYBRID OPTICAL NETWORKS (HONS)

As discussed above, each type of optical switch has advantages and disadvantages. So, selecting one type over another depends in issues like: traffic characteristic, traffic load, and network topology. Various backbone networks have been deployed in the industry, network operators have integrated different networks, ranging from cable TV, mobile phone, and internet services into a unified platform referred as next generation network (NGN) in order to optimize network resources and reduce operating cost. On the other hand, Hybrid optical networks (HONs) [17-26] have been discussed as backbone networks, in which multiple switching paradigms are integrated in the same network node in order to maintain existing strengths of a particular switch, and eliminate some weaknesses in order to improve overall network performance.

Regarding the network architecture, if either OBS or OPS is employed as the access gateways (i.e., edge nodes) depicted in Figure 1, the HON will gain higher flexibility and capability. Since the access gateways aggregate the arrival traffic based on burst/packets, the delivery of bundled traffic through the core layer yields more efficient use of optical channel. In

contrast to the OBS/OPS, OCS can provide a dedicated channel to the destination access gateway as a QoS qualified connection; but relatively lower utilization.

In addition, OBS/OPS are promising switching schemes for Internet traffic due to their compatibilities with fluctuated traffic. In fact, Internet traffic can be modeled as bursty traffic discussed in [27]. OBS/OPS edge nodes are able to aggregate the arrival traffic in a buffer, and allocate only sub wavelength channel in the core layer. These yield higher multiplexing gain, and increases overall network utilization. However, there are tradeoffs. For instance, certain levels of delay occur at the aggregation and burst assembly processes (i.e. offset) [5, 8]. OPS/OBS require not only the complicated switching nodes, but also sophisticated signaling protocols, like GMPLS [28-31] in OPS and JET [5] in OBS. As discussed above, costs of OPS/OBS switches are relatively high for real implementation. Moreover, quality of service (QoS) in HON is an important issue, which has not been widely discussed in the research community.

1.3 RESEARCH CHALLENGES AND PROBLEM STATEMENT

In this section, we start to provide an overview of national optical backbone architecture, regarding topology and services. Then, we will discuss some challenges in several aspects relating to traffic demands and the architecture. Finally, we express specific statements of research problems.

This section divides into two subsections: First, we discuss research challenges for optical backbone network in subsection 1.3.1. Later on, we clearly identify the problem statement of HON in subsection 1.3.2.

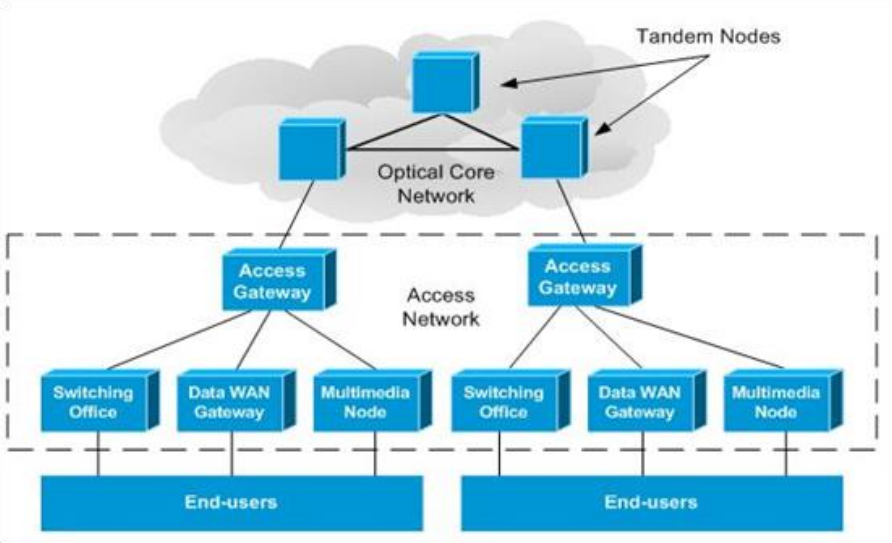

Figure 1. Framework of national optical backbone network [32]

1.3.1 Research Challenges for HONs

Figure 1 illustrates a framework of national optical backbone network is initially proposed by Thompson [32] and some others [11, 18-20, 33]. The backbone network is based on 2-tiers architecture (i.e., core and access layers) which can provide optical transport systems for several service providers (e.g., voice carriers, video providers, ISP, and datacenters). In core network, each tandem node (TN) provides transit connectivity to the other TNs via physical links. Regarding access network, each access gateway (AG) aggregates traffic from the service providers and delivers to the adjacent TN. When the network nodes employ Hybrid Optical

Switch (HOS) according to this topology, we have noticed some challenges regarding three main issues as follows:

***First*:** Each traffic demand, generated by a particular service provider, has its unique traffic characteristic. For instance, constant bit rate (CBR) applications (e.g., voice, video conferencing) require guaranteed bandwidth channel with low delay acceptance. On the other hand, we can deliver non-delay sensitive traffic (e.g., WWW, FTP, Instant messaging) under delay environment. Moreover, some applications can tolerate some level of upper-bound delay like VoIP, streaming video and online gaming. Currently, the traffic mentioned above is classified according to class of service (QoS) identification based on IP protocol or in MPLS (i.e., on network layer). However, the backbone network finally transmits all traffic on the same optical channel (i.e., optical cross connect). Consequently, QoS for the overall network likely decreases in the physical and data link layer; for instance, employing OPS for CBR traffic.

In HON literature, access nodes (or AGs) can be employed by either OPS or OBS, which perform traffic aggregation before transmitting to the core layer. Although the OCS can limit upper bound delay, there will be packet/burst assembly delay at the edge node. Several groups of literatures, relating to HONs are as follows. In Burst over circuit channel (BoCS) as proposed by Gauger and Mukherjee [21] and hybrid optical network by C. T. Chou [34], the entire traffic is aggregated by an OBS before transmitting over dedicated wavelength channels. However, both literatures lack of details on traffic aggregation and performance analysis. In recent HON publication [11], OBS is employed at the edge node, which classifies arriving traffic into several data flows, called flow transfer mode (FTM). There are four different modes based on QoS requirement. In core layer, the core nodes perform more like OBS than OCS as in previous literatures. The advantage is that edge node sends out control packet per flow instead of per

burst, allowing less control packets need to process in the core layer. However, the burst loss in the core layer due to output port contention is still a limitation of the OBS.

Instead of employing an OBS at edge nodes, OPS is replaced [13,16,20]. Since the OPS is based on the packet switching paradigm, it is highly compatible with packet-based networks such as MPLS. In this case, the edge nodes can create virtual channels between source and destination, classified by MPLS labels. However, the OPS network will create relatively high end-to-end delay due to existence of processing and queueing delays in all nodes, which will reduce QoS for real time applications (e.g., video conference).

Second: the nature of traffic demands between edge nodes fluctuate all the time. For instance, voice call traffic reaches the peak during rush hours; in addition, the demand always varies over a short period of time called 'tide' as discussed by Thompson [35]. This allows more difficulties to the backbone network to provide optimized capacity in the wavelength channel. In other words, the edge nodes need to reserve capacity based on the peak traffic demand (over-provisioning); otherwise, the fluctuated traffic will be blocked. As a result, utilization in the channel will significantly drops during non-rush hours. Hence, it is a challenge if the network is able to employ a dynamic capacity sharing among several traffic demands.

According to Optical Burst Transport Network (OBTN) [21], the overflow channels are employed to release the network contention in the primary channel. In fact, every OBS node aggregates all types of traffic and transmits over an optical circuit channel. It is difficult to predict the amount of overflow traffic due to various types of traffic mixed in the primary channel (i.e., long flow, short flow, or burst). This certainly affects the design of overflow channel including number of channels and QoS control. In fact, the paper lacks several details on traffic aggregation, classification, and overflow traffic analysis.

Menon's works [36, 37] and Washington [38] also discuss overflow channel to alleviate the contention of OBS hybrid node. Each hybrid node pre-allocates end-to-end circuit channels (i.e., primary) for specific destinations and traffic classes. If the primary light path is not available, the hybrid node routes the traffic to overflow channels shared by all classes. In addition, the overflow traffic can be inserted back in primary channels at any node if available [37]. In our proposed network, we also employ OBS for overflow channel as well. However, the overflow channel is used to absorb traffic fluctuation from our premium channel, which treats only top class service like CBR traffic (i.e., strictly delay sensitive). The purpose is to increase utilization and decrease the number of premium channels. For the other traffic types, the edge node will assign to secondary channel (i.e., packet over OCS channel) without overflow technique. Another difference is that there is no traffic insertion or overflow in our intermediate nodes (i.e., core nodes). We provide exclusively end-to-end channel for top class traffic without any interruption in the core layer. By this approach, we can identify upper-bound delay for each traffic request based on traffic intensity and packet size distribution. In our research, the analysis is based on network performance, and mathematical models to present all types of optical channels instead of cost model.

Third: Optical network resources (i.e., O/E convertors, repeaters, and fibers) are limited and costly. Mainly, cost of HONs varies by several factors including number of transponders, switching type, and number of optical components (e.g., wavelength convertors, optical amplifiers, and FDLs). For instance, OPS and OBS are more expensive than simple OCS; network cost varies by total number of optical transponders; the optical components as wavelength convertors would be avoid. Therefore, the more wavelength channels are used, the

higher cost for the network. It is challenging to minimize optical channels for all types used in the entire network, while the network satisfies the QoS requirements for each traffic category.

Consequently, the design of future optical switching networks must include the following issues: how to provide appropriate optical channels to suit a particular type of traffic and satisfy QoS requirement? How to integrate different optical channels into single optical network infrastructure in order to reduce cost of implementation, operation, and maintenance? How the switching architectures should be designed in order to meet the above requirements?

1.3.2 Problem Statement of HONs

Mostly, literature in HONs area discusses the overview of architecture framework employed HOSes in several parts of the network nodes. Some research focus on the wavelength channel assignment through the core network referred as wavelength routing assignment (WRA) problem in order to achieve optimized channels in the entire network. These research do not investigate the nature of traffic variation and fluctuation especially classification of arrival traffic in their performance analysis. In fact, the HON in our proposal will support different types of traffic in which each type has unique characteristic (i.e., different QoS requirement) which directly affects the number of wavelength channels needed for the network. Especially, in practice, traffic fluctuates over the time; how can we efficiently utilize optical channels including OCS, OPS, and OBS paradigms with the respect of QoS consideration. Specifically, we are seeking to answer the following questions: how to efficiently assign certain types of optical channels in HON to match various types of traffic in term of classification, aggregation, and wavelength assignment? How many channels are required for each type of traffic based on certain

performance parameters? What is lower bound end-to-end delay for particular traffic environment?

1.4 CONTRIBUTION

First, we provide an overview of what we are contributing in this research study as shown in subsection 1.4.1. Moreover, we provide more details for the performance analysis in order to answer the research question as discussed in subsection 1.4.2.

1.4.1 What Will We Do?

We aim to propose a new approach of national optical backbone network, which is able to support a variety of traffic with regard to QoS constrains for particular application. The network can provide certain levels of channel granularities allowing efficient utilization of optical resources. In this research study, we discuss 2-tiers architecture of dynamic hybrid optical network (DHON) along with comprehensive details of traffic classification, aggregation, and wavelength channel assignment. In addition, we investigate mathematic models for particular type of optical channels to obtain several performance parameters.

Regarding the architecture, edge and core nodes employ a hybrid switch with a capability of dynamic wavelength assignment. The network separates optical channels into three categories: premium, secondary, and overflow. The premium and secondary channels are assigned for real time circuit-based traffic and packet-based traffic respectively. The overflow channel,

implemented by OBS, absorbs burst overflow traffic from the premium channel in order to release the traffic contention and increase QoS in premium channels.

The secondary channel supports packet-based traffic, which employs statistical buffer in order to obtain higher utilization in wavelength channel. The channel is divided into two classes of QoS buffers: Class I based on delay sensitive traffic (i.e., long flow) has relatively a strict delay constraint. While Class II based on non-delay sensitive traffic (e.g., best effort) has less effects by the delay. In addition, we investigate a model and performance analysis for a mixture of traffic, corresponding to M/G/1 and M/G/2. Finally, we show our DHON based on O-O-O switching paradigm has improved the performance over typical (O-E-O) switching network architectures.

1.4.2 More Detail to Answer the Research Questions

- We investigate performance analysis of premium and overflow channels regarding the following parameters: blocking probability, delay, and utilization.
  - o In premium channel, real time applications are compatible with constant bit rate (CBR) channel, allowing minimal end-end delay and jitter. Therefore, we represent a group of reserved wavelength channels between ingress-egress nodes as M/M/c/c queueing model, in which the blocked traffic will be rerouted to the overflow channel.
  - o We consider the blocked traffic as an input of the overflow system, in which the overflow load is varied by number of wavelength channels and traffic demand of premium channel. Note that we adopt 3-moments of method technique (Wilkinson [39]) to estimate the overflow traffic behavior with respect to Interrupted Poisson Process (IPP) parameters.

o The overflow channel employing timer-based buffering will be represented as G/G/1 queueing system in order to investigate performance parameters, where the arrival process of the overflow system is associated with previous IPP parameters.

o Regarding the departure process, we represent the pattern of burst delivery in the channel as an Interrupted Poisson Process (IPP). In fact, timeout and offset time varies the IPP parameters of burst assembly

o In order to obtain numerical results of overflow system regarding G/G/1 queue, we need to employ matrix based approach to solve for certain performance parameters.

o We compare utilization and number of wavelength channels required for DHON to those based on a competitive optical network without overflow channel deployment.

- We design and investigate performance analysis of secondary channels for packet-oriented traffic (i.e., both Class I and Class II).

o Class I channel supports delay sensitive traffic. In our DHON, the edge node will treat HD video traffic differently from the other data traffic since the videos will be the majority of Internet traffic in the near future, which require low end-to-end delay connection.

o We represent Class I as a M/G/1 queueing system, in which the arrivals are bundled streams of compressed videos (e.g., H.264), which are based on frame granularity, comparatively larger size and less bursty than best-effort traffic. In fact, the compressed video frame has variable sizes in order to optimize transmitted data associated with a statistical distribution.

o We design Class II channel to handle non-delay sensitive traffic based on packet granularity, in which high end-to-end delay channel does not significantly interrupt user experiences. In this case, the performance analysis is based M/G/1 queue. The arrival packets are

aggregation of best effort traffic, which is relatively short in packet size associated with long-tail distributions.

- In addition, we also investigate performance of the secondary channel in some specific traffic environments: mixture of traffic with regard to video priority and traffic allocation in multiple wavelength channels.
- We compare lower-bound end-to-end delay employed in DHON to the delay occurring in IP/MPLS over DWDM.

- We discuss architectures of the core layer relating to topology and switching fabric. Regarding wavelength setup, we explain an overview of wavelength routing assignment deployed in the core layer between ingress-egress nodes, which is compatible with channel assignment at the access layer.

1.5 METHEODOLOGLY

In this section, we discuss methodologies using to conduct our research studies in order to answer the research questions as follows:

- Regarding premium and overflow channel, we write Matlab program based on queuing analysis to explore effects of particular performance parameters to the others. In addition, we will find a minimum number of wavelength channels with QoS constraints.
  - In premium channel, we represent the system as M/M/c/c. At a given traffic load, we vary the number of wavelength channels to find out blocking probabilities and utilization. On

the other hand, if the blocking probability and utilization are the constraints of particular traffic demand, the minimum number of wavelength channels can be determined.

- In addition, we vary traffic loads and calculate blocking probability and utilization so that number of premium channels can be determined when traffic load is fluctuated.
- Based on overflow channel, we investigate the amount of overflow traffic by varying number of premium channel. In addition, the interarrival time and holding time of the overflow traffic are identified.
- At a given buffer timeout, the aggregation delay occurring at the overflow buffer will be plotted as varying premium channels. Also, we will investigate the effect of buffer timeout on the aggregation delay by varying several values of buffer timeout.

- Regarding secondary channel for both CoS I and CoS II, we write Matlab scripts based on M/G/1 and M/G/2 queuing system to study effects of several performance parameters at certain traffic environments.

***Experiment 1*:** Effect of video frame sizes (section 6.4.1)

- Given two different frame sizes of video steams (i.e. 1300B vs 2900B) where the service time is random variable
- Fix video frame rate: 30 frames/sec (i.e., standard)
- X-axis: Vary numbers of video streams.
- Y-axis: Find these performance parameters at each specific load: mean video frame waiting time in queue, queue size, utilization.
- Compare those results obtained from Opnet simulation.

***Experiment 2*:** Effect of video frame rates (section 6.4.2)

- Compare two different frame rates of video steams (i.e. 15 frames/sec vs. 30 frames/sec)
- With comparison, we normalize traffic loads by adjusting frame sizes:

  2900B at 30 frames/sec vs. 5800B at 15frames/sec
- X axis: Vary traffic loads
- Y-axis: Find performance parameters at certain traffic loads as follows: mean queueing delay and queue size.

Experiment 3: Effect of wavelength capacity (section 6.4.3)

- Compare two different capacities of wavelength channels (i.e., 1.25 Gb/s vs. 2.5 Gb/s)
- Assign two low capacity vs. one high capacity: 2 *1.25 Gb/s vs. 1*2.5 Gb/s
- Fix video frame rate: 30 frames/sec
- X-axis: Vary numbers of video streams
- Y-axis: Find these performance parameters at each specific load: mean video frame waiting time in queue, queue size.
- Repeat and show two cases of video frame sizes: 5800B vs. 11600B

Mixture of video and data in a single channel (section 6.4.4)

We define video traffic as larger size and less variance than data traffic

- Video frame size 2900B with $CoV = 0.62$
- Data packet size 760B with $CoV = 1.5$

We perform three different scenarios of traffic mixtures:

I. Low video traffic ratio: 10% video bundled with 90% data
II. Medium video traffic ratio: 50% video bundled with 50% data
III. High video traffic ratio: 70% video bundled with 30% data

***Experiment 4*:** Comparison between video frame delay versus data packet delay

Low video traffic ratio: 10% video bundled with 90% data

- Compare two different scenarios: video prioritized traffic and non-prioritized traffic
- X axis: Vary traffic loads with the same mixture ratio
- Y-axis: Plot video frame delay versus data packet delay for both scenarios associated with the 10:90 ratio.

Medium video traffic ratio: 50% video bundled with 50% data

- Compare two different scenarios: video prioritized traffic and non-prioritized traffic
- X axis: Vary traffic loads with the same mixture ratio
- Y-axis: Plot video frame delay versus data packet delay for both scenarios associated with the 50:50 ratio.

High video traffic ratio: 70% video bundled with 30% data

- Compare two different scenarios: video prioritized and non-prioritized traffic
- X axis: Vary traffic loads with the same mixture ratio
- Y-axis: Plot video frame delay versus data packet delay for both scenarios associated with 70:30 ratio

***Experiment 5*:** Effect of traffic mixture ratio to particular type of traffic

On the video traffic

- Compare two different scenarios: video prioritized traffic and non-prioritized traffic
- X axis: Vary traffic loads
- Y-axis: Plot video frame delay for both scenarios
- Repeat several mixture ratios of video traffic : 10%, 50%, and 70%

On the data traffic

- Compare two different scenarios: video prioritized and non-prioritized traffic
- X axis: Increase traffic loads
- Y-axis: Plot data packet delay for both scenarios
- Repeat for several mixture ratios of video traffic : 10%, 50%, and 70%

End-to-end delay comparison between DHON and IP/DWDM (in section 6.5)

- Investigate a general formula to calculate end-to-end delays for both DHON and IP/DWDM network (in section 6.5.1)
  - Provide an example of end-to-end delay calculation based on realistic network
- Define arrival traffic is a mixture of video and data
  - Scheduling in DHON is based on video prioritization; but not for IP/DWDM

***Experiment 6*:** End-to-end delay comparison DHON v.s IP/DWDM regarding video and data traffic (in section 6.5.2)

- Given 50% video traffic ratio and based on 3 hops link (average hops)
- Given video frame size 2900 B with *CoV*= 0.62 and packet size 760B with *CoV*=1.5
- Vary traffic loads from 0.1 – 0.9
- Plot and compare end-to-end delay of video traffic between DHON and IP/DWDM
- Plot and compare end-to-end delay of data traffic between DHON and IP/DWDM

***Experiment 7*:** Effect of video frame size toward video frame delay (in section 0)

- Given three ratios 50% video traffic ratio and based on 3 hops link (average hops)
- Given video frame rate = 30f/s, video frame size 2900 B with *CoV*= 0.62 and packet size 760B with *CoV*=1.5
- Vary traffic loads from 0.1 – 0.9

- Plot and compare end-to-end delay of video traffic between DHON and IP/DWDM
- Given video frame size 8000 B
- Plot and compare end-to-end delay of video traffic between DHON and IP/DWDM

Compare only video delay in DHON

- Vary frame sizes: 2900B,5000B, 8000B
- Plot end-to-end delay at certain traffic loads

Compare only video delay in IP/DWDM

- Vary frame sizes: 2900B,5000B, 8000B
- Plot end-to-end delay at certain traffic loads

***Experiment 8*:** Effect of traffic ratio toward video traffic delay (in section 0)

- Given video frame rate = 30f/s, video frame size 8000 B with *CoV*= 0.62 and packet size 760B with *CoV*=1.5
- Given 50% traffic ratio and based on 3 hops link
- Vary traffic loads from 0.1 – 0.9
- Plot and compare end-to-end delay of video traffic between DHON and IP/DWDM
- Repeat with different ratio: 70%, 90%

1.6 RESEARCH ASSUMPTIONS AND LIMITATIONS

The research studies in this dissertation are based on the following assumptions and limitations:

(1) The proposed architecture focuses only backbone network (i.e., edge and core nodes. We do not take into account regional networks in the dissertation.

(2) DHON is GMPLS-compatible architecture. However, the algorithm of the control system does not take into account in this dissertation, which mainly focuses on performance analysis of the proposed architecture.

(3) The traffic demand refers requested traffic between a pair of DHON edge nodes (i.e., ingress - egress), where the edges can monitor and measure amount of traffic.

(4) The traffic between demand pairs surges during peak hours and remains for a period (i.e., 30-60 minutes). In contrast to the ripple, it occurs frequently but relatively in small magnitude (see Figure 6). Hence, we can assume that wavelength establishment/release for fluctuated traffic does not require fast switching.

(5) We assume the overflow channel is lightly used for each traffic demand. Due to the dynamic wavelength assignment, the edge node can adjust appropriate number of wavelength channels closed to the present traffic load.

(6) There is some possibility of out-of-sequence data between OCS and OBS channels. However, we assume the buffer employed at the egress node with the playback feature will alleviate the issue.

(7) Assume the arrival traffic to ingress node will be de-multiplexed to DS-0 so that certain parameters of arrivals can be determined and used for overflow traffic estimation. However, it may not be the most economical approach.

(8) In premium channel, we illustrate a voice application as an example of delay sensitive traffic when the traffic overflows to OBS channel. In fact, it could be video traffic as well with different traffic parameters, and the analysis of premium channel is based on homogenous traffic.

2.0 LITERATURE REVIEW AND BACKGROUND

We start to discuss a variation of optical switching techniques in optical switches research area. Then, we will focus only on hybrid optical networks (HONs), in which we review and classify a number of HON literature into three categories. Finally, we compare some similar works to the proposed network.

This chapter is outlined as follows: In section 2.1, we present a classification of optical switching techniques and their implementation. In section 2.2, we will provide classification of HONs along with a comparison with DHON

2.1 OPTICAL SWITCHING TECHNIQUES

There are numbers of literature regarding optical switching networks. In fact, most of them are related to one of these switching scheme: OCS, O/E/O, OPS, and OBS. Basically, optical switching nodes can be classified into four categories according to switching techniques, presented by C.Qiao [8].

2.1.1 Optical Circuit Switch (OCS)

In OCS, the switch creates end-to-end connections based on traffic demands. Once the switch fabric is established, the connection holds for a certain periods as a data pipe. The data travels in optical domain, in which an input wavelength will remain the same to the output port. Regarding switching control part, the fabric is electronically controlled by two types of signaling (i.e. setup and release) which may take a few hundred milliseconds; and the connection remains in the range of minutes or hours [8]. Since there is no O-E-O conversion at port interface, data is transparency in terms of bit rate, protocol, and data format. Therefore, it is relatively flexible and easily scalable without any concern on line card upgrading/replacement when the traffic increases or change types of services [4]. However, it lacks of statistical multiplexing at the switch, which is different from the other switches. As a result, the optical channel implemented by OCS has comparatively low utilization. In addition, OCS is comparatively reliable and low delay channel since the end-to-end connection is preconfigured.

We have found this OCS implemented in the following optical networks: IP over optical cross connect (IP/OXC) [2] and IP over Optical Transport Network (IP/OTN) [3, 40]. Basically, OTN consists of OXCs [4, 41] connected to over WDM system, which is able to perform routing, grooming and restoration in optical domain. In some types of OXC (i.e., wavelength-routing switch (WRS) [41]), the switch fabric can be reconfigurable in a short period of time; therefore, real time recovery can be done in optical layer instead of in IP layer [2, 3]. Note that OTN is based on fully mesh topology, and the end-to-end connection is pre-determined (i.e. two-way reservation). Obviously, OTN eliminates the bottleneck (i.e. O-E-O) and network congestion at intermediate nodes. In [35], core nodes employ OCS in space and wavelength to

set up semi-permanent end-to-end channels, which vary by traffic loads during different time of a day.

2.1.2 O-E-O Switch (O-E-O)

An O/E/O switch employs O-E converters at input and output of the switch. Considering an arrival optical packet needs to be converted to electrical format so that the controller can process the information in packet header and then configure switching fabrics. Not only is the control header, but also data payload is converted into electrical domain as well, which is different from the other three categories. In O/E/O switch, the switch aggregates traffic in a buffer achieving statistical multiplexing, in which the switch can presumably utilize sub wavelength in the channel. In other words, the connection is not dedicated for a particular source and destination. As a result, link utilization in the core network can be improved (i.e. less coarse granularity). Since each O/E/O switch requires converter at each port interface, the network definitely consumes large numbers of converters, yielding high network cost. As a result, scalability is a weak point for this switch; also high power consumption and heat dissipation are the drawbacks as well [4].

Examples of networks employing O/E/O switches include IP over DWDM [3] and IP over SONET (opaque case) [4]. In contrast to IP/OTN, IP/DWDM does not require OXC but IP routers are connected over point-to-point WDM links. If the failures occur either at IP routers or optical links, the restoration will perform at IP layer based on Open circuit shortest path first (OSPF) or Intermediate System to Intermediate System (IS-IS) protocol. Typically, it takes fairly long time to recover the traffic in IP layer, which may take ten seconds to minutes to perform

routing convergence [2]. Since traffic terminates in electrical domain at intermediate nodes, end-to-end delay is relatively high and none deterministic. In addition, network cost for IP/DWDM is shown to be higher than IP/OTN for several topologies [3, 40]. In term of channel utilization, each link requires over provisioning bandwidth to handle recovery traffic from neighbor nodes. In practice, the utilization of router interface is set to 50% of the link capacity [3].

In the case of opaque switch in IP over SONET [4], the O-E converter at every switch interface is used to solve the interoperability issue among different vender (i.e. different optical frequency). In addition, O/E/O switch enables to read SONET header at switch interface so that every opaque switch is able to perform grooming and network in-band control functionalities (i.e. monitoring, fault detection, and restoration) [4].

2.1.3 Optical Packet Switch (OPS)

Contrary to OCS creating end-to-end connection, OPS is based on connectionless scheme where the switch fabric is set up according to each packet. At intermediate nodes, packets will be stored and forwarded to the destination. As a result, different demand pairs can share an optical channel; presumably, sub channel is assigned to the traffic. In classical electronic OPS, the contention packet can be stored in electronic buffer and sent out every single packet. Contrary to OPS, there is no optical random access memory (RAM). The optical buffer, referred to fiber delay lines (FDLs), is fixed length producing constant waiting time in the buffer [15].

Typically, OPS [12-16] requires O-E converters at interfaces of the control unit in order to convert packet header into electrical domain. For the data payload, it remains in the optical domain throughout the network. An OPS needs optical delay lines (i.e., optical buffer) to hold

data payload while the header is being processed at the control unit. In contrast to O/E/O where both control and data parts are converted to electrical domain, OPS does only control header which has much less information than the whole packet. As a result, OPS will have less processing delay at intermediate nodes than the O/E/O.

In general, OPS network can be categorized into two subcategories: slotted (synchronous) and un-slotted (asynchronous). In slotted OPS [12], all packets have the same size in which they are allocated inside a fixed timeslot consisting of a header, data payload, and guard band between them (see Figure 2). The wider guard band allows less strict requirement for the alignment; however, it will decrease network utilization [15]. In addition, synchronization bits are required before the routing tags and payload in which all incoming packets need to be aligned before entering the switch fabric. As a result, a group of FDLs that generate multiple of timeslot durations are required at the input interface to align unregulated packets with a local clock [15]. In this case, the need of complicated synchronization stage is the drawbacks for practical implementation.

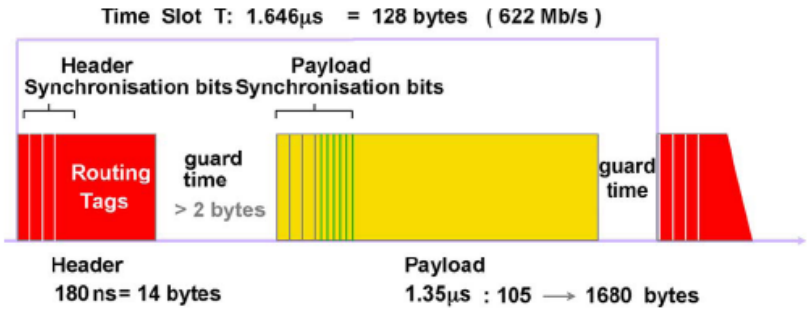

Figure 2. Slotted OPS frame format [14]

In un-slotted OPS [15, 42], each packet has variable lengths and requires no synchronization stage. However, fixed-length FDLs are still needed to hold the incoming packets while the header is being processed in electrical domain and configured the switch fabric [15]. In other words, all packets are delayed at the same duration regardless of the time that they arrive. Considering optical format, the control signaling (i.e. header) are separated from the data part by sub-carrier multiplexing (SCM) in which the signaling and data can be sent in the same wavelength band discussed in [12]. In fact, the header rate in the electrical domain is much slower than the data (i.e., payload) rate in optical domain. Therefore, the bottleneck at intermediate nodes will alleviated compared to O/E/O, in which the data is converted to electrical domain as well. Examples of un-slotted OPS networks include Optical label switching (OLS) [29, 42], Labeled Optical Burst Switching (LOBS) [42, 43], and LOB polymorphic network [17]. Some slightly different on LOBS and OLS is that there are additional burst aggregation at the edge node instead of statistical multiplexing shared. Regarding the optical label, the core nodes process this label to receive the routing information, and perform fast-forwarding the optical payload. Actually, this technique inherits the concept of Multiprotocol label switching (MPLS) which also has improved version for the optical network; that is GMPLS [30].

In conclusion, the un-slotted OPS efficiently employ optical channel, support high-speed packet network, and reduce the bottleneck. However, there are some constraints including practical optical buffering, no optical RAM, and contention resolution. Moreover, OPS needs high performance switch which is scalable and performs fast switching [12, 42].

2.1.4 Optical Burst Switch (OBS)

Since there is a discrepancy between optical and electrical transmission rate, the bottleneck occurs when the O-E conversion exits. As a result, the network should keep data transmission in optical domain. However, some practical difficulties exist in OPS as mention earlier (e.g., optical RAM, synchronization). The OBS is an alternative switching scheme, which combines advantages of OCS and OPS. In OBS network, the data remains in optical domain from ingress to egress nodes based on advanced channel reservation. The channel is efficiently utilized without the use of optical RAM and synchronization. However, OBS introduces some delay at the edge node, caused by burst assembly (i.e. offset) [5, 8]

In term of control channel, O-E conversion is required for header processing (see Figure 3). However, the OBS employs less control channels than OPS (one control channel per fiber) [8]. As a result, the OBS needs less O-E-O converters, leading to cost saving.

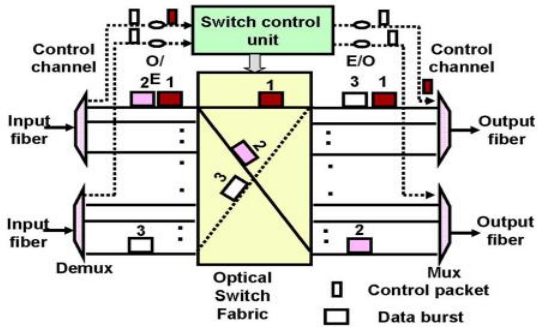

Figure 3. Optical Burst switch (core node) [14]

Figure 3 illustrates an OBS core node. The OBS establishes connections for the arrival bursts according to the headers. The OBS employs relatively fast switch; the connection holds for a particular burst and immediately released when it leaves the switch. In fact, a burst is switched in optical domain without the need of FDLs whilst processing its header. This is because the advantage of advanced reservation protocol (i.e., JET) proposed by Qiao [5]. Since OBS does not employ FDLs, wavelength converters can be placed at the switch interfaces to reduce contention in the core layer [5].

OBS network achieves statistical multiplexing shared at the edge node and provides data transparency in the core layer. An OBS edge node aggregates the traffic and assembles several packets into a burst; In addition, with the burst reservation protocol, the network allows data transparency without processing delay in the core layer. The Burst Assembly and reservation protocols will be in the following discussion.

Burst Assembly and scheduling

Consider the Assembly units of the edge node in Figure 4, packets that have the same destination are aggregated in the same buffer. In fact, there are several buffers classified by QoS [8]. As soon as packets are buffered until reaching the threshold (could be time or burst length), the burst scheduler contains these bursts in a burst data packet (BDP). In the same time, a burst control packet (BCP) is immediately created and sent out prior to the burst transmission in a separated channel (out of band) [8]. The control packet contains the following information: egress address, offset time, burst size, and CoS [9] so that core switches reserve resources for the burst along the route to egress nodes. In addition, the scheduler finds an appropriate wavelength to send the

burst with respect to burst starting time and its duration. Examples of scheduling algorithms include Min-SV, Min-EV, LAUC, and Best-Fit. [8, 44].

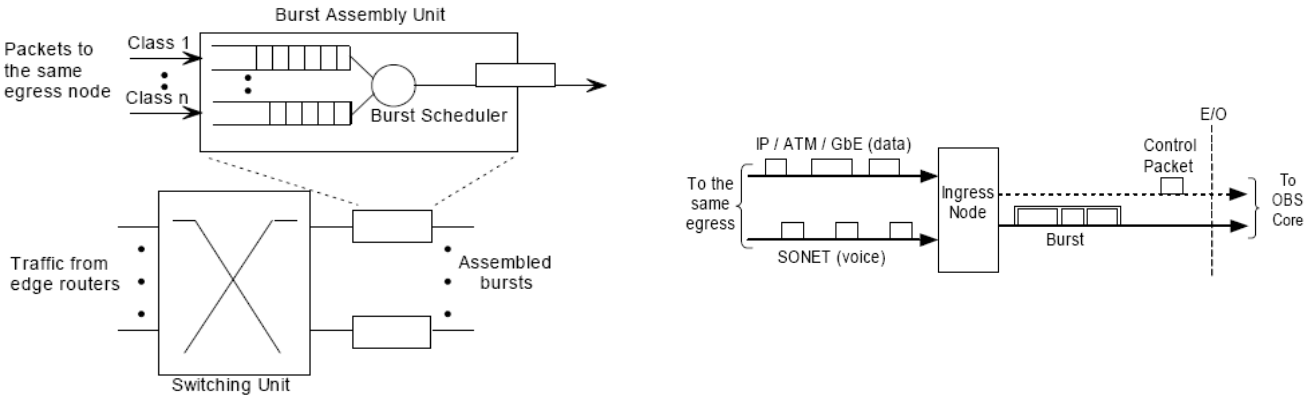

Figure 4. Burst assembly at the edge node [8]

Burst Reservation

Burst reservation protocol is responsible to reserve channels for burst transmission in the core layer. In general, the resource reservation protocol is classified into two major approaches as discussed in [8]. First, two-way reservation or Tell-And-Wait (TAW); for example, Just In Time (JIT) protocol [45], which requires the acknowledgement from destination nodes before sending a burst (similar to circuit channel approach. However, the channel holding time is not as long as circuit channel. On the other hand, one way reservation or Tell-And-Go (TAG) for instance, Just Enough Time (JET) protocol, which does not require the acknowledgement. In fact, the TAG protocol was initially employed in Terabit burst switching [6]. While most OBS networks in the literature employ JET protocol as their burst reservation, which is initially proposed by Qiao [5].

According to [5, 7], JET protocol is an distributed reservation protocol, which requires no optical buffer at intermediate nodes. Figure 5 illustrates how the JET protocol reserves switching resource between a source node to the destination node. Once the source node finishes burst aggregation, it sends a burst control packet (BCP), containing burst information in a separate signaling channel along with burst data packet (BDP). The time difference between the header and the data is referred to *"offset," T*. In each intermediate node, once the BCP is processed, the switch reserves the bandwidth at a specific time (associated with BCP) to establish a wavelength. In other words, the switch selects an available wavelength and the output port, according to the destination. In Figure 5b), suppose the header is sent at time t_a, the burst can start sending at time t_s (where $t_s = t_a + T$). Since the control packet identifies the burst length l, the channel is reserved from t_s to t_{s+l} with the automatic release.

In Figure 5a), the offset time T, between the burst and control packets gradually decreases due to the header processing time (δ), occurring at every intermediate node. In order to ensure enough time for processing the BCP at the destination before the burst arrival, the offset time T must be greater than $\delta \times H$, where H is the number of hops [5].

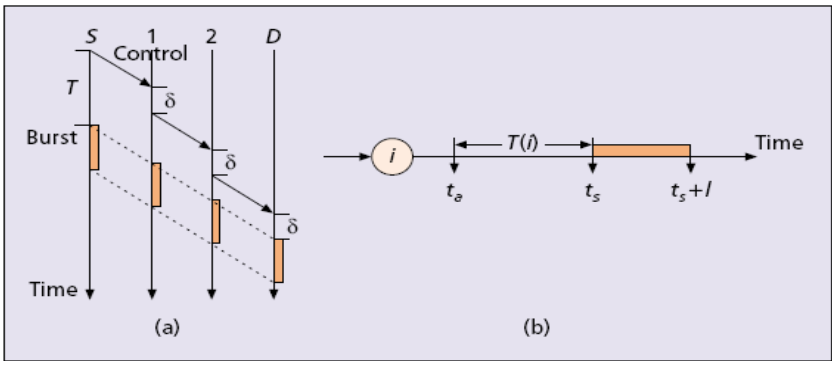

Figure 5. JET reservation protocol [7]

At a high burst load, it is more likely to have high contention at intermediate nodes, resulting in higher probability of burst loss. An priority-based reservation called "an offset-time-based QoS scheme" was proposed in [7] to provide service differentiation. Since the offset duration will affect the QoS of burst transmission, a high priority burst is assigned to a long offset; on the other hand, a low priority burst is assigned to a short offset. In fact, the longer offset provides the better flexible time for core nodes to allocate the switch resources (i.e., output port and wavelength). As the result, the burst probability can be reduced and the burst length is suggested to be between 1 μ sec and few millisecond [17].

In Conclusion, the comparisons among switching paradigms according to certain criteria are shown in Table 1. **Characteristic comparisons among switching paradigms**.

Table 1. Characteristic comparisons among switching paradigms

Criteria/Types	OCS	O/E/O	OPS	OBS
BW Utilization	LOW	HIGH	HIGH	HIGH
Setup time	SLOW	FAST	FAST	FAST
Connect Duration	LONG	SHORT	SHORT	SHORT
Connection	connection	connectionless	connectionless	connectionless
Implementation	EASY	EASY	DIFFICULT	DIFFICULT
loss rate	NO	LOW	HIGH	HIGH

2.2 HYBRID OPTICAL NETWORKS (HONS)

As discussed above, each optical switching paradigm has its own advantages and some drawbacks. In addition, we have witnessed that diverse traffic types are exchanged across Internet backbone networks [1]. These encourage an advent of new-era optical transmission systems, Hybrid optical networks (HONs) [17-21] which combine multiple optical switching techniques into a unified network platform that is able to transport certain traffic types across backbone networks more efficiently than conventional optical networks. In fact, each switching technique is suitable for a particular traffic type, but creates drawbacks for the others. In order to enhance overall network performance, the HONs remain strengths, but eliminate weaknesses of a particular switching technique. Recently, a massive growth of data centers (DCs) and High performance computing (HPC) expedites enormous traffic exchange over the Internet. This requires powerful and scalable switching architectures to support such huge traffic volume and various traffic types generated by DCs applications. In [22-26], Hybrid optical switch (HOS) also plays an important role in DCs research area for the replacement of existing electronic

devices to eliminate O-E-O conversion. Since current DC architectures are based on multilevel electronic interconnections, the networks lack of scalability, energy efficiency, and cost effectiveness to efficiently support such traffic like cloud computing and HPC. Mainly, the literatures aim to propose new optical switching architectures, which are flexible to various traffic requirements, efficient resource utilization, and low energy consumption. Regarding HONs literatures relating to our proposed network, we are able to classify their architectures into the following categories:

2.2.1 HON as Bundled Traffic (Client-Server Approach)

In this scheme, the network recognizes all incoming traffic at edge nodes as bundled arrivals which will be transported on the same type of optical channel, in which the core layer will allocate for the edge layer (without network separation). Analogy with Client-server model [19], an edge node locating in access layer performs its optical channel request to the core layer. Then, the core layer controller allocates optical resources for connecting the requesting edge node and the destination edge node through wavelength channels. The edge node can be either OBS or OPS, which is more sophisticated, and be able to support finer granularity than core switches. In fact, the edge node performs traffic aggregation based on statistical multiplexing, and then delivers the traffic on the assigned optical channels for efficient channel utilization. As a result, transit traffic is not required to switch at intermediate nodes, which can eliminate processing delay, queueing delay and significantly reduce the deployment of costly electrical transponders, in which the cost of transponders is subject to optical data rates. Examples of OBS deployment at

edge nodes include Burst over circuit channel (BoCS) by Gauger and Mukherjee [21] and OBS over OXC by Chou and et. al., [34].

In BoCS, the OBS nodes aggregate arriving traffic in a burst buffer, in which the OBS nodes connect all together in a fully meshed topology. In practice, the network could be logical mesh topology if there is no physical link available according to mesh connection. In contrast to OBS where few links are shared by different traffic demands, BoCS deploys large number of optical links which are dedicated to the same traffic demands [21]. Another variation includes having OPS at the edge and circuit-based OTN in the core layer proposed by Mahony [13] and by Caenegem and et. al. [16]. The OPS functions as an interface between service and transport layers, and provides fast switching and packet aggregation for efficient bandwidth utilization. The OPS has direct interfaces to an OXC which provides static wavelengths and fiber routes to the OPS traffic [13]. The OPS edge node can handle the traffic as the same granularity as customer's electronic routers (i.e. per packet) which allow the integration of the control plane between IP and OPS, in which GMPLS is deployed at the OPS control plane [13]. In addition, Mukherjee [20] also proposed the combination between OPS and OCS with dynamic bandwidth allocation. The OCS core layer can provide "dial for bandwidth" rather than static bandwidth channel. However, the higher degree of dynamic traffic, the faster setup time for the switching fabric is required.

The most recent HON is proposed in [11] where the edge nodes classify arriving traffic as several data flows, called flow transfer mode (FTM) associated with QoS requirement. For this architecture, the control plane separates from data plane thus, no processing delay in the core layer. FTM consists of four modes: continuous streaming, periodic streaming, burst, and packet. In the core layer, the switching facilities will serve the edge layer with different scheduling

algorithms, corresponding to the mode. In fact, this HON is more like OBS, but the advantage occurs when the traffic is on continuous and periodic modes, where the edge node sends out control packet per flow instead of per burst. In other words, less control packets need for processing in the core layer, making this architecture an energy-efficient advantage. However, the burst loss in the core layer due to output port contention is still the limitation of the OBS.

In Hydra employed in DC [25], the authors replace 2-tiers of fat-tree Ethernet interconnect by 1-tier of optical circuit switch (i.e., MEMs) with low optical ports, which is much smaller than serves ports. In fact, top of rack (ToR) Ethernet switch is oversubscribed and not scalable compared to a reconfigurable optical switch. Since MEM switch has slow set-up time, which is suitable for high-rate, long-lived, point-to-point flow. The authors also presented software stack and network controller, using VLAN to forward traffic over Ethernet switch. The Hydra is able to accelerate the execution of real parallel workload when employing the same cost of network as the fat tree topology.

2.2.2 HON with Network Separation (Parallel Approach)

An alternative approach associated with the HON is combining two parallel transport systems (i.e. OCS and OBS) on a common platform, in which the ingress node selects an appropriate switching facility based on the characteristic of the requested traffic. Examples include polymorphic multiservice optical network (PMON) [17], Optical hybrid switching system [33, 46]. In the PMON, two parallel switching architectures are combined in the same platform. One employs OCS paradigm and the other is based on labeled optical burst switch (LOBS), proposed by Qiao [43], with additional capability of wavelength provisioning. The ingress node classifies

the arrival traffic to an appropriate network based on traffic characteristics. In addition, the network is compatible with GMPLS unified control plane. Regarding the OCS core node, it could be simply implemented by optical cross-connect, arrayed waveguide gratings (AWG), or MEMs. Conversely, LOBS requires more complex core switches, which need to analyze all bursts in order to distinguish class of services and transmission types. The core node requires FDLs to hold the data packet during label processing. Also, the core nodes can perform label swapping for certain arrival traffic [17]. Moreover, Xin and et.al also discuss the combination of OCS and OBS. [33], in which the OCS network supports long-live IP flow, and the OBS network carries only the short-lived IP packets (burst traffic). They also pointed out that two-way reservation is required for the circuit network while the OBS is enough for one -way reservation. In fact, the channel deployment in the OCS will not be efficient utilized due to the channel over-provisioning design.

Regarding HONs used in DCs architectures [22-26], most of literature proposed optical HONs with two parallel switching facilities in the core layer to remove some drawbacks of 3 tiers electronic switch interconnect based on multilevel fat tree and *point-to-point* topology, which create overprovision, crosstalk, high energy consumption, and distance attenuation. In [22, 23], the authors proposed 2 tiers optical layers (i.e. HOS edge and HOS core layers), excluding top of rack (ToR) Ethernet switches located on servers racks. However, with higher capacity of server 40Gb/s, we can remove ToR and connect the servers directly to HOS edge switches. The edge nodes classify arriving traffic into three types (i.e., circuit, burst, and packet), and the core layer will allocate the most suited optical transport system corresponding to the application requirements. Each core node combines two switching paradigms, which will switch off when it is inactive [22]: fast switch (supports short burst & packets) employed by semiconductor

amplifiers (SOA), and slow switch (supports long burst & circuit) employed by MEM switches. The unique feature of HOS control plane is that packets can be inserted into unused TDM circuit channel with the same destination, allowing higher utilization [22]. In core layer, there is no contention resolution in time domain but in frequency domain (i.e., WC). As a result, no delay in the core layer but loss may occur in core nodes [22, 23]. Regarding the analysis, the paper focuses on energy consumption model, very little on network delay analysis, also lacks of multiple channels regarding performance results. In LIGHTNESS DCN [24], the authors proposed a testbed prototype of Hybrid OPS/OCS DCN with unified software defined network (SDN)-enabled control plane architecture. The prototype employs two parallel switching facilities (OPS and OCS) in the core layer, in which OCS supports long-lived data flow and OPS for short-lived flow. The unique of LIGHTNESS DCN is the SDN capability, allowing their OPS is highly distributed controlled for port-count independent reconfiguration time [24]. However, the paper shows only the concept of the new prototype without any analysis and results.

2.2.3 HON with Overflow Channel

There are only few literatures related to overflow channel deployment in optical networks. The overflow channel is used for overflow traffic management regarding a contention resolution. However, they do not provide network separation for the traffic classification purpose in the literatures. First examples include Optical burst transport network (OBTN) by Gauger and Mukherjee [21]. The OBTN employs both switching paradigms (i.e., OCS and OBS). The BoCS network, which provides primary channel, has virtual direct end-to-end wavelength between OBTN nodes. In fact, the direct wavelength across the core layer can reduce the OBS ports in

core layer. The additional overflow channel, provided by an OBS network, is designed to release the network contention in the BoCS network. In fact, the paper lacks discussion on traffic classification in the primary channel, which transmits all types of traffic in the static wavelength channel. The other two research studies for the overflow approach include Menon [36] and Washington's [38], the overflow channel is proposed to alleviate the contention of a primary OBS network same as the OBTN. The difference is that the overflow traffic occurs in every intermediate nodes can be reallocated/aggregated in the primary channel at any intermediate node if the primary capacity is available. As a result, there will be some delays (i.e., processing, queuing) introduced in every intermediate nodes. In addition, the overflow channel is provided dedicatedly for a particular destination (i.e., mesh topology) without achieving the statistical multiplexing gain by burst assembly process. This probably leads to inefficient use of overflow channel, and requires significant number of costly overflow channels. The network cost model for the OBS network with overflow deployment is also studied in [36].

3.0 HYBRID OPTICAL NETWORK WITH OVERFLOW CHANNEL

3.1 OVERFLOW CHANNEL AND ALTERNATIVE PATH

3.1.1 Traffic Demand and Overflow Channels

Initially, overflow channel was discussed in telephone networks to alleviate traffic congestion during peak load, in which a group of circuit trunks is allocated between transit exchanges. During busy hours, blocked calls which cannot be placed in the primary trunks are rerouted to secondary (i.e., overflow) trunks. The overflow trunks are analogy to a capacity buffer, shared by different groups of primary trunks. Since optical wavelength channels are based on the same switching paradigm as the telephone trunks, the overflow concept can be applied. In optical network, the traffic exceeding the capacity of dedicated wavelength channels can be allocated to an overflow optical channel. The overflow channels can be either the whole wavelength or partial granularity depending on switching types (e.g., OCS, OPS, and OBS). As a result, costly wavelength channels, which are very costly, can be efficiently employed leading to network cost saving. The relationship between wavelength reservation, traffic demand, and the overflow traffic is shown in Figure 6.

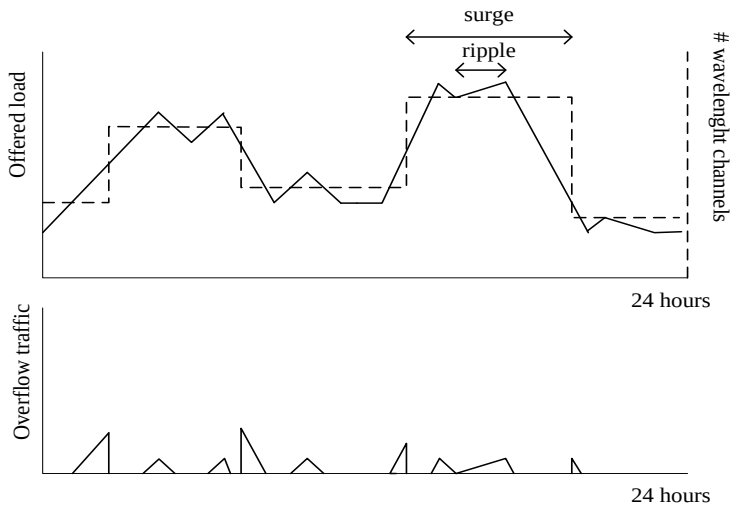

Figure 6. Reserved channels and overflow traffic

Figure 6 shows number of wavelength channels corresponding to traffic demands (offered loads) along with overflow traffic between two edge nodes. The dedicated wavelength channels are reserved end-to-end for a particular demand pair. An overflow channel (lower picture) will deliver fluctuated traffic from the reserved channels. In practice, the traffic demand fluctuates during the day for instance; voice offered load surges to the peak during rush hours (i.e., 9-10 a.m. or 4-5 p.m.). Moreover, traffic demand also fluctuates (called "ripple") during short periods. In Figure 6, one can see that once a “surge” begins, it will remain for a period (i.e., 30-60 minutes), until the traffic decreases to the normal situation, while the “ripple” randomly occurs throughout the time domain [35]. For implementation, core nodes employ OCS in space and wavelength domain to set up semi-permanent end-to-end channels, which vary by traffic loads during different time of a day.

Regarding channel assignment, the "surge" will be handled by additional wavelength channels (as dotted line in Figure 6), and the "ripple" will be carried by the overflow channel. Once traffic load increases greater than a threshold, the edge node will request a new channel to the core layer, which will set up the end-to-end channel for the surge based on routing and wavelength assignment (RWA) algorithm.

3.1.2 Overflow Channels and Alternative Path

From the previous section, one could see that the overflow traffic is relatively small amount comparing to traffic load in the premium channel, reserved according to the average traffic load. Therefore, the overflow channel logically performs as a capacity buffer. The overflow channel can be shared by any OBS node in order to efficient use of costly OBS channel. In each intermediate node, the network reserves switching fabric according to burst control header and release the fabric immediately after the burst left for the new burst arrival.

In Figure 7, solid lines represent the reserved wavelengths, dedicated for several traffic demand pairs, including traffic from node A-to-B, A-to-C, and A-to-D, and the overflow path is depicted in the dotted line. Regarding the demand pair (A-D), the main traffic is transmitted over the direct wavelength from A-to-D; but the overflow traffic can be delivered on the alternative route either via node B or C. In the same time, the traffic demand of B-to-D can also share this overflow channel. The advantages of alternative overflow path are not only the capacity sharing, but also the benefit of network redundancy as well.

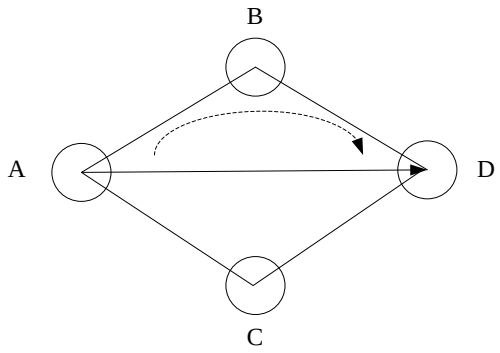

Figure 7. Overflow channel and the path

The wavelength channel is solely reserved for each particular traffic demand pair, provided by a type of OCS (i.e., wavelength routing switches). On the other hand, the overflow channel can be shared among the entire OBS nodes. Hence, an OBS or OPS network implements the overflow channel.

In this proposal, a Dynamic Hybrid optical network (DHON) is proposed, which combines several switching paradigms channel in order to support dynamic traffic with efficient use of wavelengths. The details of the network architecture and its topology will be discussed in the following sections.

3.2 DHON WITH OVERFLOW CHANNEL

In this section, we investigate the framework of dynamic hybrid optical network (DHON) with overflow channel deployment. The proposed network is able to support all forms of traffic types, including voice video and data with transparency of data format (e.g., ATM, MPLS, and IP). A group of dedicated wavelength channels is reserved for premium traffic, which requires low

delay channel with QoS guarantee. The deployment of overflow channel will improve the overall network performance: increasing the utilization in the *premium* channel and in the same time decreasing the number of wavelengths assigned for *premium* channel. In addition, the traffic aggregation at ingress node for the secondary channel will promote the efficient use of wavelengths for packet-based traffic (e.g., IP, frame relay). The network topology of DHON will be discussed in the next section.

3.2.1 DHON Architecture and Topology

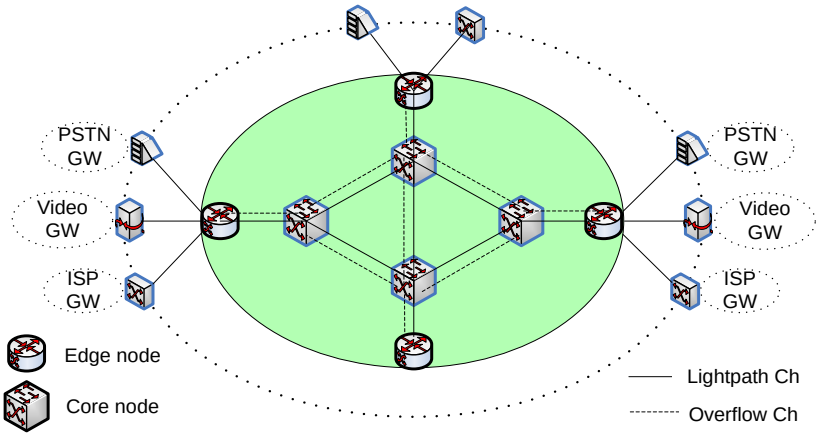

Figure 8. DHON physical topology

Figure 8 illustrates the basic concept of the Dynamic Hybrid Optical Network (DHON). The proposed optical network serves as a nationwide backbone network, providing a unified optical transport system for all service providers (e.g., ISPs, data center, CATV, and voice). Mainly, the network consists of two network layers, including access and core layers depicted in shaded area.

The access and core layers are composed of a group of DHON edge nodes and core nodes respectively. The edge nodes connect several types of service providers via their gateways, which aggregate traffic from end users in the region. However, the gateways are not a part of our proposed network. Although future traffic consuming applications like Internet of things, or high performance cloud computing (HPC) located in data centers (DCs) are not illustrated in our proposed architecture, DHON still could be a model in the future with additional optical switching nodes aggregating servers in the DCs.

The network separates the channels into *wavelength* and *overflow* channels. In Figure 8, the solid line represents wavelength channel, based on end-to-end channel reservation for each traffic demand (ingress-egress). In the core layer, the traffic travels in optical domain and remains in the wavelength channel without any adding/dropping at intermediate nodes. On the other hand, the dotted line refers overflow channel based on hop-by-hop reservation, in which each switching fabric is reserved according to bursts. In Figure 9, lightpath channel (i.e., wavelength) is divided into two traffic channels: *premium* and *secondary*. The *premium* channel supports long-flow or real time traffic (i.e., voice, video conference), which requires lowest end-to-end delay. Therefore, the network pre-reserves a number of *premium* channels according to average traffic load without waiting for available capacity. On the other hand, the *secondary* channel delivers non delay-sensitive traffic, associated with packet-based applications (e.g., IP traffic). The reason of channel separation is to provide channel efficiently based on QoS requirement (channel classification will be discussed again in 4.3).

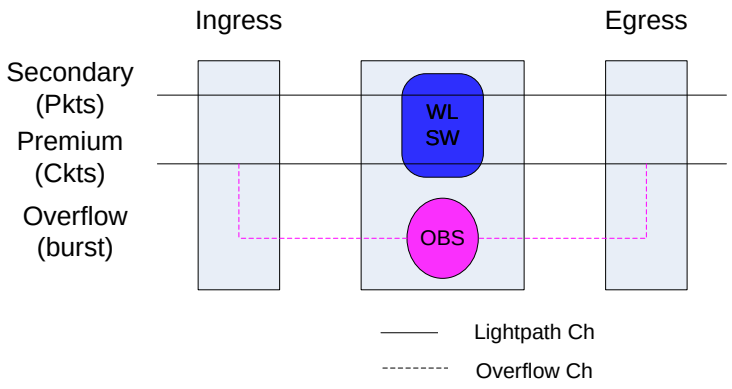

Figure 9. Wavelength V.S overflow channel in DHON

The overflow channel is based on hop-by-hop routing is used to alleviate the congestion on the premium channel, allowing the decrease in wavelength assignment for the *premium* channel. Since the overflow traffic from the reserved premium channel is bursty which has interrupted Poisson distributed (shown in 5.3.2), the OBS is a suitable switching paradigm to carry the overflow traffic. In this case, the OBS virtually operates as a capacity buffer of the *premium* channel, which is shared among overflow traffic according to several demand pairs.

The DHON is designed based on the philosophy of smart edge nodes; yet less complicated core nodes. The edge node has relatively sophisticated functions, which performs traffic monitoring, classification, aggregation, and wavelength assignment. Furthermore, the edge node provides the interconnection between electronic domain and optical domain, associated with the gateways and the proposed core network. As a result, the edge nodes need to operate in both electrical and optical domains.

In contrast to the edge nodes, the core nodes perform transit connection between each pair of ingress-egress nodes, according to the offered load generated by the ingress nodes. The core network is responsible for fast-forwarding any traffic aggregated by the edge nodes; all the

traffic transmitted through the core node is transparent to the data format. The core nodes are implemented by OCS (i.e., reconfigurable wavelength switch) in order to eliminate delays (i.e., processing, queueing, and transmission) occurring at intermediate nodes, and minimize the complication of switching architecture and network cost. However, the core nodes also integrate OBS in the same switching node to deliver the overflow traffic, and share the same optical resources (i.e., chassis, optical multiplexers, fiber, etc.).

In contrast to existing IP/DWDM, DHON requires sophisticated edge nodes, and employs an extra OBS overflow channel per hop to enhance utilization and reduce number of premium (i.e., wavelength) channels. However, IP/DWDM requires comparatively fewer channels because it aggregates traffic in a buffer at every node, allowing higher utilization but lower QoS. Although DHON requires slightly more wavelength channels and its nodes are more complicated, the added cost could be compensated by improved performance. We cannot compare costs until we can estimate cost of the conventional IP/DWDM.

3.2.2 Multilayer Topology of DHON

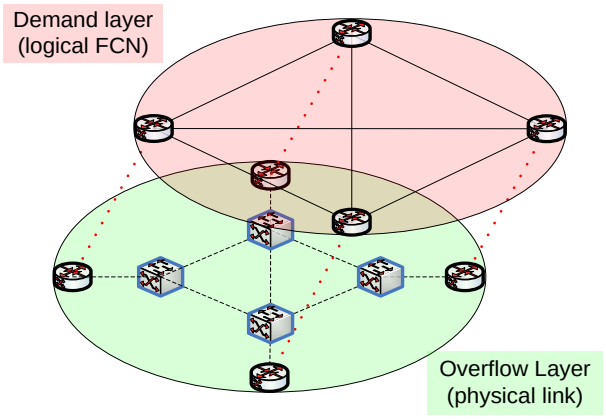

Figure 10. Multilayer of network architecture

Regarding the topology in Figure 8, we can also differentiate in this approach: the traffic demand layer and the overflow layer illustrated in Figure 10. The demand layer represents the traffic demand between each pair of edge nodes (ingress-egress), which has logical fully connected totopology and dedicated for each pair (upper layer in Figure 10). The offered traffic associated with the traffic demand layer travels in physical optical link lower plane.

In reality, the offered load associated with each demand can be transmitted over a number of end-to-end wavelength channels. Each channel are not required on the same route (see Figure 62), which actually depends on optical resources available along the path (i.e., switching fabric, wavelength, and optical fiber). The routes of end-to-end connections are identified by

wavelength routing assignment (WRA) algorithm, which is beyond the scope of this research study. However, we provide the general concept of WRA in the appendix.

Considering the overflow channel, the traffic transmission is based on hop-by-hop routing; therefore, the overflow traffic occurred at each ingress node is transmitted to the next hop toward the destination edge nodes (egress), illustrated in the lower plane. Any OBS node along the route can share the overflow channel. A group of OBSes forms the overflow layer. The OBS network employs advanced burst reservation (i.e. JET) in order to ensure that the channel is already reserved from the ingress to egress nodes prior to transmitting an overflow packet. As a result, the overflow channel implemented by OBS is able to reduce network blocking, and efficiently use the optical channels.

4.0 PROPOSED DHON EDGE NODE

In this chapter, we will discuss the proposed hybrid edge node in details before providing the performance analysis in the next chapter. We start with the required functionalities of the node in section 4.1, and then variety of traffic that the node has to handle in section 4.2 . In section 4.3, we discuss node architecture, and illustrate how optical channels operate together. At last, section 4.4 discusses overflow theories, necessary for understanding the performance analysis regarding overflow channel in the next chapter.

4.1 DHON EDGE NODE FUNCTIONALITIES

The proposed edge must perform the following functionalities: traffic classification, monitoring, aggregation/disaggregation, and wavelength channel assignment.

Traffic Classification: Edge nodes classify traffic into three categories based on QoS characteristics. The nodes assign traffic to appropriate optical channels (i.e. premium, secondary, and overflow channels) which are transported by different type of optical switches. In addition, they are able to differentiate several standards and protocols (e.g., IP, TCP/UDP, MPLS, SONET, SS7, etc.)

Traffic monitoring: Edge nodes monitor traffic loads between each pair of edge nodes. The edge nodes collect statistical data of arrival's time stamps and their holding times in order to analyze traffic characteristics: mean, variance, distribution. Based on monitoring feature, the nodes are able to request the centralized controller to configure/release wavelength channels throughout the network based on statistical data for an efficient utilization of optical resources.

Traffic Aggregation/Disaggregation: Edge nodes aggregate/disaggregate arrival traffic based on traffic category and destination. The edge nodes are compatible with existing optical transport system (e.g., SDH/SONET), and able to capsulate/de-capsulate arrival traffic in any payload format. In premium channel, ingress nodes are able to perform multiplexing/de-multiplexing. In a specific case, if an instant traffic demand exceeds reserved capacities; the node will reroute the traffic to an overflow channel. In secondary channel, packet-based traffic is aggregated in CoS buffers in order to achieve higher channel utilization; while satisfy QoS requirements for certain applications.

Wavelength channel assignment: The ingress nodes are able to evaluate a number of wavelength channels for each switching paradigm (i.e., OCS, OPS, and OBS). The number is calculated based on queuing analysis concerning QoS parameters (i.e. delay, blocking, and utilization).

4.2 TRAFFIC CLASSIFICATION IN DHON

Since the DHON performs as a unified backbone network, supporting various traffic types for telecom providers. The traffic arriving to ingress nodes will be categorized so that it can be

assigned to appropriate optical channels. In Figure 11, we divide the traffic into 4 types based on traffic flow behavior and QoS requirements. In addition, the matching between optical channel and the traffic characteristics is also discussed as the follows:

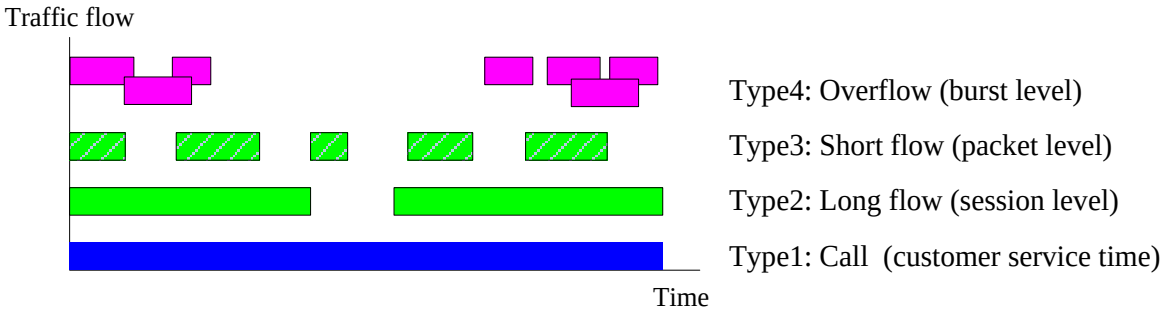

Figure 11. Traffic Classification in DHON

1. Constant rate stream (call) represents call requests from service providers, which require constant bitrate (CBR) bandwidth during call durations (service time). Examples include (e.g., premium voice call, video conference, CATV). This traffic type requires real- time channel that provides highest QoS associated with very minimal end-to-end delay, corresponding to *premium* channel.

2. Variable stream (long flow) refers to variable rate traffic associated with long flow session applications. This traffic type is able to tolerate some degrees of end-to-end delay but limited to upper bounds of their QoS requirements. Examples include voice over IP (VoIP), Internet video streaming, online gaming. Regarding the limited delay, the traffic would be exclusively handled in a specific QoS buffer, referred to CoS I buffer located in *secondary* channel.

3. Elastic stream (short flow) refers to data transmission, which is randomly transmitted as asynchronous packets. This traffic type is able to tolerate relatively high delay and large jitter during transmission. Examples include Web, File sharing, and E-mail. Since the traffic is considered as low delay sensitive traffic that can be aggregated in statistical buffer for efficient use of wavelength channel. Therefore, it would be corresponding to our CoS II in *secondary* channel.

4. Overflow stream (burst) refers to call requests, which cannot place in the premium channels due to fully occupancy. The overflown calls will be sampled, encoded, and rerouted to overflow channel. In fact, the overflow traffic has a bursty pattern, which will be aggregated in a burst buffer before transmitting in an optical fiber, corresponding to our *overflow* channel.

In conclusion, the *premium* channel is reserved for "constant rate streams" which consume relatively fixed bandwidth of wavelength channel. The *secondary* channel is responsible for packet-based traffic, including long flow and short flow, associated with a particular class of service buffer.

In this research study, we assume call arrivals (i.e. voice/video calls) and IP long flow session as Poisson process since the traffic is randomly originated by user decisions. Contrary to short IP packets and burst data, the traffic is generated by protocols, in which numbers of arrivals are not Poisson distributed.

4.3 NODE ARCHITECTURE & CHANNEL CLASSIFICATION

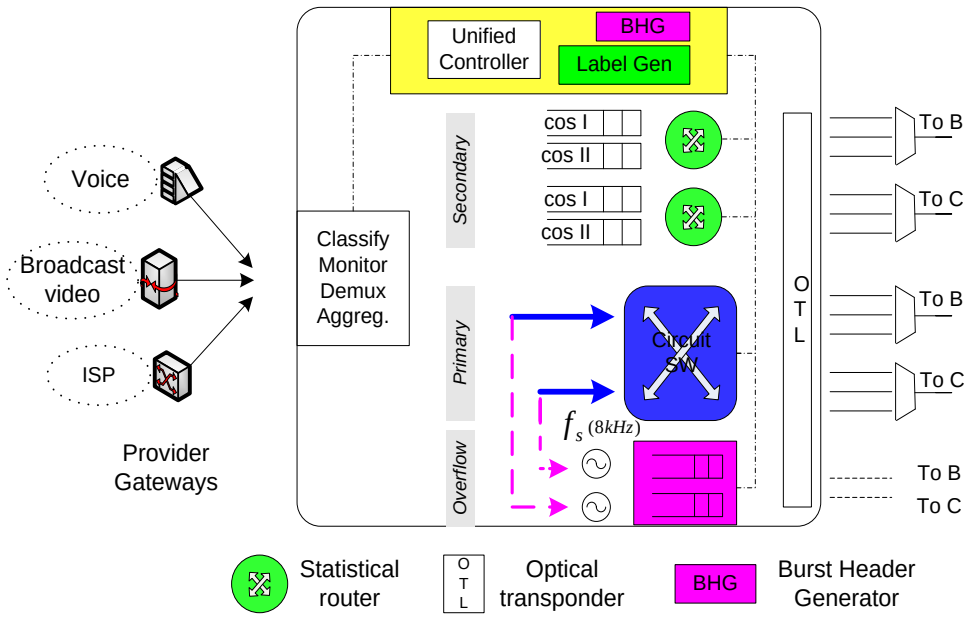

Figure 12. DHON ingress node architecture

Figure 12 illustrates details of the edge node architecture. The node consists of 3 main parts: control system, input/output interfaces, and channel assignment. Based on GMPLS control system, the node is able to recognize all types of optical switching (i.e. OCS, OPS, and OBS). The input interfaces connected to provider's gateways are compatible with existing format (e.g., IP, MPLS, ATM and etc.). In addition, the edge node performs O/E/O conversion by reformatting optical input to electrical signal, and transmitting via optical interfaces. Regarding

channel assignment, the node allocates arriving traffic to one of these optical channels: *secondary, premium,* and *overflow* (top-down approach). The *premium* channel operates together with *overflow* channel, which supports fluctuated traffic. At the same time, we can significantly reduce number of *premium* channels due to less over-provisioning (discussed later in the next section 4.3.1.). In *secondary* channel, two classes of QoS buffers are employed for maximum use of channel capacity (details in section 4.3.3).

4.3.1 Premium and Overflow Channels

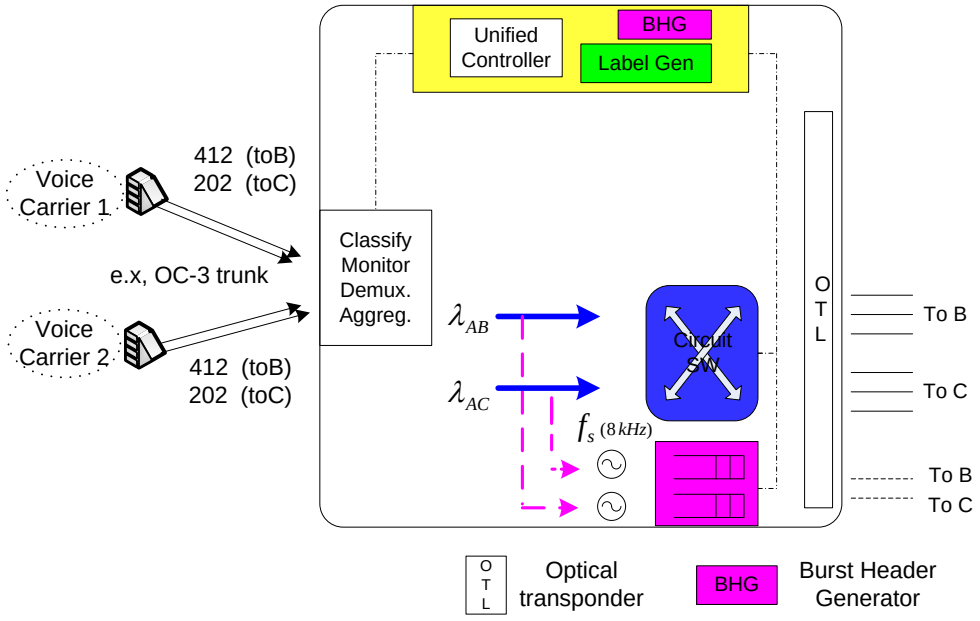

Figure 13. Ingress node architecture with premium and overflow channels

In this section, we discuss traffic aggregation in *premium* channel associated with *overflow* channel. Figure 13 illustrates partial architecture regarding only *premium* and *overflow* channels. Considering call requests from carriers, the calls are transported over SONET/SDH link (e.g., OC-3, OC-12) to the ingress node, in which the calls are bundled based on destination (i.e., 412, 202 area codes). The ingress node extracts calls from SONET envelope and de-multiplexes traffic to call level (DS-0) in order to monitor traffic load. Then, the ingress node aggregates calls from several carriers, which have a route to the same destination, and transports the aggregated calls in the same wavelength channel.

Regarding *premium* channel, ingress nodes require not only time synchronization for control signaling (i.e., SS7, SDH/SONET), but also compatibility with optical transport system. Therefore, we need 3-dimensions switches (i.e., space, time, and wavelength) for edge nodes. However, the core layer provides transparent transmission, which requires only 2-dimensions photonic switches (space and wavelength).

Premium channels are initially configured based on traffic intensity between a particular pair of edge nodes. When traffic fluctuates greater than pre-allocated channels, an overflow channel will handle the excess traffic. Regarding traffic surge during busy hours (referred to 3.1.1), overflow calls from *premium* channels will be placed in additional wavelength channels. In other words, when traffic monitoring unit detects an increase of traffic intensity, it will send signaling to a central controller to establish new wavelength channels between particular node pairs (i.e., dynamic channel allocation).

Regarding *overflow* channel, it is implemented by OBS to improve overall network efficiency in terms of utilization increase and channel saving. In fact, overflow traffic is characterized as bursty arrivals, consisting of on-off states. The overflow calls are converted into

packet-based format (i.e., sampling and quantization), and then aggregated in a buffer before transmitting over OBS. Since the *overflow* channel is designed to alleviate traffic congestion in *premium* channel, the delays occurring at the edge node are factors of concern. Therefore, several timer-based buffers are employed at an edge node to limit the end-to-end delay according to QoS restrictions.

To better understand how the system works, we illustrate an example of traffic aggregation in premium and overflow channel in Figure 14.

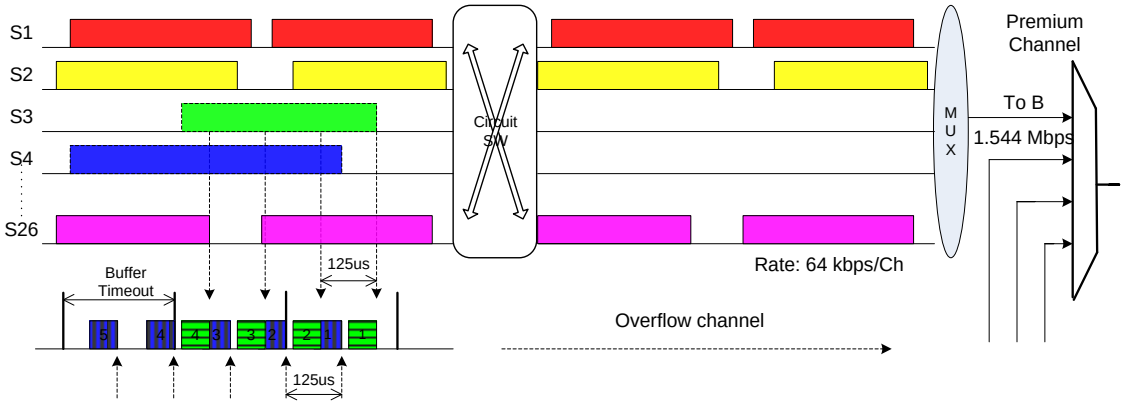

Figure 14. Traffic aggregation in premium channel and overflow traffic grooming

Assuming hundreds of calls arrive to an ingress node, only 26 of those calls have the same destination to an egress B (shown in the figure). In this example, the ingress node has 1.544 Mb/s wavelength channel allocated to the destination B. Basically, the link is able to carry 24 calls simultaneously (based on 64 kb/s per each call). Therefore, the last two arriving calls (i.e., S3, S4) cannot be allocated in the primary channel, which will be relocated to an overflow channel. In our DHON, the overflow calls are sampled at 8 kHz (every $125\,\mu s$), and quantized

with 8 bits/sample. Then, the call samples will be aggregated in a burst buffer. One can see that the samples are mixed among those two overflow calls which will be differentiated at the egress B corresponding to the burst header.

Regarding a specific case with 3 edge nodes in the network (Figure 13), the ingress A has dedicated wavelength channels to egress nodes B and C where λ_{AB}, λ_{AC} represents premium traffic rate between node A-B, and A-C respectively. Due to dedicated channels, neither processing nor queuing delay occurs at intermediate nodes. Consequently, throughput and end-to-end delay are determined depending only on delays at the edge node.

4.3.2 Overflow Burst Assembly, Reservation and Departure

In this section, we discuss mechanism relating to *overflow* channel: burst assembly, channel reservation, and burst departure. The overflow channel employs JET for channel reservation. In other words, an ingress node sends out a burst control header (BCH), containing information of overflow samples associated with the burst. Then, intermediate OBSes (on the path from ingress-egress) reserves their switching resources before the ingress node sent out the burst. In fact, the control header travels separately from the burst (out-of-signal), analogy to a SETUP message. As a result, during burst delivery, processing and queuing delay can be eliminated in the core layer. Since overflow traffic is a part of voice calls, it requires low end-to-end delay. Through an adjustment of buffer *timeout* and numbers of *premium* channels, an upper bound delay of burst transmission can be determined.

Theoretically, burst assembly has some effects to network performance. Since the delay is a constraint issue for overflow channel. In the proposed DHON, we employ *timer-based* buffer

(fixed assembling time) to aggregate overflow traffic. Regarding our contribution, overflow theory combined with sampling theory are used to represent arrival process of the system. For the departure, it relates to several factors (e.g., arrival rate, buffer timeout, and offset time). Once both processes are defined, the performance of overflow channel can be derived by queuing analysis. Figure 15 illustrates the relationship between overflow traffic arrivals, burst assembly associated with BCH, and departure of bursts.

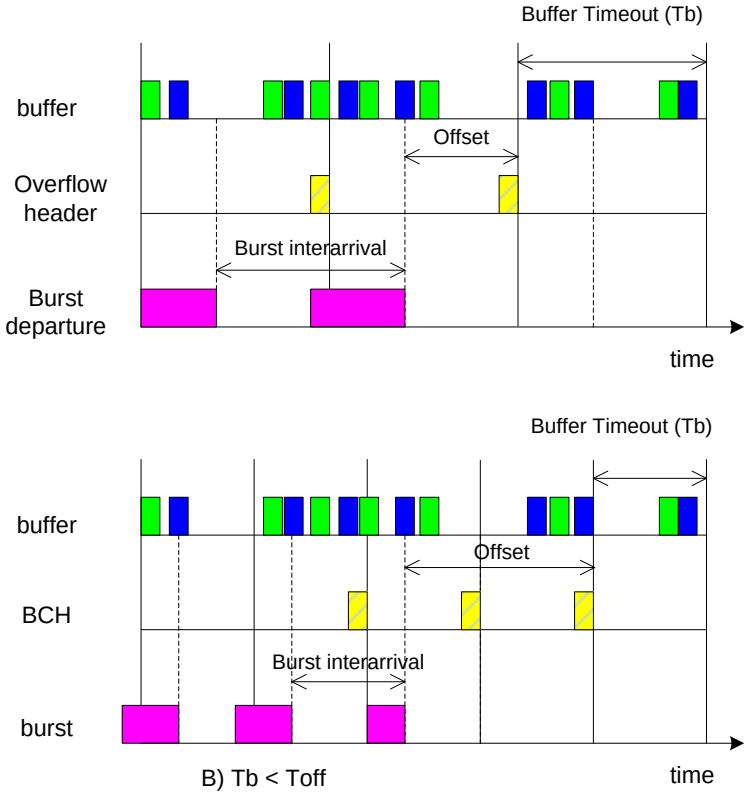

Figure 15. Overflow arrivals, burst assembly, and departure a) $T_b > T_{off}$, b) $T_b < T_{off}$

In Figure 15a), the overflow traffic (samples of calls) is aggregated into the buffer. Based on timer-based scheme, the samples are accumulated until reaching *buffer timeout* (T_b), in which a burst (variable-sized) has been formed during this time. After timeout, the BCH is immediately sent to OBS core nodes in order to reserve switching resources beforehand. In fact, the buffer holds the burst for a time duration referred as *Offset* (T_{off}) before transmitting.

One can notice the departure of bursts has ON and OFF states, which can be represented as IPP. ON refers to burst is being transmit out of ingress node and OFF means no burst sending. Another observation is that burst inter-arrival time equals *buffer timeout* (T_b), which always happens for both cases: (a) $T_b > T_{off}$, b) $T_b < T_{off}$. However, burst size decreases in case b) as shorter buffer time. The details of queuing analysis will be investigated in 5.2.2.2.

4.3.3 Secondary Channels

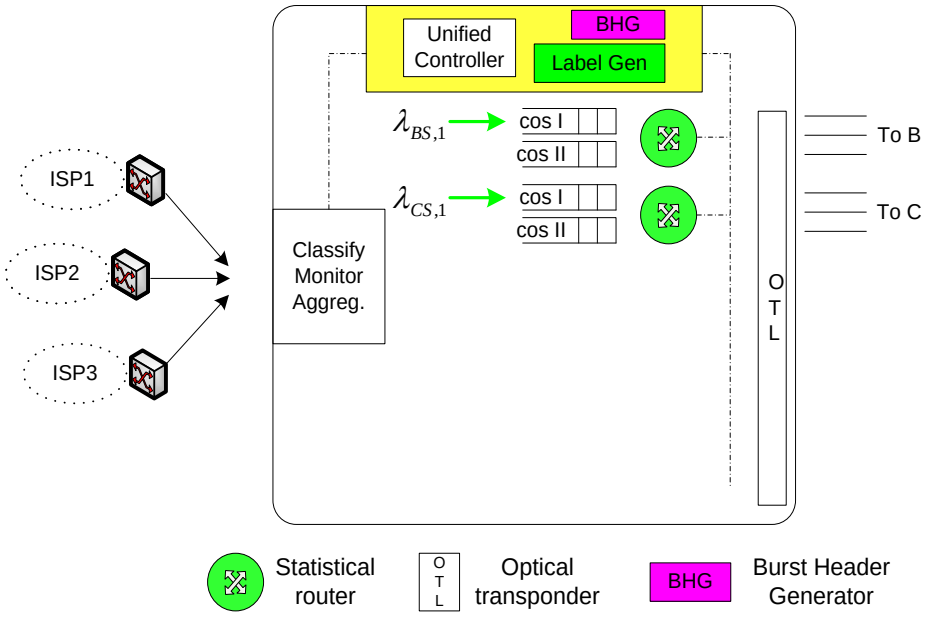

Figure 16. Edge node associated with secondary channels

The *secondary* channel is mainly designed to support packet-based traffic ranging from long flow stream (i.e., VoIP, multimedia stream) to elastic applications (i.e., http, mail, FTP). Since these traffic types can tolerate greater delay than the constant rate traffic in *premium* channel, they can be aggregated in a buffer prior to delivery on the dedicated wavelength channels in order to achieve statistical multiplexing gain in the wavelength channel. In fact, the buffers are independently separated, depending on the destination and class of service (CoS). In addition, the

buffers allow efficient use of the wavelength channels via the deployment of statistical multiplexing switch.

According to *secondary channel* shown in Figure 16, the buffers at the secondary channel are classified into two classes of services (Cos I, II), depending on the delay tolerance. The traffic demands from several ISPs have different destinations (not similar to premium). The ingress node will classify each arriving packet based on the destination according to the packet header, and aggregate the traffic from several ISPs, which have the same destination into the same buffer. Since the variable stream associated with CoS I requires more restriction on the end-to-end delay than the elastic traffic (best effort), the CoS I buffer should be a finite size in order to limit the over-bounded delay. If the number of existing packets remaining in the buffer is greater the buffer size, the new arrival will be dropped and the ingress node will request the gateway to retransmit the packet.

Hence, the DHON is able to treat the customers (i.e., providers) with several types of QoS based on customer's service level agreement (SLA). The secondary channel is also employed dedicated wavelength channel in order to eliminate processing delay at core nodes (not similar to other OPS networks). However, the electronic buffers introduce some delay to the network. As a result, the edge node needs a careful design of buffer size and the numbers of wavelength channels assigned to various degree of traffic load.

4.4 OVERFLOW TRAFFIC THEORY

In this section, we explain some of overflow traffic theories, relating to our proposal and will be applied to our performance analysis in overflow channel in section 5.2. Riodan [47] described some formula to calculate mean and variance of overflow calls from telephone trunks system. He discussed that the overflow traffic is not Poisson distributed, in which mean and variance are not equivalent. In fact, only mean and variance cannot represent overflow traffic characteristic precisely. Since the overflow traffics is bursty, an interrupted Poisson process (IPP) is a better model for bursty traffic representation. Kuczura [48, 49] proposed a mathematic model (i.e., IPP) by using three moment method to approximate overflow traffic from circuit based trunks. He also discussed combinations of several types of arrival flows, including Poisson and non-Poisson flows.

Now, we are going to apply the above theories to investigate overflow traffic analysis for our research study. Let a_{ij} is a total offered load from several carriers associated with a demand pair *(i,j)*, where c_{ij} channels are reserved between node *i* and *j* for the offered load. Based on the traffic demand a_{ij} regarding the premium channel, we can find mean α_{ij} and variance v_{ij} of overflow calls as follows:

$$\alpha_{ij} = a_{ij} B(c_{ij}, a_{ij}) = \lambda_{ij} B_{ij}(c_{ij}, a_{ij}) / \mu_{ij}$$

$$v_{ij} = \alpha_{ij}\left[1 - \alpha_{ij} + \frac{a_{ij}}{c_{ij} + 1 + \alpha_{ij} - a_{ij}}\right]$$

According to the Erlang-B properties, we can write the overflow arrival rate in terms of α_{ij} as the follow:

$$\lambda_{o\_ij} = \lambda_{ij} B_{ij}(c_{ij}, a_{ij}) = \mu_{ij} a_{ij} B(c_{ij}, a_{ij}) = \mu_{ij} \alpha_{ij}$$

The peakedness *Z* (or burstiness) used to measure a variation of overflow traffic for a particular demand pair (i, j) is as follow:

$$Z_{ij} = \frac{v_{ij}}{\alpha_{ij}} = \left[1 - \alpha_{ij} + \frac{a_{ij}}{c_{ij} + 1 + \alpha_{ij} - a_{ij}} \right]$$

It should be noted that if the value of *z* is equal to one, the traffic is Poisson distributed.

Given traffic intensity a_{ij} and numbers of wavelength channels c_{ij}, the first three moments of overflow traffic based on a demand pair *(i,j)* are given by Kosten:

$$m_1 = a_{ij} \frac{\sigma_0(c_{ij})}{\sigma_1(c_{ij})}$$

$$m_2 = a_{ij}^{\ 2} \frac{\sigma_0(c_{ij})}{\sigma_2(c_{ij})} + m_1$$

$$m_3 = a_{ij}^3 \frac{\sigma_0(c_{ij})}{\sigma_3(c_{ij})} + 3m_2 - 2m_1$$

where $\sigma_0(c_{ij}) = \frac{a_{ij}^c}{c_{ij}!}$, and $\sigma_j(c_{ij}) = \sum_{i=0}^{c} \binom{j+i-1}{i} \frac{a^{c-i}}{(c-i)!}$

According to three moments of methods approximation, the overflow traffic can be modeled as Interrupted Poisson process (IPP) with ON-OFF states. The matching between the first three moments and IPP parameters are as follows (Kuczura 1973) [48]:

$$\lambda_{on} = \frac{\delta_2(\delta_1 - \delta_0) - \delta_0(\delta_2 - \delta_1)}{(\delta_1 - \delta_0) - (\delta_2 - \delta_1)}$$

$$\omega = \frac{\delta_0}{\lambda}\left[\frac{\lambda - \delta_1}{\delta_1 - \delta_0}\right]$$

$$\gamma = \omega\left[\frac{\lambda - \delta_0}{\delta_0}\right]$$

where λ_{on} is overflow arrival rate during ON state. In fact, the above parameters are based on service time normalization ($\frac{1}{\mu} = 1$). Thus, $\lambda_{on} = A_{on}$ (i.e., overflow traffic load) in this case. Also, $1/\omega$ and $1/\gamma$ are mean duration of ON and OFF states respectively, which are exponential distributed.

In the above equations, δ_n represents the ratio of factorial moments of the overflow stream:

$$\delta_0 = m_1$$

$$\delta_1 = \frac{m_2}{m_1} - 1$$

$$\delta_2 = \frac{m_3 - 3m_2 + 2m_1}{m_2 - m_1}$$

Moreover, the overflow stream can be represented in another form called renewal process, in which inter-arrival distribution $G_{ij}(t)$ of the overflow traffic corresponding to offered load a_{ij} can be obtained by IPP transformation to hyper-exponential distribution IPP→ H_2:

$$G_{ij}(t) = p_1(1 - e^{-\lambda_1 t}) + p_2(1 - e^{-\lambda_2 t}), \text{ where } p_1 + p_2 = 1$$

where

$$\lambda_1 = \frac{1}{2}[A + \omega + \gamma + \sqrt{(A + \omega + \gamma)^2 - 4A\omega}]$$

$$\lambda_2 = \frac{1}{2}[A+\omega+\gamma+\sqrt{(A+\omega+\gamma)^2 - 4A\omega}]$$

$$p_1 = \frac{A-\lambda_2}{\lambda_1-\lambda_2}$$

$$p_2 = 1-p_1$$

And the Laplacian transform of the G(t) is given by:

$$G(s) = \frac{p_1\lambda_1}{s+\lambda_1} + \frac{p_2\lambda_2}{s+\lambda_2}$$

Remark: Hyper exponential distribution H_k (k=2) has probability density and cumulative functions as follows [50]:

CDF: $F_x(x) = \sum_{j=1}^{k} q_j(1-e^{-\mu_j x}), x \geq 0$

PDF: $f_x(x) = \sum_{j=1}^{k} q_j \mu_j e^{-\mu_j x}, x > 0$

5.0 PERFORMANCE ON PREMIUM AND OVERFLOW CHANNEL

Premium channels support high-priority traffic, such as real time applications, which have long flows or a constant-bit rate stream. Such applications usually have strict delay constraints. In some situations (with low probability), traffic load fluctuates over a short period, in which case any excess traffic would be absorbed by an overflow channel. In this chapter, we discuss the analyses of premium and overflow channels. The chapter divides into two parts: performance analysis on *premium* channel discussed in section 5.1, and later, we investigate performance analysis of overflow channel in section 5.2. Lastly, we illustrate network performance plots for both channels and evaluate the results in section 5.3.

5.1 PERFORMANCE ANALYSIS ON PREMIUM CHANNEL

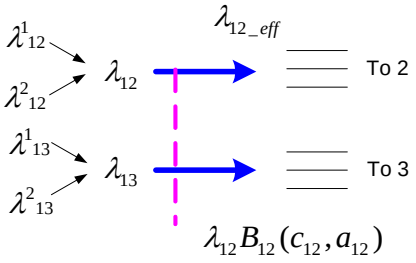

Figure 17. Queuing model of premium traffic

Premium channels are similar to trunk channels in that they are configured end-to-end as a group of wavelength-defined channels. Since real time applications usually have strict delay constraints, the arriving traffic needs a pre-assigned channel without queuing in a buffer. Therefore, we represented the channel as M/M/*c*/*c* model. In Figure 17, we assume the traffic from several providers arrive to an ingress node. The ingress node aggregates traffic, which has the same destination in the same group of wavelength channels. The number of channel varies by traffic loads. For example, calls from carriers 1 and 2 which have destination to egress node 2 ($\lambda^1_{12}, \lambda^2_{12}$) are aggregated as the total traffic demand from ingress1-egress2 (i.e., λ_{12}). We assume the call arrivals from each carrier (i.e., $\lambda^1_{12}, \lambda^2_{12}$) is Poisson process, in which call inter-arrival and holding time (service time) are exponential distributed. Since the merging of *i* independent Poisson processes with the inter-arrival time distribution $1-e^{-\lambda_i t}$ into a single process is also a

Poisson process with inter-arrival time distribution $1-e^{-\lambda_i t}$ where $\lambda = \sum_{i=1}^{m} \lambda_i$. That means $\lambda_{12} = \lambda_{12}^1 + \lambda_{12}^2$ is also Poisson process.

In general case, each ingress node associated with traffic demand pair (i, j) has arrival rate λ_{ij} , where $i \in 1,2...n$ and $j \in 1,2...n; j \neq i$. The call arrivals are placed on c wavelength channels, which can be represented by M/M/*c*/*c* model. The parameters used in performance analysis for *premium* channel are described below:

Call blocking:

Based on traffic demand (*i, j*), blocking probability of *premium* channel can be found by Erlang B model,

$$\pi_0 = \frac{1}{\sum_{n=0}^{c}\left(\frac{a_{ij}{}^n}{n!}\right)}, \qquad \pi_n = \frac{\frac{a_{ij}{}^n}{n!}}{\sum_{n=0}^{c}\left(\frac{a_{ij}{}^n}{n!}\right)}$$

Hence, the probability that the entire c_{ij} channels are occupied is given by:

$$\pi_c = B_{ij}(c_{ij}, a_{ij}) = \frac{\left(\frac{\lambda_{ij}}{\mu_{ij}}\right)^c \frac{1}{c_{ij}!}}{\sum_{n=0}^{c}\left(\frac{\lambda_{ij}}{\mu_{ij}}\right)^c \frac{1}{n!}}$$

where λ_{ij} = arrival rate of demand *(i, j)*;

$\mu_{ij} = \frac{1}{\tau}$, in which τ = average service time of calls in the wavelength channels of node (*i, j);*

c_{ij} = number of wavelength channel between node (*i, j);*

$a_{ij} = \frac{\lambda_{ij}}{\mu_{ij}}$ = offered load (Erlang), or written as: $a_{ij}(t) = \frac{1}{T}\int_0^T n_{ij}(t)dt$

$n_{ij}(t)$ = number of calls in wavelength channels at time *t*, regarding node (*i, j)*

Between any demand pair (i, j), an average overflow rate (λ_{o_ij}) is given by:

$$\lambda_{o\_ij} = \lambda_{ij} B_{ij}(c_{ij}, a_{ij})$$

In other words, λ_{o_ij} can be rewritten in terms of traffic intensity a_{ij} :

$$\lambda_{o\_ij} = a_{ij}\mu_{ij} B_{ij}(c_{ij}, a_{ij})$$

Given offered load for each demand pair a_{ij} and blocking probability B_{ij} , the numbers of wavelengths requirement for premium traffic associated with node *i* can be determined as:

Number of wavelengths at node *i*: $LP_i = \sum_j c_{ij}$ where $i \in 1,2...n$, $;\forall j \in 1,2...n-1$ $;(j \neq i)$

Total wavelengths in the network: $TP = \sum_i LP_i$, $\forall i$

<u>Carried Traffic:</u>

Since the rate of overflow traffic between node (i, j) is defined by $\lambda_{ij} B_{ij}(c_{ij}, a_{ij})$, an effective arrival rate λ_{ij_eff} is given by:

$$\lambda_{ij\_eff} = \lambda_{ij} - \lambda_{ij} B_{ij}(c_{ij}, a_{ij}) = \lambda_{ij}(1 - B_{ij}(c_{ij}, a_{ij}))$$

According to Little's Theorem, the *average number of calls* allocated in a wavelength channel between node (i, j) can be found by:

$$L_{ij} = \lambda_{ij\_eff} * W_{ij} = \lambda_{ij\_eff} * \mu_{ij}^{-1} = a_{ij}$$

where W_{ij} = mean waiting time in the system, equivalent to μ_{ij}^{-1} (only M/M/c/c);

a_{ij} = offered load or traffic intensity (Erlang) between node (i, j)

Hence, $$L_{ij} = \frac{\lambda_{ij\_eff}}{\mu_{ij}} = \frac{\lambda_{ij}}{\mu_{ij}}(1-B_{ij}(c_{ij}, a_{ij})) = a_{ij}(1-B_{ij}(c_{ij}, a_{ij}))$$

Wavelength channel *utilization* can be found by:

$$U_{ij} = \frac{\lambda_{ij\_eff}}{c_{ij}\mu_{ij}} = \frac{L_{ij}}{c_{ij}} = \frac{a_{ij}}{c_{ij}}(1-B_{ij}(c_{ij}, a_{ij}))$$

We also define wavelength saving Gain (LSG), which represents a relative wavelength saving for premium channel when the overflow channel is deployed:

$$WSG = (WL_{no\_oflw} - WL)/WL$$

where $WL_{no\_oflw} = \sum_{i}^{n} wl_i$ refers to total numbers of wavelengths deployed in the network (premium channels), wl_i is numbers of wavelengths used at ingress node *i*.

5.2 PERFORMANCE ANALYSIS ON OVERFLOW CHANNEL

In this section, we investigate the performance analysis of overflow channel. In fact, there are two alternatives to implement the overflow channel based on switching paradigms: circuit based overflow channel (section 0) and burst based overflow channel (section 5.2.2).

5.2.1 Circuit-based Overflow Channel

Figure 18, overflow traffic from premium channels is delivered in a group of OCS channels. Since the edge node pre-allocates the overflow traffic per destination, there is no waiting time for accessing the overflow channels.

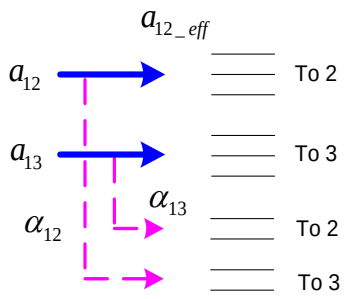

Figure 18. Overflow channel implemented by OCS

For this moment, we will focus on a blocking probability of an overflow channel, which also refers to system blocking. In other words, at a given blocking, we can find out the number of premium channels to allow the system to meet that such blocking. In order to investigate number of wavelength channels with regard to system blocking α_{b_ij} (in Figure 19), we need to employ Equivalent Random Traffic (ERT) technique proposed by Wilkinson's method [39, 51]. The ERT method is used to calculate blocking probability of a system when circuit-based overflow channel is deployed.

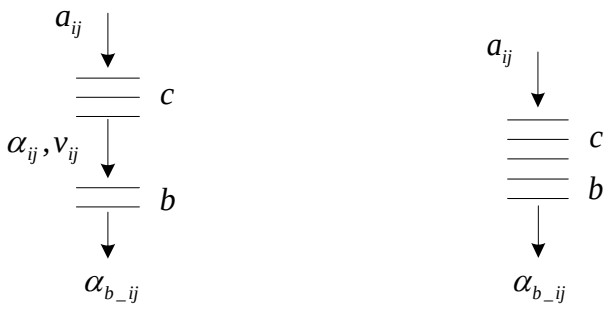

Figure 19. Blocking of the overflow channel

In Figure 19 (left), α_{ij} represents offered load of the overflow traffic from the premium channels, α_{b_ij} refers to the overflow traffic from the overflow channels (i.e., ultimate blocking). Assume the edge node *(i,j)* has traffic demand with the offered load a_{ij}, the offered traffic is assigned to the *c* premium channels and the overflow traffic is assigned to *b* overflow channels, in which the overflow traffic is characterized by α_{ij} and v_{ij}

$$\alpha_{ij} = a_{ij} * B_{ij}(c_{ij}, a_{ij})$$

The blocking probability B at the overflow channel is given by:

$$B = \frac{\alpha_{b\_ij}}{\alpha_{ij}}$$

One can see that the overflow blocking *B* does not equal Erlang-B based on the secondary trunks. That is $B \neq \alpha_{ij} * B_{ij}(b_{ij}, \alpha_{ij})$.

It is the matter of fact that $B > \alpha_{ij} * B_{ij}(b_{ij}, \alpha_{ij})$ because the overflow traffic is non Poisson distributed, which is more bursty than the regular Poisson arrival.

According to the overflow theory, the ultimate blocking calls α_{b_ij} is equivalent to the blocking of the same offered load to the combined trunks (see the right figure) which can be written as:

$$\alpha_{b\_ij} = a_{ij} * B_{ij}((c_{ij} + b_{ij}), a_{ij})$$

In the specific case of several independent types of premium trunk group (several data rate of premium traffic), the parameters of equivalent overflow traffic to the overflow channel is given by:

$$a_{ij}^{*} = \sum_{k}^{m} a_{k\_ij} \, , v_{ij}^{*} = \sum_{k}^{m} v_{k\_ij}$$

5.2.2 Burst-based Overflow Channel

In this case, the fluctuated traffic from the premium channel is handled by OBS channel, in which the overflow calls (i.e., bursty traffic) will be sampled and quantized to be compatible with burst-based channel. The overflow traffic parameters are derived from three-moment method discussed earlier. In this section, we will investigate performance analysis of overflow system implemented by OBS shown in Figure 20. An arrival process of the system is defined as overflow calls from the premium channel which are very bursty (i.e., Off-On traffic). In addition, the traffic coming off the burst buffer is also bursty. Since both arrival and departure processes are not Poisson distributed, we propose G/G/1 queuing model to represent our overflow channel. In order to solve G/G/1 for numerical results, we will investigate the stochastic processes by Matrix-Geometric approach (i.e., phase type model Ph/Ph/1). We further provide comprehensive analysis on overflow channel into three subsections: arrival process (5.2.2.1), departure process (5.2.2.2), and overflow system (5.2.2.3).

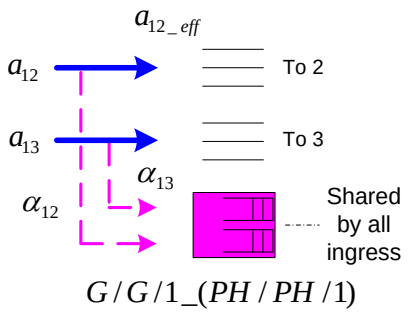

Figure 20. Overflow channel implemented by OBS

5.2.2.1 Arrival process of OBS overflow channel

Since the overflow traffic from premium channels is a renewal process, an arrival process of the overflow system is represented as IPP, consisting of ON and OFF states with parameters $\omega, \gamma, \lambda_{on}$ (mentioned in section 4.4)

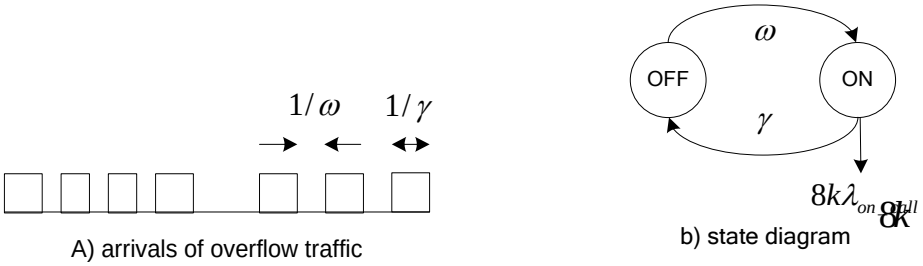

Figure 21. Arrival process of the overflow channel system

Figure 21 a) illustrates arrivals of overflow traffic with mean time between ON and OFF state as γ^{-1} and ω^{-1} respectively, which corresponds to a state diagram in Figure 21 b). OFF state refers to the call arrivals are being transmitted into premium channels (between ingress-egress).

While, ON state represents all premium channels are fully occupied, in which the new call arrivals will be performed A-D conversion before delivery in the overflow channel with ON state call arrival rate $\lambda_{on\_call} = A_{on} * \mu_{ocs}$, in which all IPP parameters (i.e., ω, γ, A_{on}) are derived from matching of the three moments (explained in 4.4). Regarding the state diagram in Figure 21b), we can calculate stationary probability and mean arrival rate of the overflow traffic as the follows:

A transition probability matrix Q is given by:

$$Q = \begin{bmatrix} -\omega & \omega \\ \gamma & -\gamma \end{bmatrix}$$

Based on steady state approach, a stationary probability is obtained by $\pi Q = 0$

$$\begin{bmatrix} \pi_{off} & \pi_{on} \end{bmatrix} \begin{bmatrix} -\omega & \omega \\ \gamma & -\gamma \end{bmatrix} = 0$$

which is written in linear equation expressions as follows:

$$-\omega\pi_{off} + \gamma\pi_{on} = 0$$

$$\omega\pi_{off} - \gamma\pi_{on} = 0$$

From the first linear equation, the probability of overflow state $\pi_{on} = (\omega/\gamma) * \pi_{off}$

From $\pi e = 1$, we have

$$\pi_{off} + (\omega/\gamma) * \pi_{off} = 1$$

Hence,

$$\pi_{off} = \frac{\gamma}{\omega + \gamma}$$

$$\pi_{on} = \frac{\omega}{\omega + \gamma}$$

Finally, the stationary probability vector π is given by:

$$\pi = [\pi_{off}, \pi_{on}] = \left[\frac{\gamma}{\omega+\gamma} \quad \frac{\omega}{\omega+\gamma} \right]$$

Mean overflow rate (calls/sec) can be calculated as:

$$Mean\_rate = \sum_i \lambda_i \pi_i = \lambda_{on}\pi_{on} + \lambda_{off}\pi_{off} = \lambda_{on\_call} \frac{\omega}{\omega+\gamma}, where\ \lambda_{off} = 0$$

At a given time interval [0, t], the average number of arrivals in a certain period N_t can be calculated as $E[N_t] = \left[\frac{\lambda_{on\_call}\omega}{\omega+\gamma} \right] * t$

Bustiness of overflow traffic is defined by:

$burstiness = \frac{peak}{mean} = \frac{\omega}{\omega+\gamma}$, where peak equals to λ_{on_call}

$$overflow\_iterarrival = \frac{1}{\omega} + \frac{1}{\gamma}, mean\_holding = 1/\gamma, mean\_silent = 1/\omega$$

In our proposed overflow channel, the overflow calls will be digitalized (sampling at 8 kHz with 8 bits encoding/sample). Hence, the *Mean overflow rate* (in calls/second) mentioned earlier must be converted to a unit of bits/second as follow:

$$\lambda_{overf} = 8k * \lambda_{on\_call} \frac{\omega}{\omega+\gamma} \text{ Bytes/sec}$$

$$= 64k * \lambda_{on\_call} \frac{\omega}{\omega+\gamma} \text{ bits/sec}$$

Note that λ_{on_call} is equivalent to $A_{ij} * \mu_{OCS\_ij}$,

where A_{ij} = an offered load of overflow traffic between edge node *i* and *j*, (obtained by the three moments matching), μ_{OCS_ij} is a service rate (call/sec) of premium channel between edge node *i* and *j*.

Now, considering an example of calculations for an overflow arrival rate with two different approaches (direct calculation vs. IPP matching):

In Figure 14, 24 calls (2 calls blocked) are allocated to a premium channel, in which each call requires 64kbps transmission rate. Assume each premium (wavelength) channel has capacity of 1.544 Mbps (using small capacity to clarify the calculation). Also, assume call arrival rate, λ is 4 calls/sec and average call duration is 120 seconds. Considering performance analysis in the wavelength channel (i.e., 1.544 Mbps link) which can carry 24 DS-0 calls simultaneously, time for each call spending in optical switching fabric is $T = \frac{120}{24} = 5\,\text{sec}$ or $\mu = \frac{1}{T} = 0.2\,\text{calls/sec}$. The offered load is found by, $a = \frac{\lambda}{\mu} = \frac{4}{0.2} = 20E$. In practice, an optical wavelength channel can start from 2.5 Gbps link (OTU-1) for an optical transport unit according to G.709. Hence, Sojourn time in the channel would be $T = \frac{120}{1000 * 24} = 0.005$ sec.

Considering the overflow system, the overflow traffic (traffic intensity) is given by:

$$\alpha_{ij} = a_{ij} * B_{ij}(c_{ij}, a_{ij}) = 20 * B(1,20)$$

The overflow rate (calls/sec) can be found by:

$$\lambda_{overfcall} = \alpha_{ij}\mu_{ij} = a_{ij}\mu_{ij}B_{ij}(c_{ij}, a_{ij}) = 20 * 0.2 * B(1,20)$$

Since the overflow calls are digitized (sampled and encoded), mean overflow rate will be:

$$\lambda_{overf} = 8k * \lambda_{overfcall} = 8*10^3 * 20 * 0.2 * B(1,20) = 30.46 \text{ Btyes/sec}$$

$$= 243.71 \text{ kbps}$$

However, the overflow mean rate (sample/sec) can be found by another approach based on IPP parameters:

$$\lambda_{overf} = 8k * \lambda_{on\_call} \frac{\omega}{\omega + \gamma} = 8k * A_{ij} \mu_{OCS\_ij} * (\frac{\omega}{\omega + \gamma}) \text{ Btyes/sec}$$

5.2.2.2 Departure process of OBS overflow channel

Now, we consider behavior of burst departure from OBS buffer to an overflow channel. According to traffic aggregation and burst reservation explained in 4.3.2, a departure process of the overflow channel can also be considered as IPP shown in Figure 22.

Figure 22. Departure process of an OBS overflow channel

where $T_{buffout}$ refers to aggregating duration for a burst,

t_{off} refers duration when no burst transmission,

t_{on} refers time used to transmit a burst given by $t_{on} = \frac{\overline{burst\_size}}{\mu_{OBS}}$.

μ_{OBS} represents OBS burst rate in bits/sec

In fact, a burst size $(\overline{burst\_size})$ aggregated in the buffer depends on overflow arrival rate λ_{on} and buffer timeout. Hence, an average burst size (Bytes) can be written as the following function: $\overline{burst\_size} = f(\lambda_{on}, T_{buffout}) = \lambda_{on} * T_{buffout}$,

where $\lambda_{on} = 8k * \lambda_{on\_call}$ Bytes/sec

Hence, $t_{on} = \dfrac{\overline{burst\_size}}{\mu_{OBS}} = \dfrac{8k * A_{on} * \mu_{OCS} * T_{buffout}}{\mu_{OBS}}$ where A_{on} is derived from Kuczura's IPP approximation; μ_{OCS} is based on calls/sec; μ_{OBS} is based on Bytes/sec.

According to Figure 22b), $t_{off} = t_{buffout} - t_{on}$

Again, we perform the same steps as earlier to investigate queuing analysis of the departure process.

Let Q is the transition probability matrix of departure IPP

$$Q = \begin{bmatrix} -1/t_{off} & 1/t_{off} \\ 1/t_{on} & -1/t_{on} \end{bmatrix}$$

Based on the steady state approach, the stationary probability is obtained by $\pi Q = 0$

$$[\pi_{off} \quad \pi_{on}] * \begin{bmatrix} -1/t_{off} & 1/t_{off} \\ 1/t_{on} & -1/t_{on} \end{bmatrix} = 0$$

The linear equation expressions are:

$$-(1/t_{off})\pi_{off} + (1/t_{on})\pi_{on} = 0$$

$$(1/t_{off})\pi_{off} - (1/t_{on})\pi_{on} = 0$$

From the first linear equation, $\pi_{on} = (t_{on} / t_{off}) * \pi_{off}$

From $\pi e = 1$, we have

$$\pi_{off} + (t_{on} / t_{off}) * \pi_{off} = 1$$

Hence, $$\pi_{off} = \frac{t_{off}}{t_{off} + t_{on}}$$

and $$\pi_{on} = \frac{t_{on}}{t_{off} + t_{on}}$$

Finally, the stationary probability vector π is given by:

$$\pi = [\pi_{off}, \pi_{on}] = \left[\frac{t_{off}}{t_{off} + t_{on}} \quad \frac{t_{on}}{t_{off} + t_{on}} \right]$$

Mean burst rate can be calculated as:

$$Burst\ rate = \sum_i \lambda_i \pi_i = \mu_{off} \pi_{off} + \mu_{OBS} \pi_{on} = \mu_{OBS} \frac{t_{on}}{t_{off} + t_{on}},$$

where μ_{OBS} is a peak burst rate

At a given time interval [0, t], the average number of bits in a certain period N_t can be calculated as:

$$E[N_t] = \left[\mu_{OBS} \frac{t_{on}}{t_{off} + t_{on}} \right] * t$$

Bustiness of overflow traffic is defined by:

$burstiness = \frac{peak}{mean} = \frac{t_{on}}{t_{off} + t_{on}}$, where peak equals to μ_{OBS}

$$burst\_iterarrival = t_{off} + t_{on}, mean\_holding = t_{on}, mean\_silent = t_{off}$$

5.2.2.3 Overflow channel system PH/PH/1

In this section, we propose a queuing model to analyze a performance of an overflow channel. In Figure 23, we integrate the arrival process (in section 5.2.2.1) and the departure process (in section 5.2.2.2) to represent the overflow channel. The system consists of two sets of stochastic processes (i.e., IPP) which can also transform to a specific case of G/G/1 queuing system (i.e., PH/PH/1).

In our queuing analysis, the calculation is based on Matrix-Geometric approach in order to obtain numerical results.

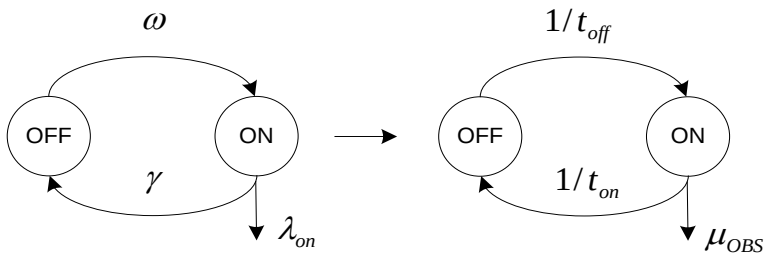

Figure 23. Representation of overflow system PH/PH/1

Firstly, we discuss a Phase Type representation $PH(\alpha, T)$, consisting of IPP parameters.

Considering the arrival process (left figure), the Phase Type process $Y(\alpha, T)$ has the following parameters:

$$\alpha = [0 \quad 1], \qquad T = \begin{bmatrix} -\omega & \omega \\ \gamma & -(\gamma + \lambda_{on}) \end{bmatrix}, \qquad T^0 = -Te = \begin{bmatrix} 0 \\ \lambda_{on} \end{bmatrix}$$

where α is an initial probability vector for a PH arrival process,

T is a generator matrix of non-absorbing arrival states,

$$\lambda_{on} = 8k * A_{on} * \mu_{OCS} \text{ Bytes/sec}$$

Secondly, the burst departure process (right figure) can be written in a Phase Type representation $X(\beta, S)$ with the following parameters:

$$\beta = [0 \quad 1], \qquad S = \begin{bmatrix} -1/t_{off} & 1/t_{off} \\ 1/t_{on} & -(1/t_{on} + \mu_{OBS}) \end{bmatrix}, \; S^0 = -Se = \begin{bmatrix} 0 \\ \mu_{OBS} \end{bmatrix}$$

where β is an initial probability vector for the PH departure process,

S is a generator matrix of non-absorbing departure states,

μ_{OBS} is the service rate of the optical burst switch (Bytes/sec)

When all parameters in both phase type representations are identified, a queuing analysis of the overflow system (i.e, utilization, delay, and throughput) can be calculated by using Matrix-Geometric method.

5.3 RESULTS OF PREMIUM AND OVERFLOW CHANNEL

In this study, we start to investigate a performance analysis in the primary channel corresponding to following parameters (i.e., blocking, utilization). At a given traffic intensity of premium traffic between a particular pair of edge nodes (*i, j*), number of wavelength channels (i.e., OTU-1 units) are varied to investigate the utilization and blocking in the channel. In fact, the traffic intensity is equivalent to call arrival rate compared to service rate in which, an OTU-1 unit can carry. In a case of 5E, it represents call arrival at a rate of 1344 calls/second with 2 minutes holding time

transported in an OTU-1 channel (i.e., 2.5 Gb/s capacity containing 32256 calls). We plot four different cases regarding traffic intensities (i.e., 5E, 10E, 20E, and 30E) shown in Figure 24.

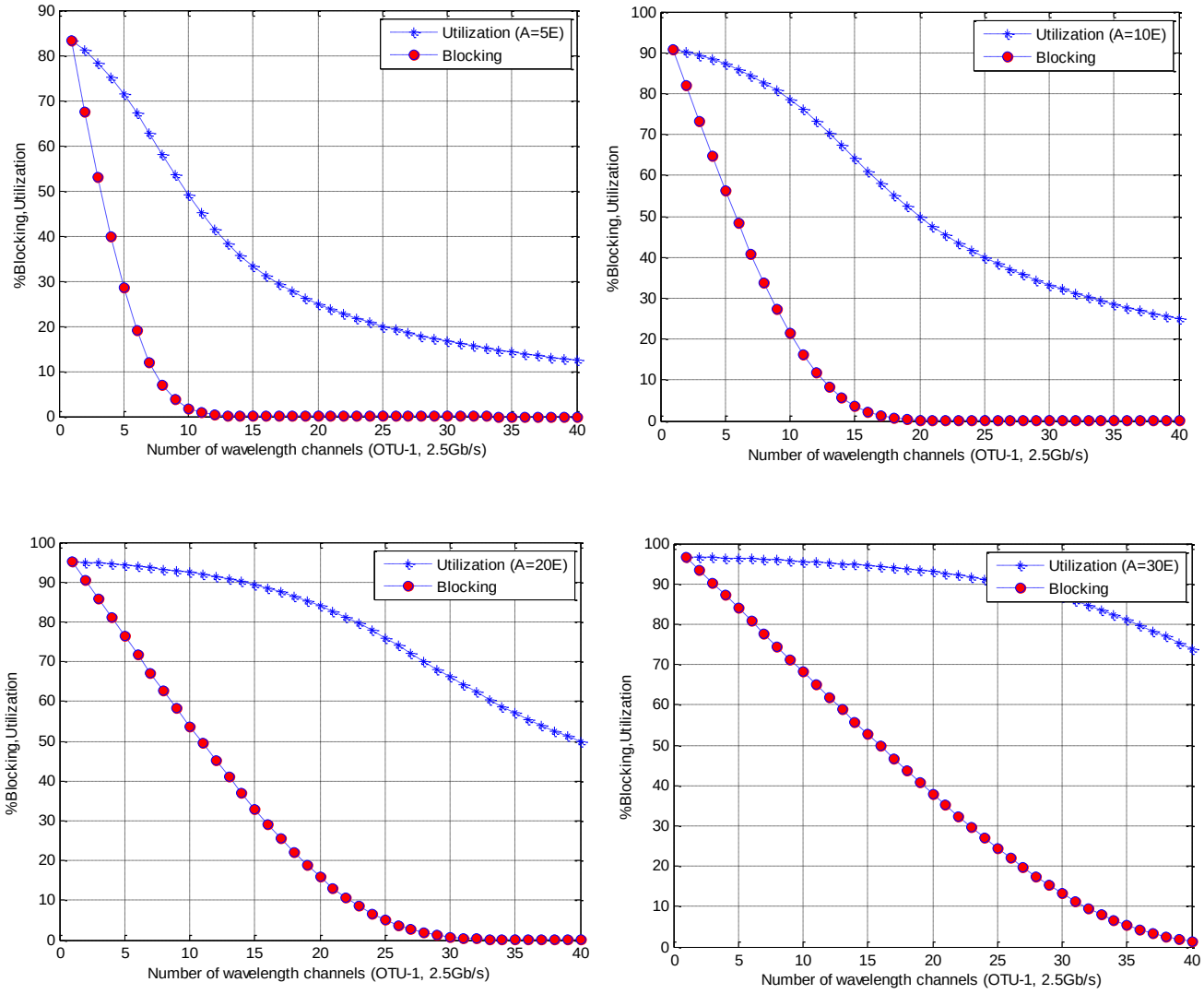

Figure 24. Performance analysis based on OTU-1 channels in premium channels

For a case of 10E, the ingress node requires 17 channels (i.e., OTU-1 line cards) in order to keep blocking less than 1%, between ingress-egress nodes. However, the utilization drops to 58%, which is quite low for a realistic implementation. On the other hands, if the node decreases channels to achieve higher utilization at 70%, the blocking will be 9% (pretty high). Therefore, we should take consideration on both parameters in the same time. In a case of higher traffic load (e.g., 20E), both parameters will be relatively acceptable, the utilization and blocking are 70% and 1.5% respectively based on 28 channels. In this case, all optical resources are pre-allocated between each node pair. As a result, the arrival traffic will be delivered in one of available channels suddenly without waiting in a buffer (no queuing delay). However, minimal delay occurs at edge node from aggregation process given by μ^{-1}.

In conclusion, an ingress node is able to lower blocking levels as an increase of wavelength channels (OTU-1 units). However, the utilization will drop as number of channels increases. In other words, the node needs some extra reserved capacity for fluctuated traffic (over provisioning) to avoid higher blocking situation. These results from a coarse granularity of optical wavelength channel. However, this circuited-based channel provides beneficial characteristics including no queuing and processing delay; also throughput guarantee.

5.3.1 Number of Wavelength Assignment at Variation of Offered Load

Regarding the previous section, the blocking probabilities based on a particular case of offered load (i.e., a=5, 10, 15, 20, 25 Erlang) are plotted on the same chart for a comparison purpose. We investigate the blocking over several numbers of wavelength channels ranging from 1 to 40.

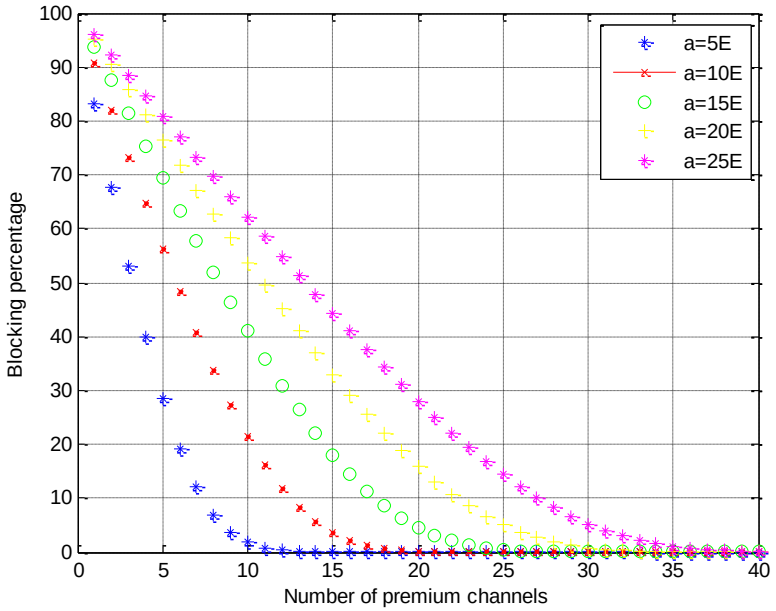

Figure 25. Wavelength assignment for premium channel

From Figure 25, an ingress node will dynamically adjust a number of OTU-1 units as current traffic intensity. For instance, in the case of 5 Erlang offered load with 1% blocking guarantee, the ingress node needs to reserve at least 12 dedicated wavelengths to the egress node. If the average traffic in a certain period of time increases to 10 Erlang, the ingress node requires 18 dedicated wavelengths to keep the same blocking level. This means the ingress node requires establishing six additional wavelength channels. Specifically, the paths for wavelength channel throughout the network are performed by GMPLS signaling protocol.

5.3.2 Effect of Optical Rate Toward Overflow Traffic and Utilization

We provide an analysis on optical transmission rate of the premium channel toward channel utilization and overflow traffic. In this study, we fix call arrival rates to 1344 calls/sec and vary numbers of wavelength channels to investigate utilization and overflow rate associated with number of assigned channels. Instead of changing traffic intensity (as earlier), the transmission rate of optical transport unit is varied (i.e., 1.25 Gb/s, 2.5 Gb/s, 10 Gb/s, and 40 Gb/s). In addition, the number of wavelength channels is varied from 1 to 20.

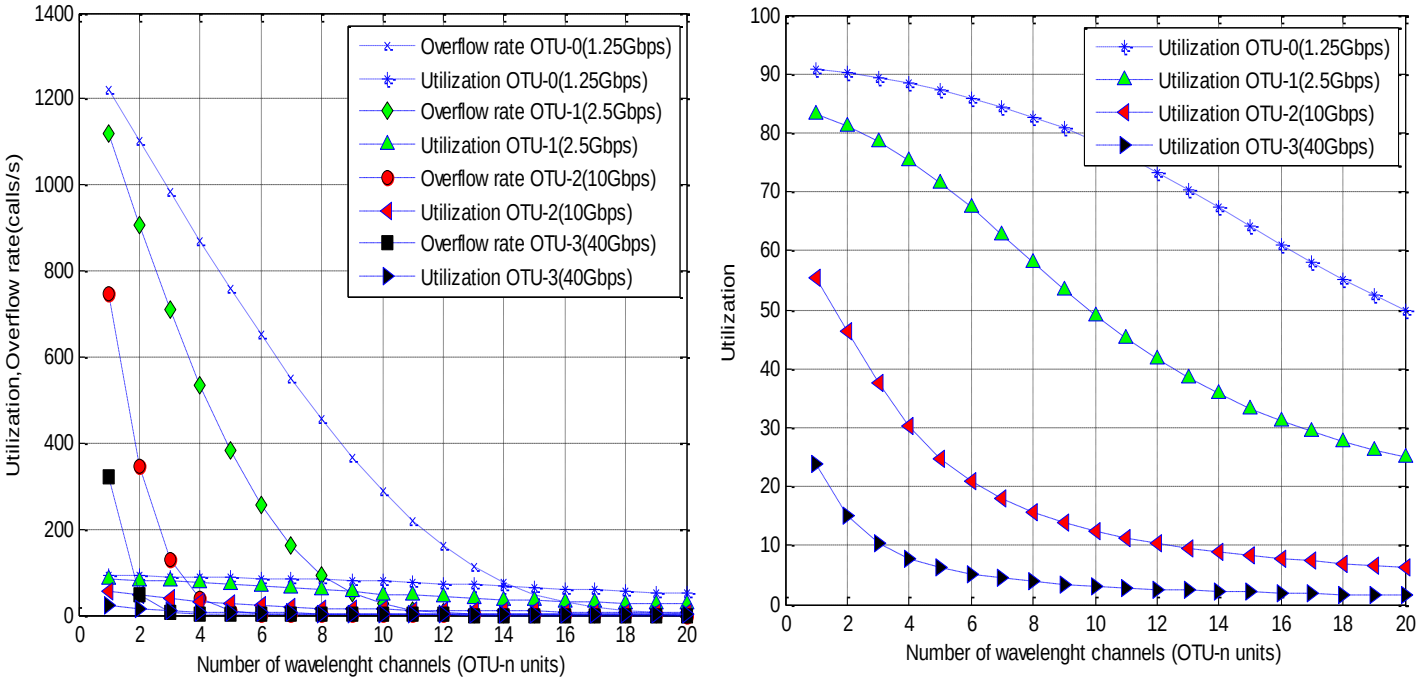

Figure 26. Effect of transmission rates of wavelength channel: a) overflow rate b) utilization

Figure 26 shows a comparison of overflow traffic and utilization at different transmission rates, corresponding to each type of OTU-n. Regarding the utilization plot of OTU-1 (2.5Gbps), one can see that the overflow rate is approximately 900 calls/sec for two units of OTU-1. The overflow traffic will decrease if the node increases the number of channels or the transmission rates in premium channels. For instance, if the ingress node needs to maintain the overflow traffic lower than 400 calls/sec, the node may either allocate the traffic to higher rate ports (i.e., 2 of OTU-2), or assigns 3 additional OTU-1 units (i.e., 5 units totally). In the case of increasing the rate (i.e., 2 units of OTU-2), the utilization is relatively low which is 46% compared to 71% for adding more cards (i.e., 5 units OTU-1). However, the selection between those two options may include cost criteria as well (but not in our research study).

The overflow rate mention earlier is obtained from the mean departure rate of the overflow process, which actually weights between two states: ON-OFF. Based on Poisson distribution's properties, the mean shall be equivalent to the variance. Also, the *Burstiness* (z) must be 1, which represents the ratio of the variance to the mean. We plot the *Business* of the overflow traffic at different offered traffic varied by number of premium channels depicted in Figure 27, which obviously shows non-Poisson distributed characteristic.

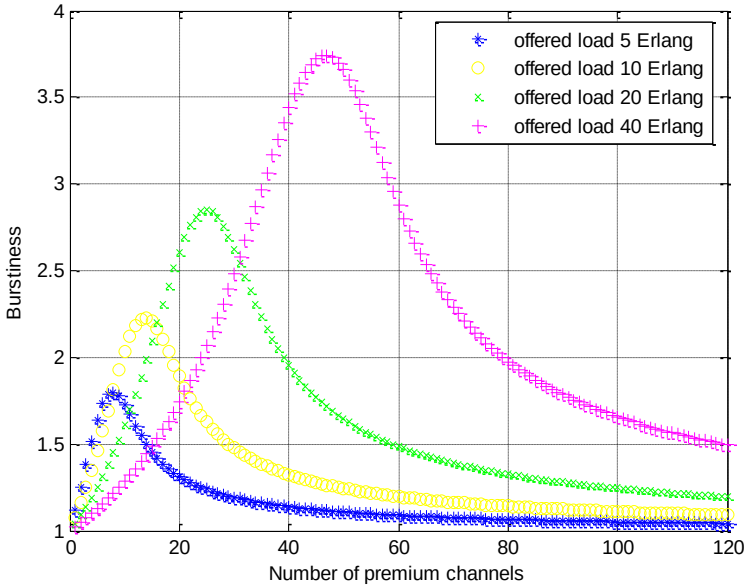

Figure 27. Burstiness of overflow vs. the premium channels

Regarding the Figure 27, most of the time, *z* is greater than 1 (i.e., bursty), and reaches the peak when the number of channels is approximately the offered load (a). One can notice that at very small number of channels ($c \approx 0$), the overflow traffic almost equals to Poisson distributed ($z \approx 1$) which means the majority of the traffic is not delivered in the premium channel (overflows to the overflow channel). On the other hands, at a large number of channels, *z* is close to 1 which represents the majority of the offered traffic is transmitted in the premium channel (i.e., minimal overflow traffic or less bursty traffic).

5.3.3 Verification of the Overflow Traffic

In order to verify the numerical results of the overflow traffic used in G/G/1 queuing analysis, we compare the results between two different methods. The first case, the overflow traffic is calculated based on Riordan formula:

$$\alpha_{ij} = a_{ij} B(a_{ij}, c_{ij}), v_{ij} = \alpha_{ij}\left[1 - \alpha_{ij} + \frac{a_{ij}}{c_{ij} + 1 + \alpha_{ij} - a_{ij}}\right], z_{ij} = v_{ij} / \alpha_{ij} .$$

Regarding the second approach, the mean overflow offered traffic is derived by our analysis in section 5.2.2.1

$$Mean\_offered = a_{on}\frac{\omega}{\omega + \gamma}$$

$$burstines = \frac{peak}{mean} = \frac{\omega}{\omega + \gamma}$$

where ω, γ are adopted from IPP parameters. In other words, the first three moments are calculated based on the number of wavelengths and given offered load, and then mapping the moments to IPP parameters. Finally, we apply the steady state approach to obtain mean rate of IPP. The corresponding results are shown in Figure 28.

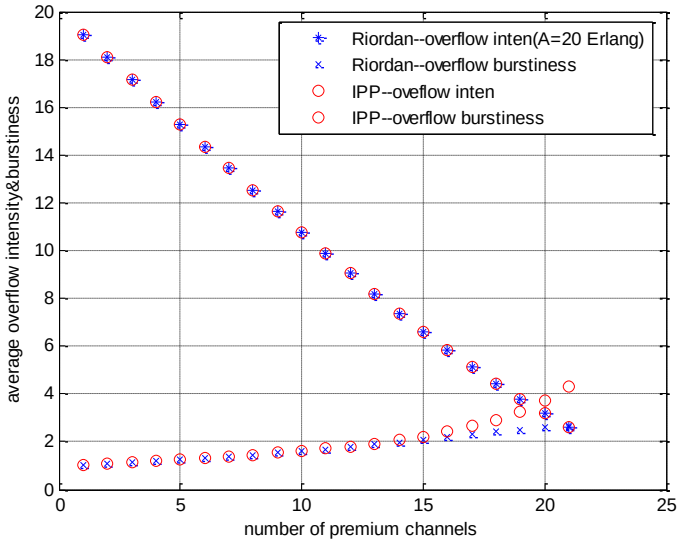

Figure 28. Verification of overflow traffic (Riordan and IPP)

The results show convergence of two different approaches: steady state vs numerical analysis associated with the overflow theory. For the numerical analysis, we will this approach later for the arrival process of overflow channel.

5.3.4 Premium Channel Assignment and Overflow Arrival Process

In this section, we investigate characteristics of the traffic, which overflows from the primary channel (i.e. OTU-1). The study of burst parameters including inter arrival time, service time, and silent time are calculated based on IPP (in 5.2.2.1). Regarding the analysis, we fix offered load in the primary channel; but vary number of wavelength channels. In fact, the offered load (i.e., traffic intensity) is associated with call arrival rate and the link capacity of the primary

channel. We will perform the analysis with two different traffic intensities (e.g., A=10, 20) based on OTU-1 wavelength channel.

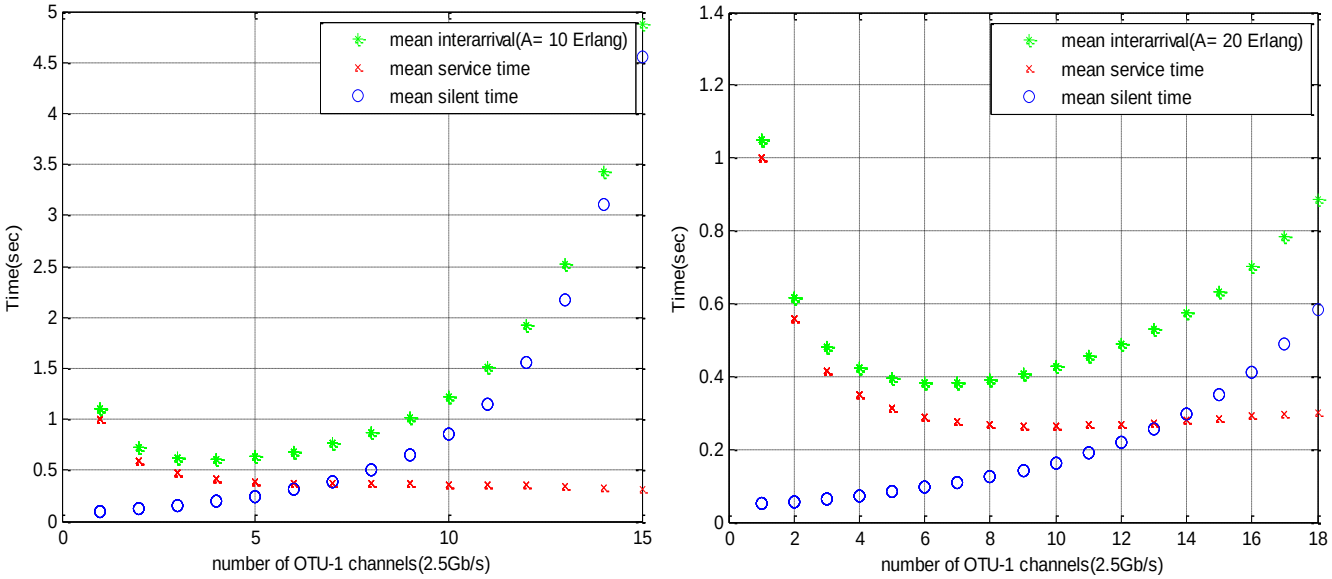

Figure 29. Inter-arrival time of the overflow traffic

In Figure 29, as numbers of wavelength channels (i.e, OTU-1) increase, average inter-arrival times between overflow calls are larger. While, service times remain relatively the same. In other words, overflow traffic decreases as the number of primary channels increases. One can notice a reversed trend of inter-arrival time when OTU-1 channel equals one, 2 (A=10 case) which is associated with Hyper exponential distributed. This can be explained as both service and inter-arrival times increase, resulting in smaller silent gap. In other words, high traffic volume goes to the overflow channel since the premium channels are fully occupied for most of the time. Regarding a higher traffic case, (i.e, A=20), all parameters provide the same trend as in

the lower case (A=10). However, the inter-arrival time is shorter at the same number of primary channels, representing higher traffic intensity flowing to the overflow channel.

5.3.5 Aggregation Delay in the Overflow Channel

In this study, we investigate how overflow traffic from the primary channel will experience queueing delay in the overflow channel employing timeout-buffering scheme. At a given offered load (i.e., traffic demand) in the premium channel and a given buffer timeout of overflow channel, we investigate a relationship between burst aggregation delay in overflow channel versus parameters in primary channel (i.e., utilization and blocking) based on certain traffic demands in the premium channel.

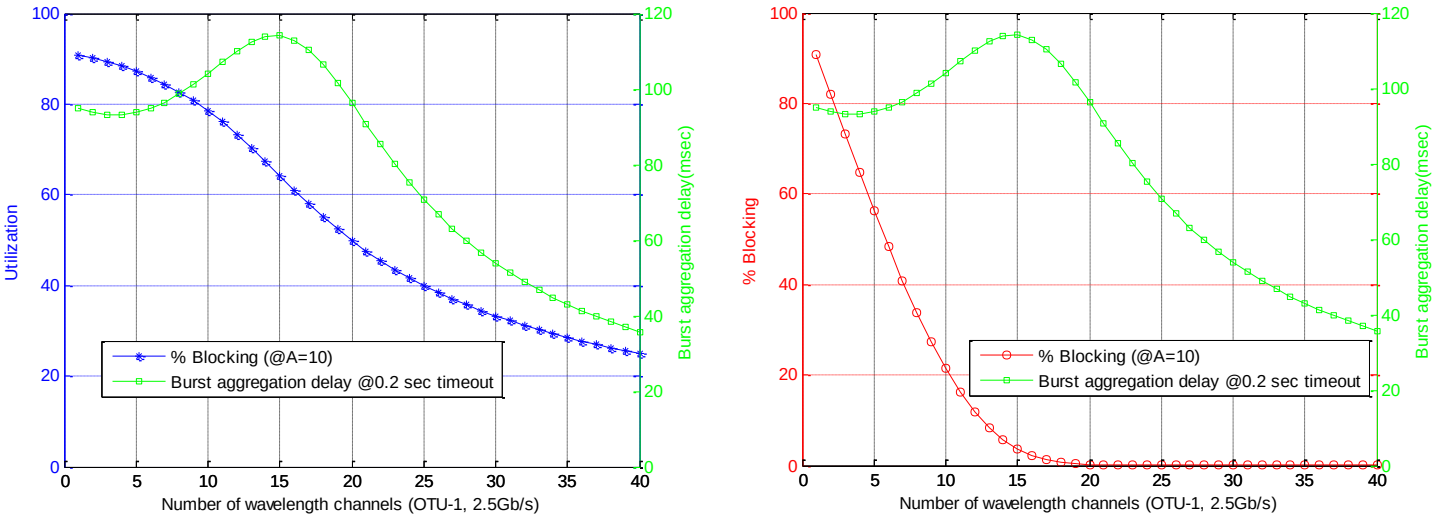

Figure 30. Burst aggregation delay in overflow channel versus a) utilization and b) blocking

Regarding plots in Figure 30, we assume traffic intensity is 10 Erlang between the demand pair with respect to OTU-1 (2.5 Gb/s) wavelength channel. For the overflow channel, the edge node deploys timeout-buffering scheme (i.e., 200 millisecond).The results illustrate that in primary channel, the increase of wavelength channel allows decrease in both utilization (see Figure 30a) and blocking probability shown in Figure 30b). In overflow channel, burst aggregation delay drops as increase of wavelength channel since the overflow traffic decreases as number of primary channel increases. However, one can see the delay plot has a "bump" in a short period (i.e. 15 channels), which is due to the bursty characteristics of the overflow traffic as depicted in Figure 27. Based on 10 Erlang, the burstiness has a peak corresponding to 15 channels. In fact, the network edge node needs to justify the number of premium channels in order to increase the utilization in the premium channel while, maintain the acceptable delay in the overflow channel.

5.3.6 Effect of Buffer Timeout on Aggregation Delay

In this section, we study how buffer timeout affects waiting time of the overflow data during burst aggregation (i.e., aggregation delay). The study starts with a given particular buffer timeout in the overflow queue (e.g. 100 millisecond) with the following initial parameters: traffic intensity A=10 (primary channel) associated with OTU-1 rate, burst service rate is 1 GB/sec. Then, we plot average delay of sampled data in the burst queue at different numbers of premium channels (OTU-1 units). We repeat the same procedure for different buffer timeouts to investigate an effect on the aggregation delay.

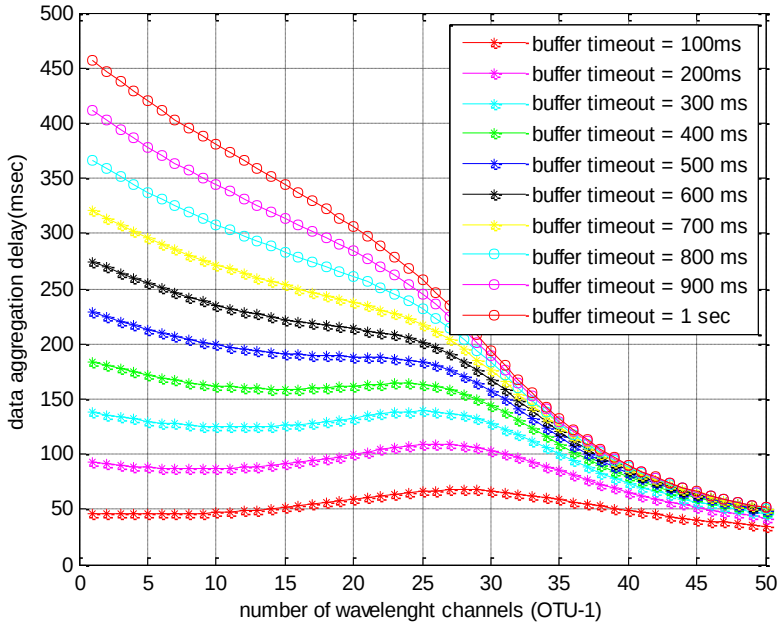

Figure 31. Aggregation delay affected by buffer timeout

Figure 31 illustrates aggregation delay of sampled data versus number of wavelength channels ranging from 1-40. Considering a particular case of 400 msec buffer timeout, the highest average delay is approximately 200 msec, based on 10 wavelength channels. Typically, the average delay decreases as the increase of wavelength channels. Nevertheless, one can notice that the curve has a reserved trend for a period of time (i.e., 9-13 channels based on 400 msec) which is affected by arrivals of the overflow traffic. However, the reversed trend will vanish if the buffer timeout is longer which can alleviate traffic congestion in the queue. Regarding buffer timeouts comparison, the larger timeout in the buffer, the longer aggregation delay added in the overflow channel. The delay is never more than 50% of the timeout.

Regarding delay-sensitive applications, end-to-end delay is the most stringent QoS parameters. In order to satisfy the delay constraint, the node needs to assign enough wavelength

channels for primary channel. For instance, a given 200 msec buffer timeout, the ingress node requires 23 reserved channels (primary channels) to satisfy 80 msec aggregation delay in overflow channel. In the case of 300 msec, the node requires 26 channels to achieve at least the same aggregation delay.

5.3.7 Optical Wavelength Saving Gain Comparison

Regarding the above analysis, the edge node can determine the number of wavelength channels employed for each traffic demand pair (ingress-egress) according to the delay and utilization requirement. The efficient use of wavelength channel is analyzed via the decrease ratio of wavelength channel assignment defined as "optical wavelength saving gain." The numbers of wavelength channels assigned for the offered traffic primary channel are compared between the case of with and without OBS overflow channel deployment wavelength saving gain is defined to measure the benefit of overflow channel deployment with the respect to several levels of queuing delay allowance at the overflow aggregation process shown in Figure 32.

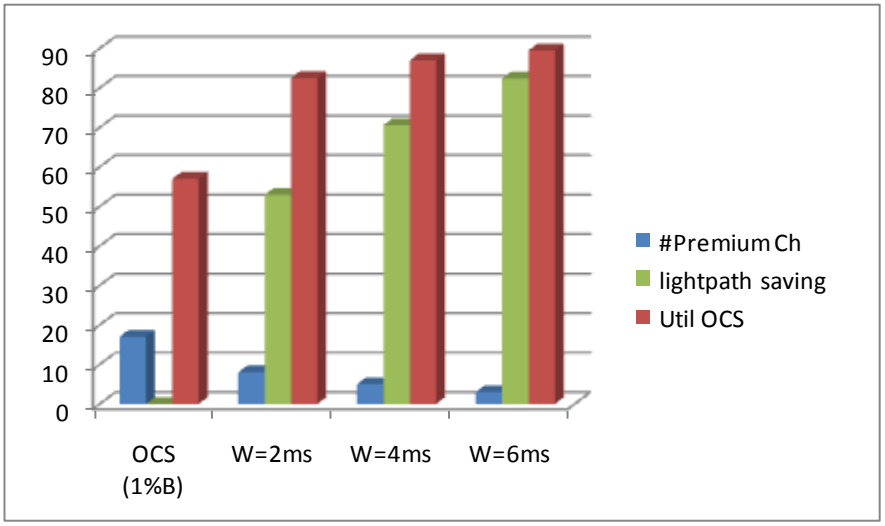

Figure 32. Wavelength saving gain

Figure 32 shows the number of wavelength channels need to assign for each demand pair at a given offered load when there is no overflow channel. In order to satisfy QoS level at 1% blocking, the edge node requires 17 wavelengths for primary channel without the OBS overflow channel. When the OBS overflow channel is deployed, the primary wavelength channel can be reduced to 8 wavelength channels with the respect of 2 msec delay allowance at the overflow aggregation process. In addition, it can be even further reduced to 3 channels according to 6 msec delay. Regarding the wavelength saving gain, the network achieves higher gain as the increase of delay tolerance according to the traffic demand. However, the higher aggregation delay will contribute to the end-end network delay, which will excess the QoS requirement for particular application.

5.3.8 Utilization Improvement on Optical Wavelength Channels

The deployment of overflow channel also increases the utilization in the premium channel. In order to measure the efficiency of wavelength assignment, the utilization gain in the wavelength channel is defined. The utilization in the premium channel is investigated, then we compared those in two cases: with and without overflow channel deployment. The utilization gain has been studied at several values of delay allowance at a given offered load (i.e., A=10E) and the overflow buffer timeout is set to 8 msec. shown in Figure 33.

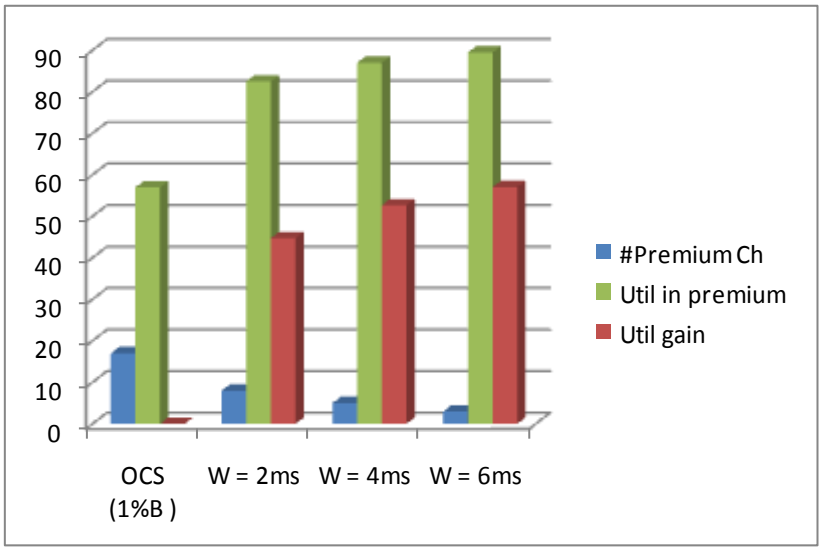

Figure 33. Utilization gain in premium channel

We found that the network could further decrease number of premium channels, if we accept higher aggregation delay (i.e., higher delay tolerance). The efficient use of premium channel is obtained via the decrease of wavelength channels. The utilization increases to 82.5%

of the channel capacity in the case of 2 msec. delay tolerance which obtains 44.7% utilization gain. In the case of 6 msec. delay tolerance, the premium channel is more efficiently used almost up to 90% of the link capacity (i.e., 57% gain). However, there will be some tradeoffs between the capacity utilization and the delay requirement for traffic demands. Therefore, the policy on the wavelength channel assignment is required to concern for both network performance parameters.

6.0 PERFORMANCE ANALYSIS OF SECONDARY CHANNEL

DHON is an optical transport system serving as a national backbone network, which is able to support various types of traffic in a single platform. Besides the premium channel, the secondary channel carries data-oriented traffic, aggregated in a buffer and transported in shared optical resources in order to achieve higher utilization. For example, content delivery network (CDN), which handles various forms of traffic, could deploy secondary channel to deliver its traffic from one data center to the others located throughout the nation. In other words, DHON ingress node is located at a regional data center, which aggregates traffic from various operators' gateways, and connects to the other data center via smart-gird wavelength channel deployment. In this dissertation, we assume control part associated with wavelength channel allocation in core layer, DCA (dynamic capacity allocation), is not in the scope of our research.

In this chapter, we develop mathematic model to represent the system of the secondary channel. Later on, we evaluate the results of network performance in certain traffic environments. Figure 34 illustrates the only the secondary channel deployment in DHON. On the left site located in city A, the video and data traffic from various gateways are aggregated in associated buffers before delivery to the other data center located in city B.

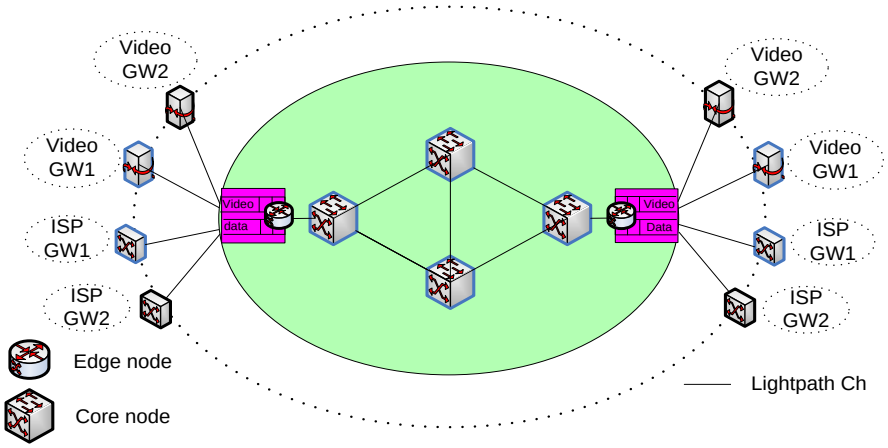

Figure 34. Secondary channel of DHON connecting between ingress and egress nodes

The ingress node (in site A) aggregates all traffic types, which has the same destination egress node in the same wavelength channel. Each ingress nodes employs two classes of buffers: Class I, delay sensitive traffic (e.g., video) and Class II, non-delay sensitive traffic (e.g., best effort applications). In fact, the ingress node aggregated video and data traffic in separate buffers.

This chapter is organized as the following subsections: performance analysis of traffic separation (in section 6.1), performance analysis of traffic mixture of traffic (in section 6.2), performance results, and evaluations (in section 6.3), and performance comparisons: DHON vs. IP/DWDM (in section 6.5).

6.1 PERFORMANCE ANALYSIS OF TRAFFIC CLASSIFICATION

In this section, the ingress node aggregates each traffic type in a particular buffer and the network will allocate the aggregated traffic in a particular wavelength channel without mixing. In other words, the traffic inside the secondary channel is homogenous. However, we will discuss mixed traffic in the same channel later.

In fact, video traffic will be a majority of future traffic in the backbone network due to popularity of HD video streaming applications (e.g., YouTube, Netflix). In our research, we consider video traffic as an example of delay sensitive traffic associated with the secondary channel. We define arrival encoded video data as long flow traffic, which differentiates from the other types of traffic. Considering traffic demand (from *i* to *j*) at edge node *i* in Figure 35, $\lambda_{i,j}^{I}$ represents traffic demand of delay sensitive traffic (i.e., HDTV), generated by video gateways. This video traffic requires relatively low delay channel (less than 100 millisecond). The other type of traffic denoted by $\lambda_{i,j}^{II}$ refers to traffic demand of non-delay sensitive traffic (i.e., best effort) which has less delay constraint than the former one. We assume inter arrival time of video or data traffic are exponential distributed, but service times of video and data are not exponential distributed. That is why generalized departure process is the best presentation for the secondary channel. Mainly the analyses of secondary channel relate to M/G/1 and M/G/C. However, the video frames size and data file size have different distributions. We will discuss more details in each particular case in the following subsections.

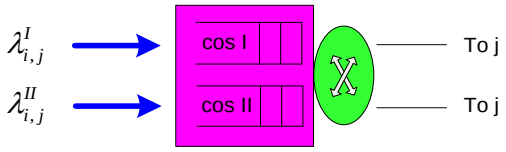

Figure 35. Queueing model of secondary wavelength channel

This chapter will be divided into 2 subsections as follows: performance analysis of video traffic in a wavelength channel (section 6.1.1), performance analysis of data traffic in a wavelength channel (section 6.1.2), and performance analysis of traffic in multiple wavelength channels (section 6.3).

6.1.1 Performance Analysis of Video Traffic in Single Wavelength Channel

We focus on video traffic and separate it from other traffic types because the encoded HD video traffic based on frame level has less traffic fluctuation than the best-effort traffic. In Figure 36, $\lambda_{v,ij}$ represents total arrival rate of delay sensitive traffic aggregated in CoS I buffer in region *i*, which has direct wavelength channels to the egress node *j*.

In our analysis, we assume the arrival video traffic is in form of MPEG-4 frame format, in which the video frame size is variable, depending on contents of any instant picture. The variable size and encoding techniques are able to compress the raw video data for efficient use of bandwidth in wavelength channel. A video stream consists of three frame types (i.e., I, B, and P), which has the following Group of picture (GOP): IBBPBBPBBPBB.

We assume a large number of video streams are delivered by video gateways at the rate λ_v frames/sec, where time between video frames $T_v = \frac{1}{\lambda_v}$ perceived by the video buffer can be assumed as exponential distributed. Assume video frame size is independent and identically distributed with random variables L^v based on following parameters: mean packet size $\overline{x_l^v}$, variance v_l^v, and covariance $CoV_l^v = \frac{\sqrt{v_l^v}}{\overline{x_l^v}} = \frac{S.D_l^v}{\overline{x_l^v}}$, in which these parameter can be obtained by measurement of real encoded video stream. In this case, we assume that ingress node *i* connects to the egress node *j* via a single wavelength channel with the transponder rate μ_j bits/sec. Therefore, we can represent this secondary channel based on video traffic and a single channel as M/G/1 queuing system. The distribution of video frames can be one of long-range distributions (i.e., Lognormal, Gamma, Weibull, and Pearson), depending on traffic circumstances: video bit rate, encoding scheme, picture resolution.

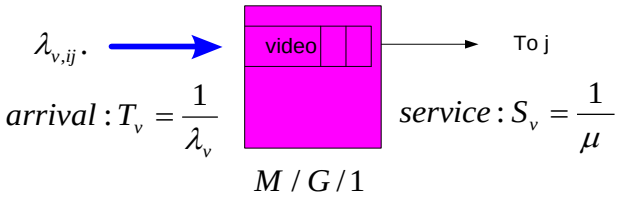

Figure 36. Secondary channel based on single wavelength channel

There are several methods to perform the analysis; for instance, residual time approach, transform approach based on imbedded Markov chain, or direct approach. For simplicity, we will perform residual time approach.

There are two possibilities of arriving video frames:

I. Arriving to non-empty frame in the system

- Video frame n_k needs to wait in the queue
- The ongoing frame has *R* residual time left to be finished, where R is random variable of the remaining service time

II. Arriving to empty video frame in the system

- No video frame waiting $n_k = 0$
- No ongoing frame, thus residual time *R=0*

Therefore, we can find the mean waiting time of video frame in the buffer as follows:

$$E[W_q] = \text{Mean service time of the frames ahead + mean residual time}$$

$$E[W_q] = E[N_v] * E[S_v] + E[R_v] * \Pr(server\_busy) \quad (6.1)$$

where $E[N_v]$ refers mean number of video frames waiting in the buffer;

$E[S_v]$ refers mean service time for video frames;

$E[R_v]$ refers mean residual time regarding video frames.

$\Pr(server\_busy)$ refers probability of busy server, equivalent to $\frac{\lambda}{\mu} = \rho$

With the Little's theorem $E[N_v] = \lambda_v E[W_q]$, we obtain

$$E[W_q] = \lambda_v E[W_q] * E[S_v] + E[R_v] * \rho_v \quad (6.2)$$

$$E[W_q] = \frac{\rho_v * E[R_v]}{(1-\rho_v)} \tag{6.3}$$

where ρ_v is video traffic load in wavelength channel obtained by $\lambda_v E[S_v]$

We need to find $E[R_v]$ in order to solve for $E[W_q]$. Using graphical technique relating to the area under triangle of residual time plot and limit theory, the mean residual time is given by

$$E[R_v] = \frac{E[S_v^2]}{2E[S_v]} \tag{6.4}$$

where mean of second moment of the service time: $E[S_v^2]$ is found by $S.D_{vs}^2 + E^2[S_v]$.

In order to find ***mean waiting time of video frame in the buffer,*** substitute Eq. (6.4) in Eq. (6.3), then we have

$$E[W_q] = \frac{\lambda_v E[S_v^2]}{2(1-\rho_v)} \tag{6.5}$$

Eq. (6.5) is known as Pollaczek-Khinchine formula:

For our numerical results in the section 6.3, we use Eq. (6.5) for the performance evaluation along with statistical data of encoded video frame size to find mean service time with respect to optical transponder speed.

The other performance parameters are calculated as follows:

Mean waiting time of video frames in the system

$$E[W] = E[W_q] + E[S_v] = \frac{\lambda_v E[S_v^2]}{2(1-\rho_v)} + E[S_v] \tag{6.6}$$

Mean number of video frames in the buffer

$$E[N_q] = \lambda_v E[W_q] = \frac{\lambda_v^2 E[S_v^2]}{2(1-\rho_v)} \quad (6.7)$$

Utilization in wavelength channel

$$U_v = \lambda_v E[S_v] * 100 \quad (6.8)$$

6.1.2 Performance Analysis of Data Traffic in Single Wavelength Channel

Now, we consider if the arrivals are non-delay sensitive traffic, which is corresponding to best effort traffic (e.g., ftp, email, and http). In Figure 37, $\lambda_{d,ij}$ represents packet arrivals of best-effort traffic to node *i*, which has a direct wavelength channel to an egress node *j*. We assume that the time between packets, (T_d) is a random variable, which has exponential distribution. The data packet size is assumed to be independent and identically distributed random variable L^d with following statistical parameters: mean packet size $\overline{x_l^d}$, variance v_l^d, standard deviation $S.D_l^d$, and covariance $CoV_l^d = \frac{\sqrt{v_l^d}}{\overline{x_l^d}} = \frac{S.D_l^d}{\overline{x_l^d}}$. Alternatively, the random variable L^d is self-similarity distributed (e.g., Pareto, Lognormal). However, the packet size is relatively small and bursty compared to the other traffic type. Based on a single channel with transmission rate μ, we represent the arrival process of best-effort traffic in an infinite queue as an M/G/1 queuing system shown below:

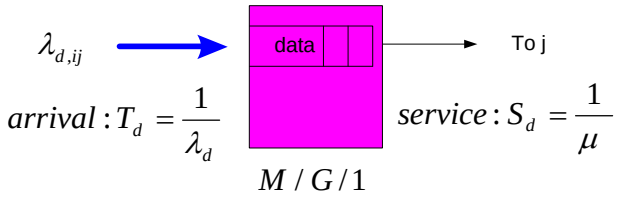

Figure 37. Queueing model of data traffic in a wavelength channel

Regarding the queueing analysis, we can follow the residual time approach as explained earlier in section 6.1.1. Then, we could solve for the following performance metrics:

Mean waiting time of packets in the buffer:

$E[W_q] =$ Mean service time of the packets ahead + mean residual time

$$E[W_q] = E[N_d] * E[S_d] + E[R_d] * \Pr(server\_busy) \tag{6.9}$$

where $E[N_d]$ is mean number of packets waiting in the buffer,

$E[S_d]$ is mean service time for packets,

$E[R_d]$ is mean residual time regarding packets, and

$\Pr(server\_busy)$ refers probability of busy server, equivalent to $\frac{\lambda}{\mu} = \rho$.

With Little's theorem $E[N_d] = \lambda_d E[W_q]$, we obtain:

$$E[W_q] = \lambda_d E[W_q] * E[S_d] + E[R_d] * \rho_d \tag{6.10}$$

$$E[W_q] = \frac{\rho_d E[R_d]}{(1-\rho_d)} \tag{6.11}$$

where ρ_d is data traffic load in wavelength channel obtained by $\lambda_d E[S_d]$.

We need to find $E[R_d]$ in order to solve for $E[W_q]$. Using graphical technique relating to the area under triangle of residual time plot along with limit theory, we get

$$E[R_d] = \frac{E[S_d^2]}{2E[S_d]} \tag{6.12}$$

where mean of second moment of the service time: $E[S_d^2]$ is given by $S.D_{ds}^2 + E^2[S_d]$.

Mean waiting time of packets in the buffer

The waiting time of packets in the buffer is derived by substituting Eq. (6.12) in Eq. (6.11):

$$E[W_q] = \frac{\lambda_d E[S_d^2]}{2(1-\rho_d)} \tag{6.13}$$

Eq. (6.13) is known as Pollaczek-Khinchine formula:

Mean waiting time of packets in the system

$$E[W] = E[W_q] + E[S_d] = \frac{\lambda_d E[S_d^2]}{2(1-\rho_d)} + E[S_d] \tag{6.14}$$

Mean number of packets in the buffer

$$E[N_d] = \lambda_d E[W_q] = \frac{\lambda_d^2 E[S_d^2]}{2(1-\rho_d)} \tag{6.15}$$

Utilization in wavelength channel

$$U_d = \lambda_d E[S_d] * 100 \tag{6.16}$$

6.2 MIXTURE OF TRAFFIC IN A WAVELENGTH CANNEL

In this section, we will investigate the arrival traffic, consisting of video and data created by certain video and data gateways respectively. In this particular case, the ingress node will allocate both traffic types in the same wavelength channel.

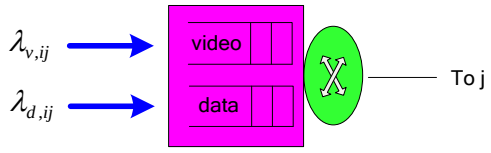

Figure 38. Queueing model of mixed traffic in a single wavelength channel

In Figure 38, $\lambda_{v,ij}$ represents total arrivals of video traffic delivered to node *j*, aggregated in a video buffer at node *i*. While $\lambda_{d,ij}$ refers total arrivals of data traffic delivered to node *j* aggregated in a data buffer at node *i*. Since both traffic types have the same destination node *j*. Assume there is a large number of video streams and data packets created by a group of video and data gateways. Thus, both traffic arrivals can be assumed as Poisson processes. Regarding the traffic characteristics, we define statistical parameters associated with video traffic as mentioned earlier in the section 6.1.1, and the data traffic parameters as discussed in the section 6.1.2.

Based on buffer scheduling schemes, we can classify the performance analysis of mixture of traffic into two categories: prioritized video traffic in a wavelength channel (discussed in 6.2.1) and non-prioritized traffic in a wavelength channel (discussed in 6.2.2).

6.2.1 Performance Analysis of Prioritizing Video Traffic

In this case, the optical switching facilities (i.e., switching fabrics and transponders) will serve video traffic for the first priority in order to smooth video traffic streams. We represent this queuing analysis as M/G/1 non-preemptive system. If there are both types of traffic waiting in the queue, the transponder will always transmit all adjacent video traffic. Then, it will start serving data traffic waiting in the queue. However, if the data traffic is being severed and a new video arrival comes, the server does not interrupt current data traffic.

Assume the arrival of each traffic type is independent and Poisson distributed with the rates λ_v and λ_d according to video and data traffic respectively. For the departure process, each traffic type is served independently by the same wavelength channel with a general service time distribution of mean (i.e., $E[S_v], E[S_d]$), and a second moment (i.e., $E[S_v^2], E[S_d^2]$) for video and data traffic respectively.

Regarding Poisson property, the total arrival rate of combined individual Poisson processes is given by:

$$\lambda_T = \lambda_v + \lambda_d \tag{6.17}$$

Based on infinite queue, utilization of the channel at steady state can be found by:

$$\rho_T = \rho_v + \rho_d = \lambda_T * E[S_T]$$

$$(6.18) = \lambda_v S_v + \lambda_d S_d = \lambda_T * E[S_T]$$

(6.19)

For stability of the system, $\rho_T < 1$

From Eq. 6.19, we have average service time:

$$E[S_T] = \frac{\lambda_v}{\lambda_T} S_v + \frac{\lambda_d}{\lambda_T} S_d \tag{6.20}$$

Then, we will employ the same approach of PK derivation discussed in the previous section.

Queueing Delay for video traffic

Since the video traffic is higher priority (i.e., not affected by the other traffic type), the queuing delay for video traffic is the same as M/G/1:

$$E[W_v] = E[N_v] * E[S_v] + E[R_T] \tag{6.21}$$

From eq. 6.21 and little's theorem $E[N_v] = \lambda_v E[W_v]$, we have

$$E[W_v] = \frac{E[R_T]}{1 - \rho_v} \tag{6.22}$$

Considering residual time $E[R_T]$, when a new packet arrives, the probability that the new arrival finds the system is busy ρ. For the mixed traffic, the mean residual time $E[R_T]$ will be the weighted sum of the residual service time of each type as below:

$$E[R_T] = \rho_v E[R_v] + \rho_d E[R_d] \tag{6.23}$$

Substituting $\rho = \lambda E[S]$ and $E[R] = \frac{E[S^2]}{2E[S]}$, we have

$$E[R_T] = \frac{\lambda_v}{2} E[S_v^2] + \frac{\lambda_d}{2} E[S_d^2] \tag{6.24}$$

From Eq. 6.22 and Eq. 6.24, we can find the queuing delay for video traffic as follows:

$$E[W_v] = \frac{\lambda_v E[S_v^2] + \lambda_d E[S_d^2]}{2(1-\rho_v)} \tag{6.25}$$

Queueing Delay for data traffic

The waiting time of data traffic in the queue consists of the following components:

Queueing delay = residual time + time to serve all traffic types ahead in queue + time to serve video traffic arriving during waiting of data traffic

$$E[W_d] = E[R_T] + (E[N_v]E[S_v] + E[N_d]E[S_d]) + E[S_v]E[N_{vw}] \tag{6.26}$$

where $E[N_{vw}]$ is the number of video packets during waiting of data traffic (i.e., $\lambda_v E[W_d]$).

By Little's theorem (i.e., $E[N] = \lambda E[W]$), we have

$$E[W_d] = E[R_T] + \rho_v E[W_v] + \rho_d E[W_d] + \rho_v E[W_d]$$

$$E[W_d] = \frac{E[R_T] + \rho_v E[W_v]}{1-\rho_v - \rho_d} \tag{6.27}$$

6.2.2 Performance Analysis of Non-prioritizing Traffic

In this scenario, all traffic is treated equally, and be served in order of time arrivals, referred to FCFS. Both traffic types are aggregated in the same physical queue and share the same wavelength channel. Without priority scheme, we can represent this system as M/G/1 queuing model, in which the statistical parameters associated with the combined traffic will be weighted by the ratios of the arrival rates.

Since we assume the arrival of each traffic type is Poisson, the summation of both types will be Poisson arrival as well with the total arrival rate given by:

$$\lambda_T = \lambda_v + \lambda_d \tag{6.28}$$

Based on infinite queue, utilization of the channel at steady state can be found by:

$$\rho_T = \rho_v + \rho_d = \lambda_T * E[S_T] \tag{6.29}$$

Substituting $\rho = \lambda E[S]$:

$$\lambda_v E[S_v] + \lambda_d E[S_d] = \lambda_T * E[S_T] \tag{6.30}$$

Thus, we have average service time:

$$E[S_T] = \frac{\lambda_v}{\lambda_T} E[S_v] + \frac{\lambda_d}{\lambda_T} E[S_d] \tag{6.31}$$

For second moment of the combined stream is given by the weight sum of each second moment:

$$E[S_T^2] = \frac{\lambda_v}{\lambda_T} E[S_v^2] + \frac{\lambda_d}{\lambda_T} E[S_d^2] \tag{6.32}$$

Regarding P-K formula as in Eq.6.5, the mean waiting time of the combined stream in the queue is given by:

$$E[W_{mix}] = \frac{\lambda_T E[S_T^2]}{2(1-\rho_T)} \tag{6.33}$$

Now, considering the queueing delay for particular traffic stream:

Queueing Delay for video traffic

The waiting time of video traffic in the queue consists of the following components:

Queueing delay = residual time + time to serve all traffic types ahead in queue

$$E[W_v] = E[R_T] + E[N_v]E[S_v] + E[N_d]E[S_d] \tag{6.34}$$

By Little's theorem (i.e., $E[N] = \lambda E[W]$), we have

$$E[W_v] = E[R_T] + \rho_v E[W_v] + \rho_d E[W_d] \tag{6.35}$$

$$E[W_v] = \frac{E[R_T] + \rho_d E[W_d]}{1 - \rho_v} \tag{6.36}$$

where $E[R_T] = \frac{\lambda_v}{2} E[S_v^2] + \frac{\lambda_d}{2} E[S_d^2]$ as obtained in Eq. 6.24

<u>Queueing Delay for data traffic</u>

We will derive queueing delay with the same approach as earlier. The waiting time of data traffic in the queue can be found by:

Queueing delay = residual time + time to serve all traffic types ahead in queue

$$E[W_d] = E[R_T] + E[N_v]E[S_v] + E[N_d]E[S_d] \tag{6.37}$$

By Little's theorem (i.e., $E[N] = \lambda E[W]$), we have

$$E[W_d] = E[R_T] + \rho_v E[W_v] + \rho_d E[W_d] \tag{6.38}$$

$$E[W_d] = \frac{E[R_T] + \rho_v E[W_v]}{1 - \rho_d} \tag{6.39}$$

where $E[R_T] = \frac{\lambda_v}{2} E[S_v^2] + \frac{\lambda_d}{2} E[S_d^2]$

6.3 PERFORMANCE ANALYSIS OF MULTIPLE CHANNELS

This section investigates performance analysis of the system when ingress nodes have a group of wavelength channels, connecting to other egress nodes.

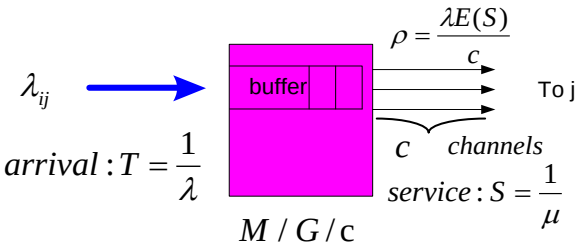

Figure 39. Queueing model based on multiple wavelength channels

Figure 39 illustrates the traffic arrivals λ_{ij} aggregated in the buffer at node *i*, in which the aggregated traffic shares *n* wavelength channels to the egress node *j*. We assume the ingress node allocates the same link speed μ for all *n* channels. The arrival is Poisson distributed with random inter-arrival time $T = \frac{1}{\lambda}$. The packet size is assumed to be independent and identically distributed random variable L according to generalized distribution with the following parameters: mean packet size $\overline{x_l}$, variance v_l, and covariance $CoV_l = \frac{\sqrt{v_l}}{\overline{x_l}} = \frac{S.D_l}{\overline{x_l}}$, in which the parameters can be obtained by measurement of the traffic demand characteristics. Based on multiple wavelength channels, we represent this model as M/G/c queuing system.

For the performance analysis, we will employ the well-known close form approximations technique associated with the first two moments of the service time and M/M/C queueing analysis to approximate the queue size, mean waiting time and other performance metrics of the M/G/C queueing system:

$$E[N] = \frac{E[S^2]}{2(E[S])^2} E[N]_{M/M/c} \tag{6.40}$$

where $E[S]$ is given by $\frac{\overline{x_l}}{\mu}$ and $E[S^2] = S.D_s^2 + E[S]^2$

$$E[W_q]_{M/G/c} = \frac{Cov^2 + 1}{2} E[W_q]_{M/M/c} \tag{6.41}$$

where covariance square of service time $Cov^2 = \frac{Var(S)}{E[S]^2}$,

the typical mean waiting time of M/M/C queue is given by $E[W_q]_{M/M/c} = \frac{1}{c\mu(1-\rho)} C(c,a)$,

where $\rho = \frac{\lambda E[S]}{c}$ and $a = \frac{\lambda}{\mu}$.

6.4 PERFORMANCE RESULTS AND DISCUSSION

In this section, we have some discussion on the results of network performance in certain circumstances. The results are based on our queueing analysis we have discussed earlier. The results are obtained by coding in Matlab. In some cases, we validate the results with those generated by OPNET simulation tool. The section is divided into four subsections: consists of effect of video frame sizes in secondary wavelength channel (section 6.4.1), effect of video frame rate in secondary wavelength channel (section 6.4.2), effect of single vs. multiple wavelength channels (section 6.4.3), and effect of traffic mixture in wavelength channel (section 6.4.4)

6.4.1 Effect of Video Frame Size in Secondary Wavelength Channel

We investigate how video frame size affects performance in the wavelength channel. The experiment performs a comparison between two different frame sizes (i.e. low vs high video resolutions). The simulation parameters are as follows:

- Jurassic Park (medium quality): video frame size (mean = 1300 Bytes, CoV = 0.84).
- Mr. Bean (high quality): video frame size (mean = 2900 Bytes, CoV= 0.62)
- Video stream format: MPEG4
- Video frame rate: 30 frames/sec
- Channel capacity: 1.25 Gb/s

In this experiment, we verify our analysis results (based on Matlab coding) with those generated by Opnet simulation tool. In Opnet, we configure network model of a wavelength channel and generate video frame with inter arrival time = 1/(30*#flows) based on exponential distributed function, where # flow refers number of video requests (from several video servers) at an ingress node sharing the same wavelength channel to a destination egress node. For the frame size generation, we employ Gamma distribution with shape and scale parameters associated with the above frame sizes and *CoV*. The secondary channel capacity is assigned to rate 1.25 Gb/s.

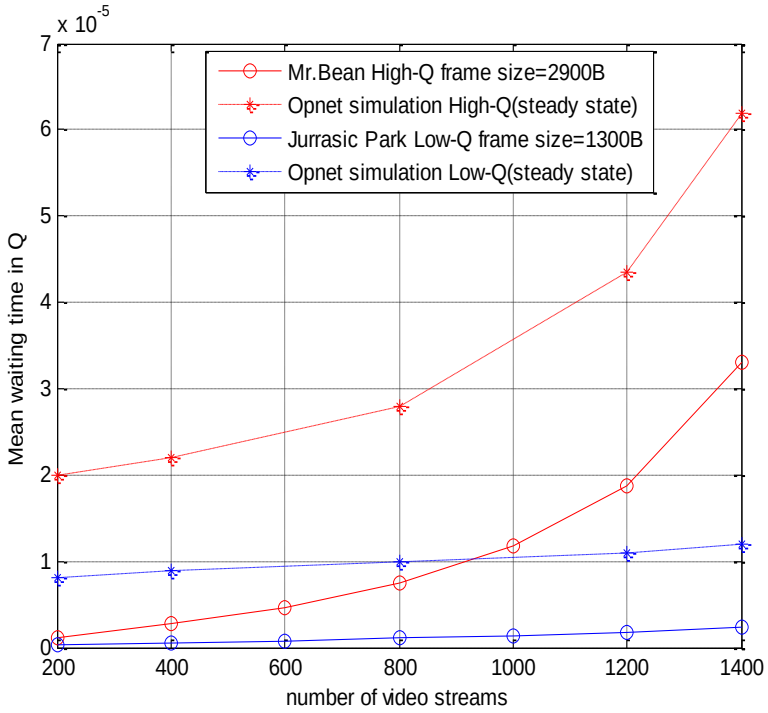

Figure 40. Queueing delay in wavelength channel

Figure 40 illustrates queuing delays in the video buffer when varying numbers of video streams (increasing traffic load). The dotted lines refer to results obtained from Opnet simulations, in which the plot shows the average delay of a number of video frames in the buffer. The solid lines refer steady state delay based on queueing model. One can see that the queuing delays based on the simulations are higher than the delay from our mathematical model for both frame sizes since the delay parameter in Opnet is obtained from system delay, which equals queueing delay plus transmission time. We could verify the simulation results by adding the transmission time to queueing delay from our analysis. In case of 2900B, the transmission time can be found by (2900*8)/(1.25*10^9) $=1.86*10^{-5}$ which is corresponding to the gap between those two graphs. For instance, at 200 streams, the queueing delay from our analysis

is $0.15*10^{-5}$. But the system delay (i.e., queuing plus transmission delays) from simulation is $2*10^{-5}$. The system delay from analysis is found by $0.15*10^{-5}+1.86*10^{-5}=2.01*10^{-5}$. Therefore, the error is $0.01*10^{-5}$, which represents a 0.5% error estimation for simulation versus analysis. Considering the comparison, the results show that larger frame size (i.e., high quality video) takes longer queueing delay than another one. However, the larger size could achieve higher utilization in the wavelength channel shown in Figure 41.

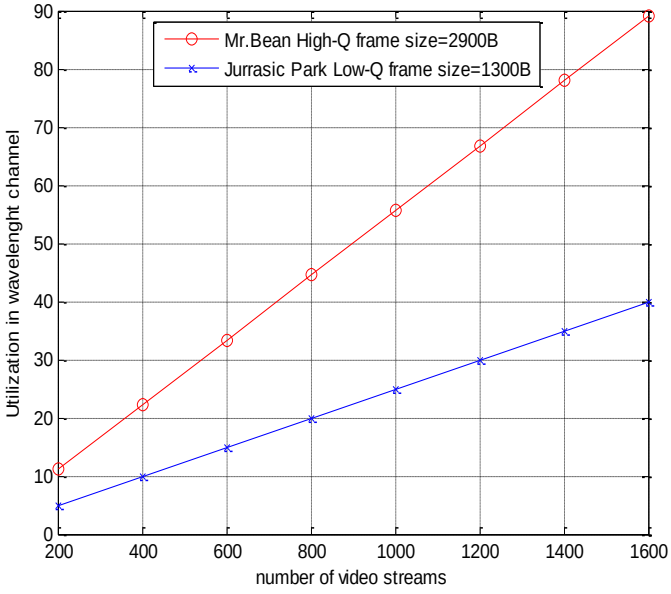

Figure 41. Utilization in wavelength channel

Regarding the queue size depicted in Figure 42, the analysis and the simulation for both cases are convergence. The higher quality video allows larger queue length of video frame in the queue, which is associated with the above queuing delay.

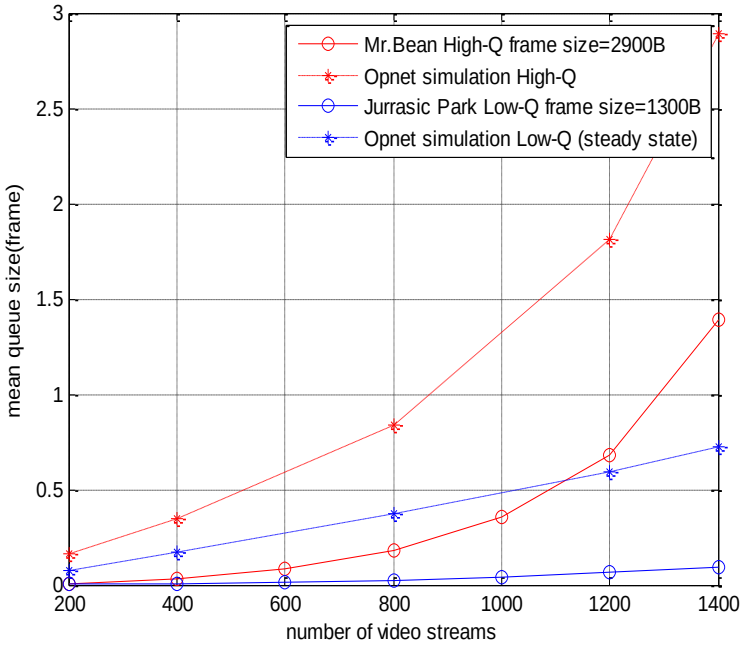

Figure 42. Mean queue size in video queue

6.4.2 Effect of Video Frame Rate in Secondary Wavelength Channel

In this study, we investigate how does either video frame rate or frame size has greater impact to the performance of the wavelength channel. At certain traffic loads, we compare the performance of the channel with regard to two different frame sizes: 2900B (at 30frames/s) vs. 5800B (at15 frames/s). In other words, the frame size 2900B is delivered at double frame rate as the one with 5800B. In the experiment, we vary traffic load in X-axis by increasing number of flows; but frame rates and sizes for each type remain the same.

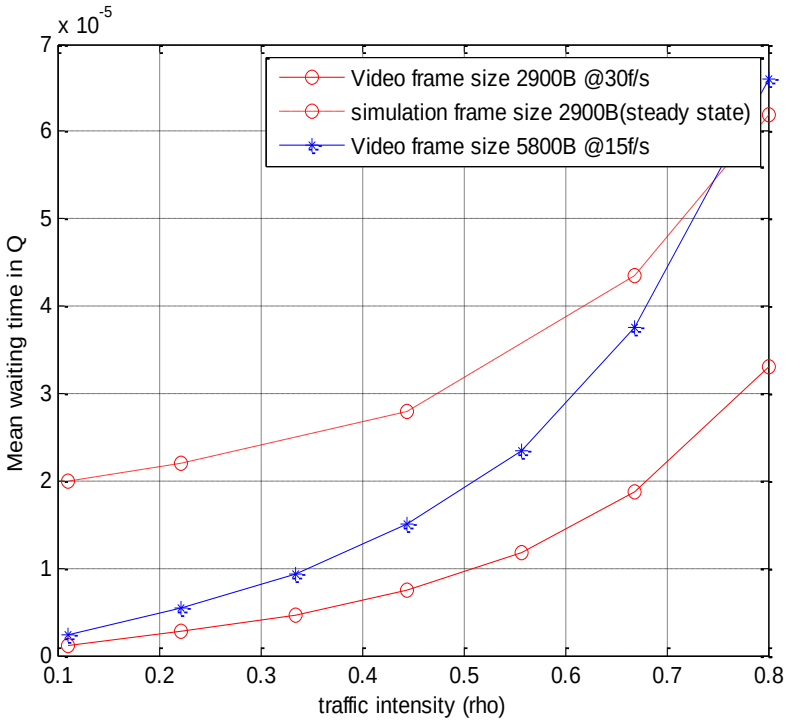

Figure 43. Mean waiting time in video queue

Figure 43 shows that the larger frame size (i.e., 5800B) allows higher waiting time in the queue although the frame arrival rate is slower. Therefore, the frame size has higher impact to the queueing delay than the arrival rate (i.e., frame rate). In addition, Figure 44 shows the same trend for mean queue length in the video buffer. The larger size yields greater queue length than the shorter one even faster arrival rate based on the same traffic load. In this case, the utilizations for both cases are the same since we compare at the same traffic loads.

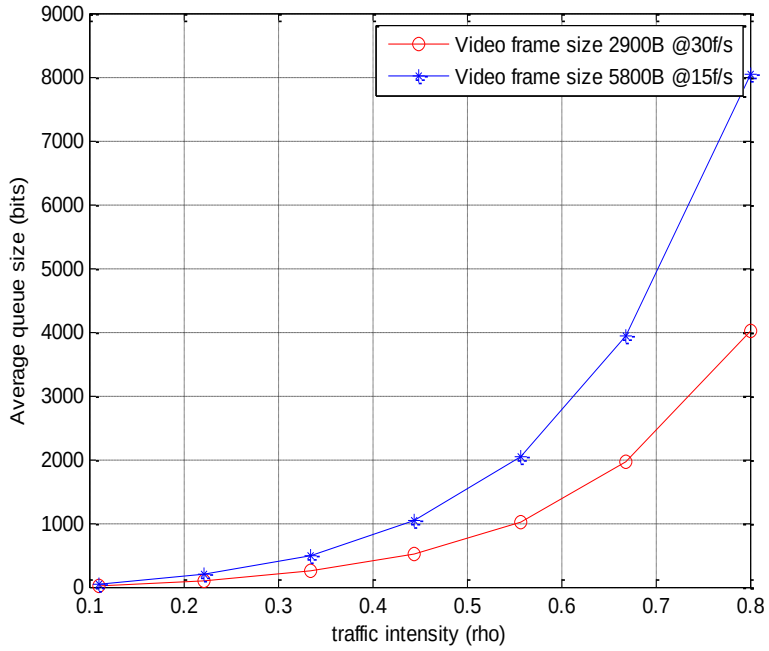

Figure 44. Mean queue length in video queue

6.4.3 Effect of Secondary Channel Capacity

Waiting time in queue

Now, we investigate whether two slower wavelength channels or one faster channel will improve network performance. In other words, should the ingress node request an additional channel based on the same speed or replace existing channel with a faster channel? In both cases, we assign the same traffic load with the following parameters: video frame rates (30 f/s) and frame sizes: mean = 2900B, *CoV* = 0.62 (Mr. Bean movie). We compare queueing delay in each scenario (i.e., 1 * 2.5 GB/s vs. 2*1.25Gb/s). According to our performance analysis, we write Matlab codes to investigate several performance parameters at certain traffic loads associated

with M/G/1 vs. M/G/2 queueing models. Regarding the M/G/2, we employ the approximation method in order to find the numerical results associated with generalized distribution of the video frame size (i.e., *CoV* = 0.62) versus exponential distribution (*CoV* = 1).

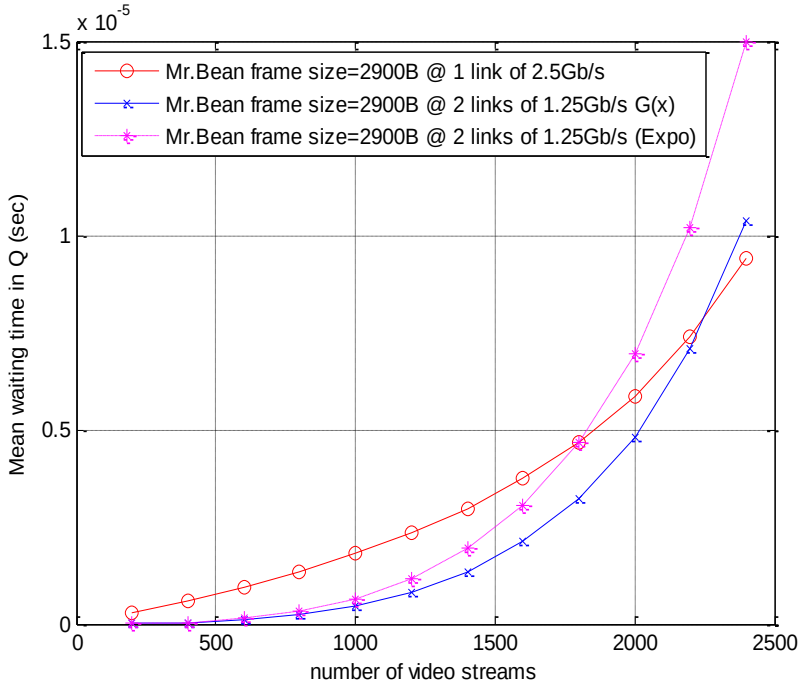

Figure 45. Mean waiting time: single vs. double links

Figure 45 depicts mean waiting time in the video buffer when varying number of video streams (i.e, increasing traffic loads). Considering the red and blue plots, the 2* 1.25Gb/s (blue) can provide lower delay channel than 1*2.5Gb/s (red) up to the crossing point (i.e., 2200 streams). That is equivalent to the traffic load, $rho = \lambda * \tau = 30 * 2250 * (\frac{2900 * 8}{2.5 * 10^9}) = 0.626$. However, when the load is greater, one faster channel (blue) will perform better (i.e., less delay).

Regarding channel utilization, there is no advantage over the other since the results are the same values traffic loads. We also show an extra plot for the case 2*1.25Gb/s (i.e. pink), in which frame size is based on exponential distributed (*CoV* =1) showing higher queueing delay than *CoV* = 0.62. However, the crossing point with the analysis moves toward fewer loads. In addition, we repeat the experiment according to several frame sizes as the follows:

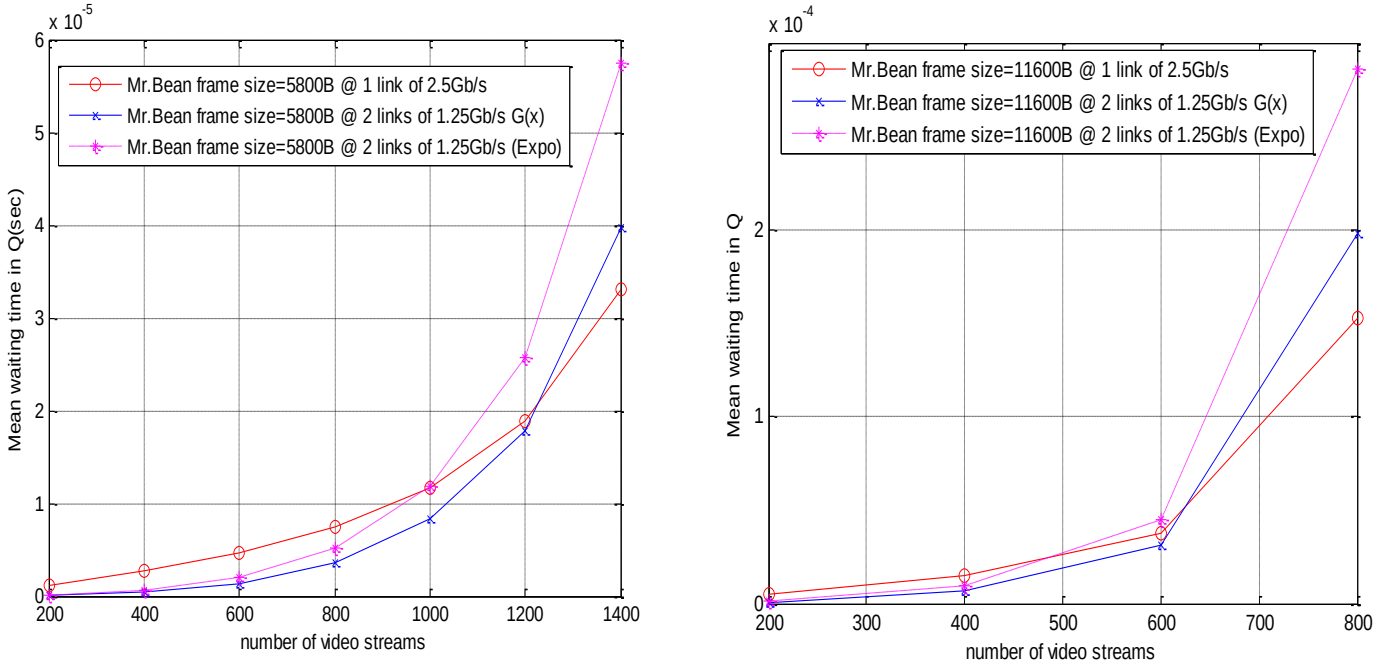

Figure 46. Mean queuing delay: 5800B vs 11600B

In Figure 46, the results depict same trend as previous figure; but only the crossing points will shift to the less loads. This is due to the larger frame sizes transmitted at the same frame rate. In the case of 5800B, the crossing is at 1200 streams, equivalent to $rho = \lambda * \tau = 30 * 1200 * (\frac{5800 * 8}{2.5 * 10^9}) = 0.668$, and also 625 streams in the case of 11600B or

$rho = \lambda * \tau = 30 * 625 * (\frac{11600 * 8}{2.5 * 10^9}) = 0.696$. One can see that all three crossing points are approximately corresponding to the same traffic loads. On the other hand, the DHON should assign one faster wavelength channel (instead of two slower ones) as the traffic loads pass the threshold (rho > 0.7).

Mean Queue size

Figure 47 illustrates mean queue size of video frames in the buffer at different traffic loads. We provide a comparison between two different frame sizes: 2900B versus 5800B. Basically, mean queue size for 2*1.25 Gb/s link are smaller than the other one. However, once traffic loads increase until passing the crossing point, the 1*2.5 Gb/s allows less video frame (bits) left in the queue. These are corresponnding to the results for queueing delay, in which the larger queue size takes longer queueing delay. However, there is no difference between in either of them based on utilization. Regarding the effect of channel capacity, we show some performance metrics, including mean queue size and mean waiting time. Other parameters, like jitter and utilization, need to be investigated as future work.

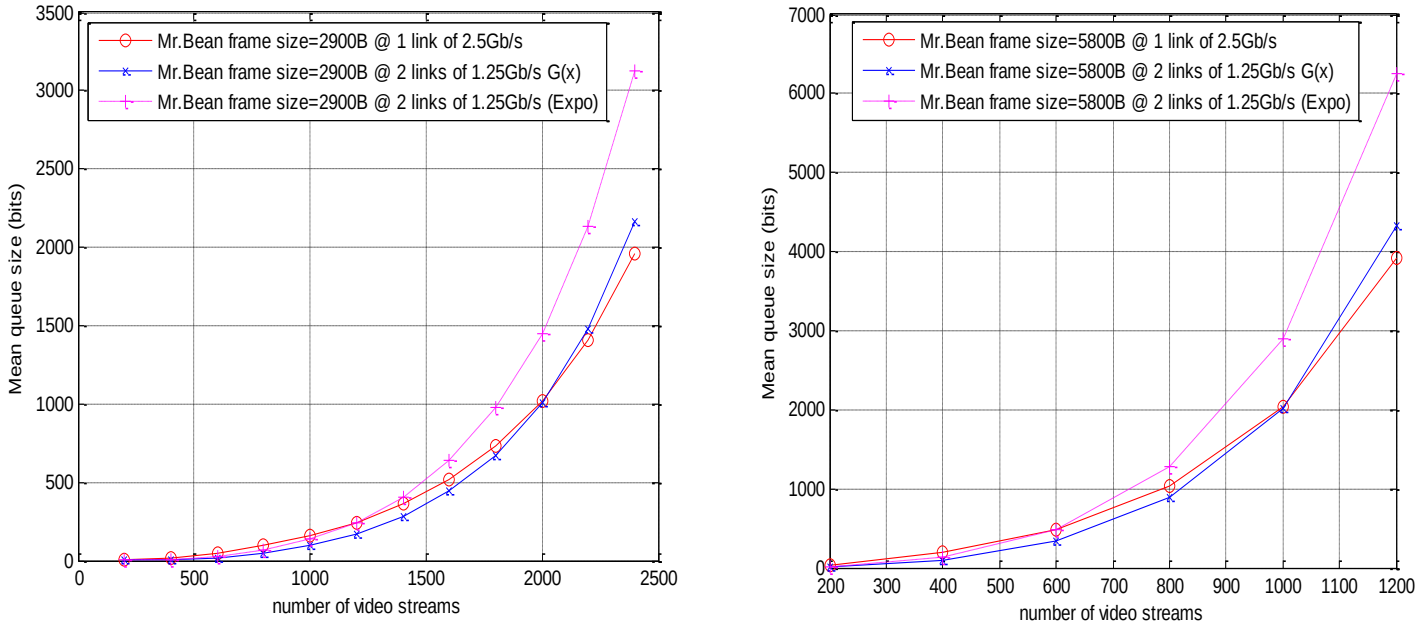

Figure 47. Mean queue size: 5800B vs 11600B

6.4.4 Effect of Traffic Mixture in Wavelength Channel

In this section, we evaluate performance analysis of mixed traffic between video and data (i.e., best effort). Ingress nodes aggregate each traffic type in separate buffers, but allocated in the same wavelength channel. In the experiment, we compare performance of the channel based on two different scheduling schemes: video prioritized versus non-prioritized. We evaluate mean waiting time in each queue type based on queueing scheduling. Throughout the experiments, we assume time between video arrivals and data packets are exponential distributed; however, the sizes and service times for both types are generalize distributed with particular variances. For the arrival rate, they vary associated with the traffic loads. The parameters details for both video and data are follows:

Video: frame size 2900B, and $CoV = 0.62$

Data: packet size 760B, and $CoV = 1.5$

For data traffic parameters, we pick the number based on bimodal traffic, in which majority of packet size falls into two sizes: 20B for header and 1500B for IP payload.

The experiments will perform three different scenarios:

I. *Low video traffic:* video 10% mixed with data traffic 90% of total traffic load

II. *Medium video traffic:* video 50% mixed with data traffic 50% of total traffic load

III. *High video traffic:* video 70% mixed with data traffic 30% of total traffic load

Video and data delay comparison

Now, considering mean waiting time in both video and data queues for two different scheduling schemes: video prioritized versus non-prioritized traffic.

I. *Low video traffic (video 10%):*

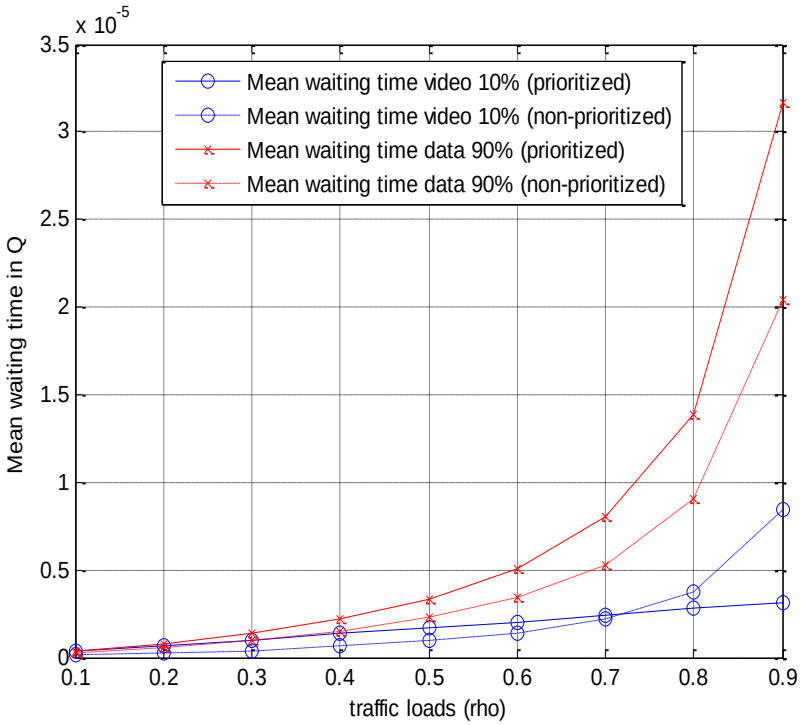

Figure 48. Mean waiting time in queue @ 10% video

Figure 48 illustrates mean waiting time for video and data traffic at certain traffic loads when 10% of total traffic load is video traffic (i.e., scenario I). Regarding video prioritized case, mean waiting time of video traffic is always lower than the data due to the prioritized service; although, the video traffic has larger frame size. For non-priority scheduling, waiting time of the video traffic is higher than the prioritized one when the traffic loads is greater than 0.7. In addition, the data queueing delay is always higher than the video since the data traffic (90%) dominates video traffic.

II. *Medium video traffic (video 50%):*

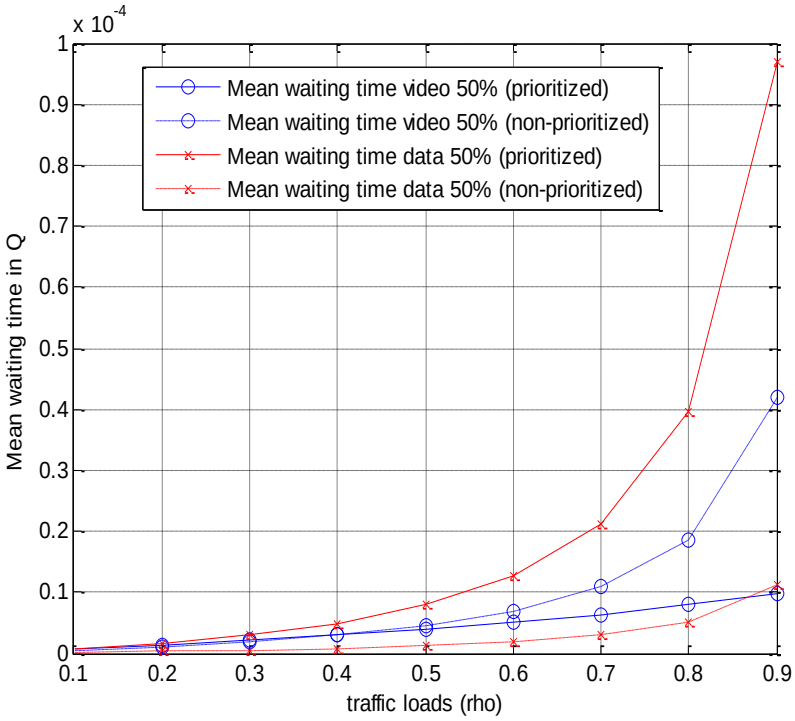

Figure 49. Mean waiting time in queue @ 50% video traffic load

For the case of 50% video traffic depicted in Figure 48, the video traffic still have lower queueing delay than data traffic. However, for non-priority scheduling, video traffic has longer delay than data traffic (i.e., reverse trend of the scenario I), because the data traffic does not dominate the total traffic load. Thus, the larger frame size takes longer waiting time in the queue than the smaller size. In addition, the crossing point between non-priority queue (dotted blue) and the priority one (solid blue) occurs around medium traffic load ($rho = 0.5$ less than the previous case), which is corresponding to the higher video traffic load than the first case.

III. *High video traffic (video 70%):*

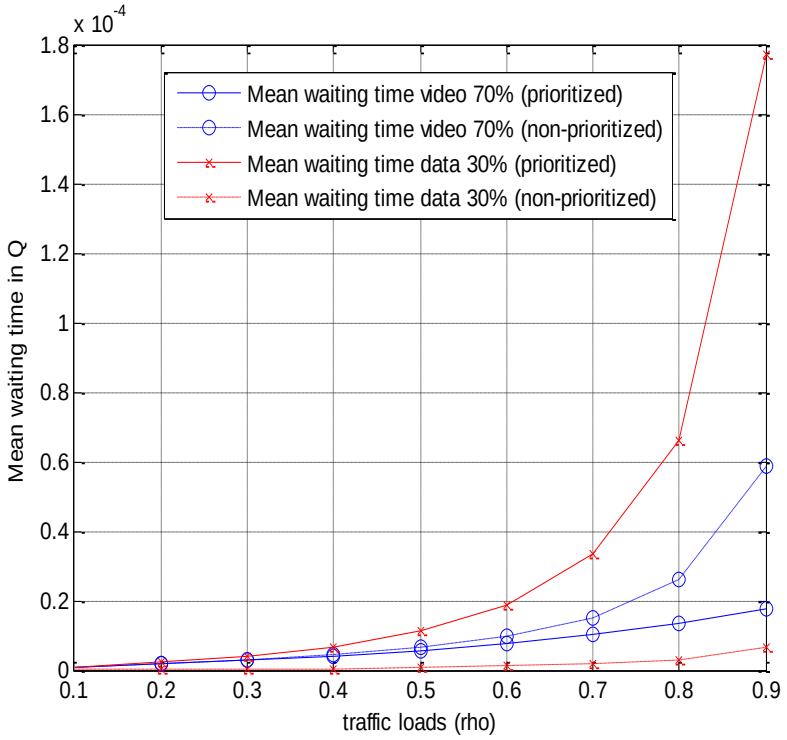

Figure 50. Mean waiting time in queue @ 70% video traffic load

Now, we evaluate the performance of the wavelength channel when the majority of the arrival traffic is video traffic (i.e., 70% of total load) shown in Figure 50. The results show that the video traffic has lower queueing delay than the data traffic for the prioritized case. However, for non-priority scheduling, video traffic has longer delay than data traffic, which is the same as scenario II due to heavy video traffic load. Thus, the larger frame size takes longer waiting time in the queue than the smaller size with the sooner crossing point among all cases due to video

traffic domination. In other words, the network should perform video priority queue if video traffic is comparatively high ratio.

Regarding utilization in the wavelength channel, they remain the same for all cases due to the steady state approach, which varies by traffic loads.

Effect of video traffic ratio on video queuing delay

Since ratio of video traffic has significant impact on the channel performance, we would better investigate how the video traffic ratio affects video queueing delay for each type of scheduling.

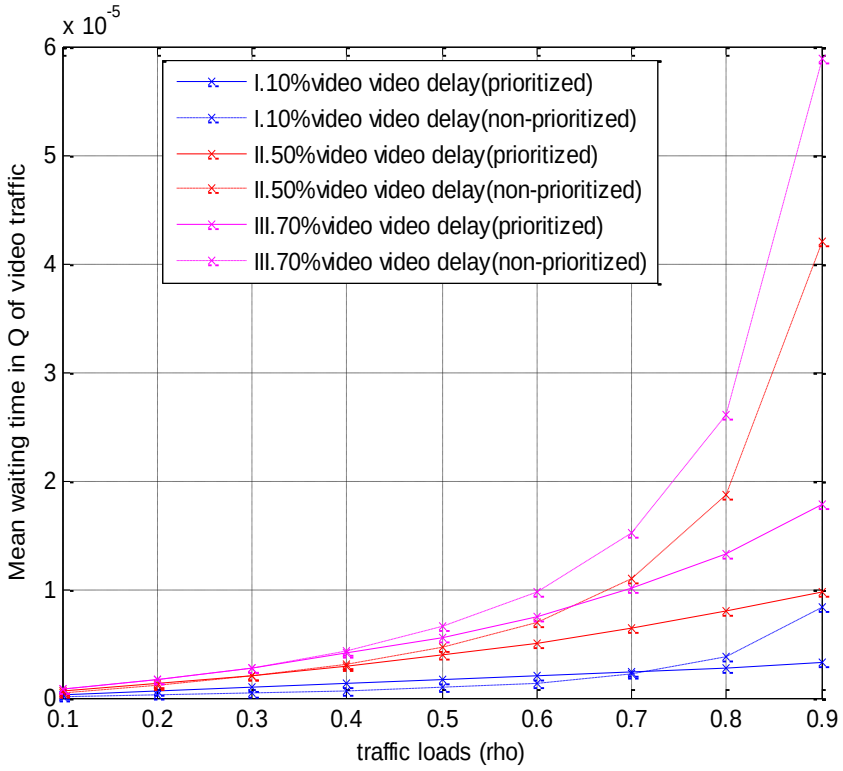

Figure 51. Impact of traffic ratio on video queueing delay

Figure 51 illustrates the comparison of queueing delay of video traffic based on prioritized and non-prioritized scheduling. We compare the results among three different scenarios of video traffic ratio as mentioned above. One can see that the higher video traffic, the longer queueing delay for both prioritized and non-prioritized cases. However, scenario I (10% video) does not have the same pattern as the others, creating a crossing point. In other words, the prioritized scheduling does not improve the performance for the video traffic since there is comparatively low video traffic is in the channel. However, the prioritized scheme will be beneficial at higher traffic load.

Effect of video traffic ratio on data queueing delay

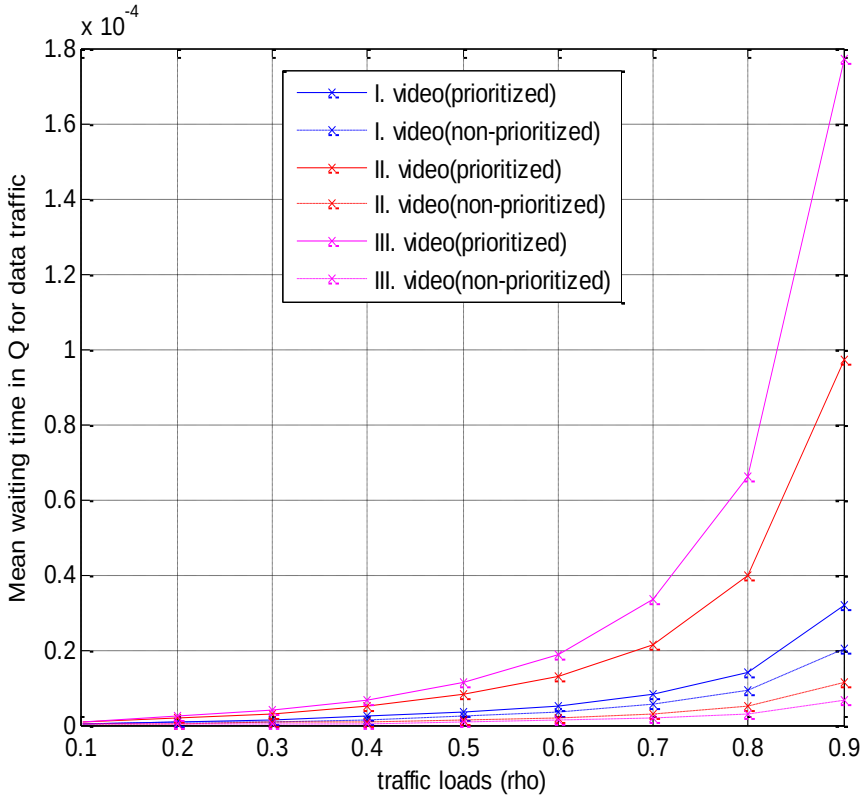

Figure 52. Impact of traffic ratio on data queueing delay

Now, we consider only the data queueing delay with regard to prioritized and non-prioritized scheduling. In Figure 52, we compare those results with three different scenarios of video traffic ratio. Considering the video prioritized case (solid lines), the higher video traffic ratio, making data packet to wait longer in the queue. That makes sense because in high video ratio, the switching fabrics are reserved most of the time for video traffic. However, in the non-prioritized scheme, one can see the reserve results. The scenario I (low video or high data) allows higher queueing delay than scenario II and II (higher video or lower data). In other words, the high data traffic load allows data packet to wait in the queue longer.

6.5 PERFORMANCE COMPARISONS: DHON V.S IP/DWDM

In this section, we compare the performance analysis between our proposed DHON and IP/DWDM network, which is commonly employed as backbone networks. However, we have to make clear assumptions in order to compare two different architectures, and ensure that the IP/DWDM network is compatible with traffic that we apply to our DHON throughout this section. The assumptions are follows:

- Our DHON deploys centralized GMPLS optical controlling so that the ingress nodes recognize all traffic granularities (circuit, frame, and packet) and be able to configure different types of optical switching fabrics. In addition, ingress nodes support priority queue scheduling.

- For IP/DWDM, all IP nodes in both access and core layers support MPLS feature (i.e. MPLS switches), in which the edge node is able to classify the traffic, and is compatible with several traffic granularities (e.g., packet and frame).
- Based on MPLS-TE, the network can search for reserved bandwidth channels from ingress node toward the destination node, called Label Switching Path (LSP).
- MPLS has fully control particular traffic and path associated with MPLS Tag. Thus, we can ensure that the traffic arriving at the ingress node (i.e., video and data) will travel in the same channel toward the sink node
- Both architectures will create queueing delay at the ingress nodes, but the difference is that DHON has logical fully meshed to egress nodes; therefore, there is no delay in the intermediate nodes (i.e., queueing, processing, and transmission delays)

The organization of this section is the follows:

6.5.1 Network End-to-end Delay

This section will provide an example of realistic traffic route, and explain the calculation for end-to-end delay associated with each type of network architectures (i.e., DHON vs. IP/DWDM).

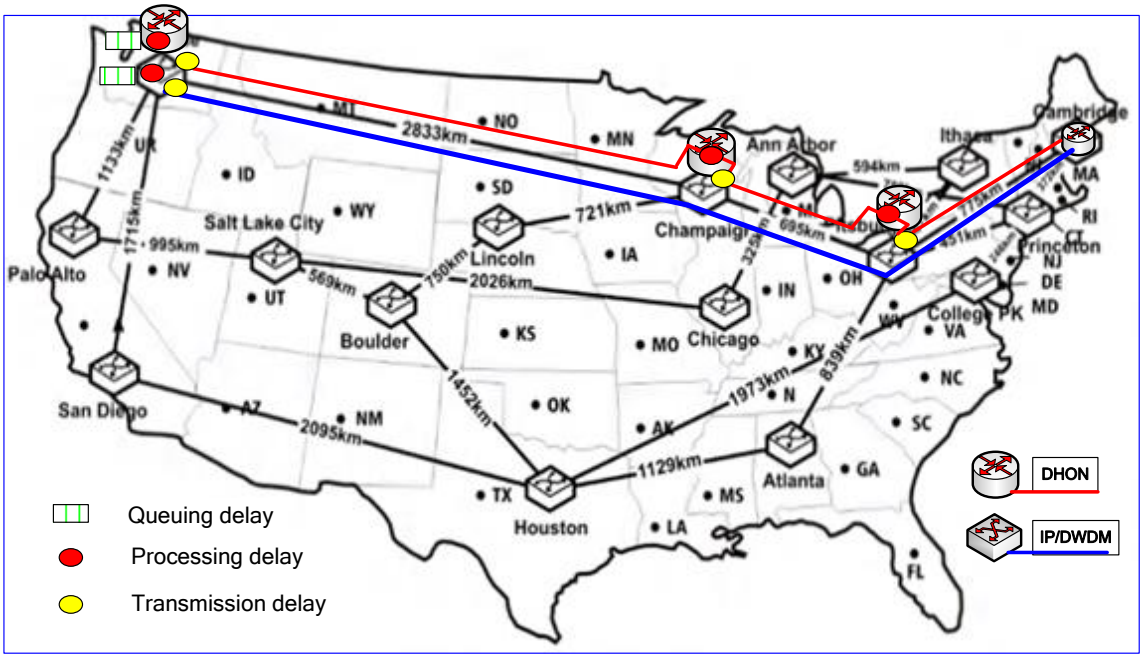

Figure 53. End-to-end delay calculation based on NSF topology

Figure 53 illustrates an example of 3-hops traffic walkthrough from the source to destination with regard to NSF network topology. The route starts from the ingress node located in Seattle via intermediate nodes in Champaign and Pittsburgh toward the sink node in Cambridge. The blue line represents a wavelength channel based on DHON, and the red one refers the LSP associated with IP/DWDM network.

Remark: the term “end-to-end delay,” that we are going to call it from now, refers the delay between ingress to egress node, which is not defined as delay between end-to-end user delays.

The end-to-end delay associated with this route is calculated as the following:

IP/DWDM

$$End\_delay_{IP/DWM} = (T_q + T_{proc} + T_{tran}) + T_{prop1} + (T_{proc} + T_{tran}) + T_{prop2} + (T_{proc} + T_{tran}) + T_{prop3}$$

$$= T_q + hop * (T_{proc} + T_{tran}) + T_{prop1} + T_{prop2} + T_{prop3}$$

, where *hop* refers number of hops the traffic travel through;

T_q refers queueing delay at IP/MPLS ingress node based on non-priority scheduling;

T_{proc} refers time to process MPLS headers;

T_{tran} refers time to deliver each packet/frame in to the channel;

T_{prop} refers propagation time along optical fiber of each packet/frame between nodes;

In addition, this end-to-end delay is compatible with both video frame and data packet delay with regard of sizes and link transmission rate.

However, the end-to-end delay for IP/DWDM is the lower bound delay. In reality, it will be higher due to queueing delay at the intermediate nodes, in which those label switching core routers are traffic congested.

DHON

$$End\_delay_{DHON} = T_{q\_prior} + (T_{proc} + T_{tran}) + T_{prop1} + T_{prop2} + T_{prop3}$$

T_{q_prior} denotes queueing delay at DHON ingress node based on priority scheduling;

T_{proc} denotes processing time for GMPLS headers;

T_{tran} denotes time to deliver each packet/frame in to the channel;

T_{prop} denotes propagation time on optical fiber on particular hop.

In this case, the delay regarding DHON is superior with the difference as the follows:

$$Delay\ Difference \geq (T_q - T_{q\_prior})_{video} + (hop - 1) * (T_{proc} + T_{tran})$$

Based on this concept, we can extend this calculation to several scenarios of network environments shown in the following sections:

6.5.2 End-to-end Delay Comparison on Video and Data Traffic

In this experiment, we compare end-to-end delay occurred in DHON vs. IP/DWM based on mixture of traffic (i.e., video and data). To simplify the comparison, the end-to-end delay plots exclude propagation delays under the assumption that traffic in both networks travels along the same path. Therefore, cancel out. The evaluation is based on 3 hops link with 50% video traffic ratio. Given video frame size 2900 B with *CoV*= 0.62 and packet size 760B with *CoV*=1.5, the plots are shown bellows:

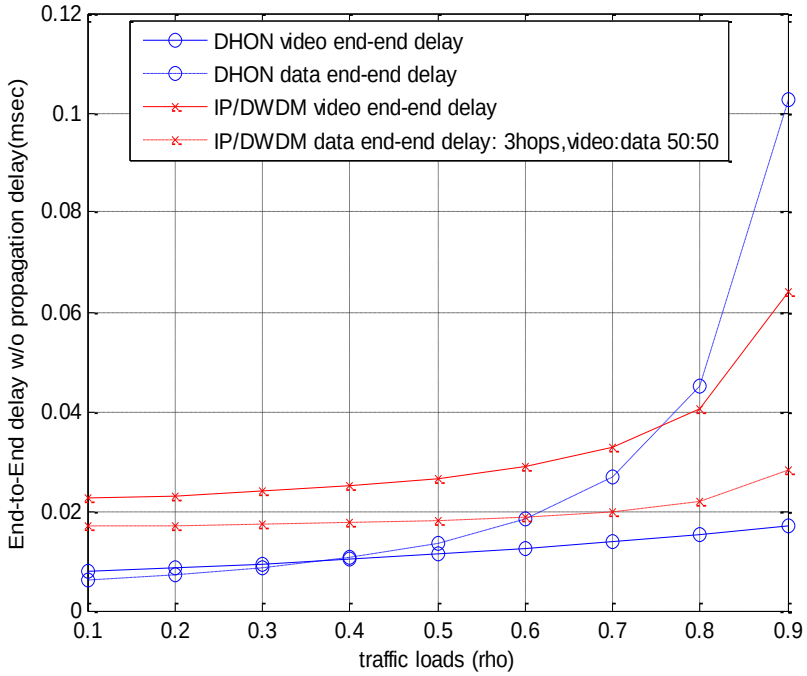

Figure 54. End-to-end delay comparison 3 hops link

Comparing video delay between both networks in Figure 54, the DHON can provide lower delay channel than the IP/DWM. Especially, at high traffic load DHON perform even better as one can see the delay regarding IP/DWDM will increase rapidly during high traffic loads. For data traffic, DHON is superior for a certain period until the traffic load is greater than a threshold ($\rho > 0.6$). Then the IP/DWM will perform better since data traffic is lower priority treated in DHON. However, the best-effort traffic is comparatively less concern than the video traffic due to higher delay tolerance.

In addition to the three hops link, we perform a similar experiment; but via a five hops link instead depicted in Figure 55. The results show the same trend; but IP/DWDM allows comparatively higher delay than the previous case due to larger numbers of intermediate nodes.

According to data type, DHON performs better than the previous case, as the crossing point moves to higher traffic load. However, DHON can decrease the delay by setting an additional wavelength channel when the load is greater than 0.7.

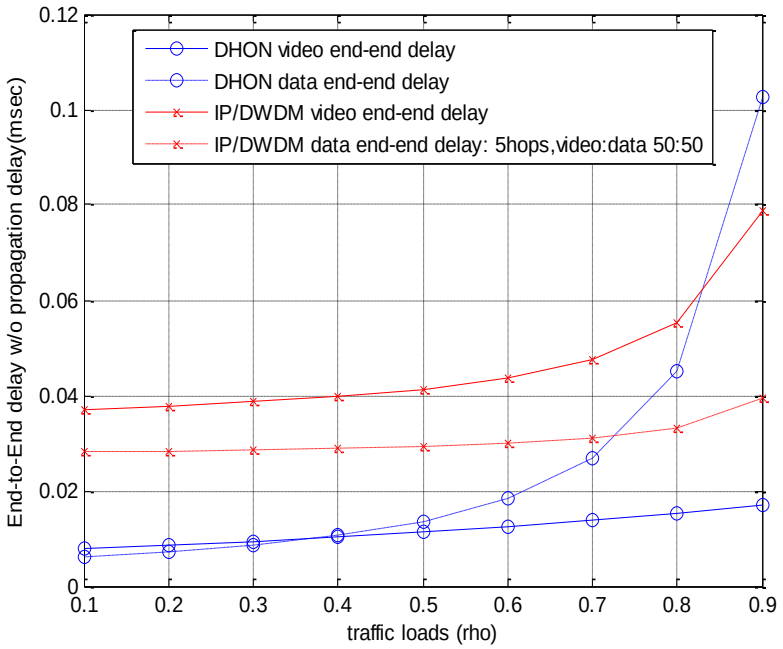

Figure 55. End-to-end delay comparison 5 hops link

6.5.3 Effect of Video Frame Size Toward Video Traffic Delay

Now, we will focus only the video frame delay, which is our primary concern. In the experiment, we will investigate how video frame size affects end-to-end delay. Frist, we show the comparison of end-to-end delay between both networks associated with particular frame size. Then, we will investigate a variation of frame sizes with respect to each particular network.

The evaluation is based on three hops link with 50% video traffic ratio. Again, end-to-end delay in the following plots does not include propagation delay. The arriving traffic parameters are the follows: frame size=2900B with *CoV*= 0.62 and packet size=760B with *CoV*=1.5. The results are shown bellows:

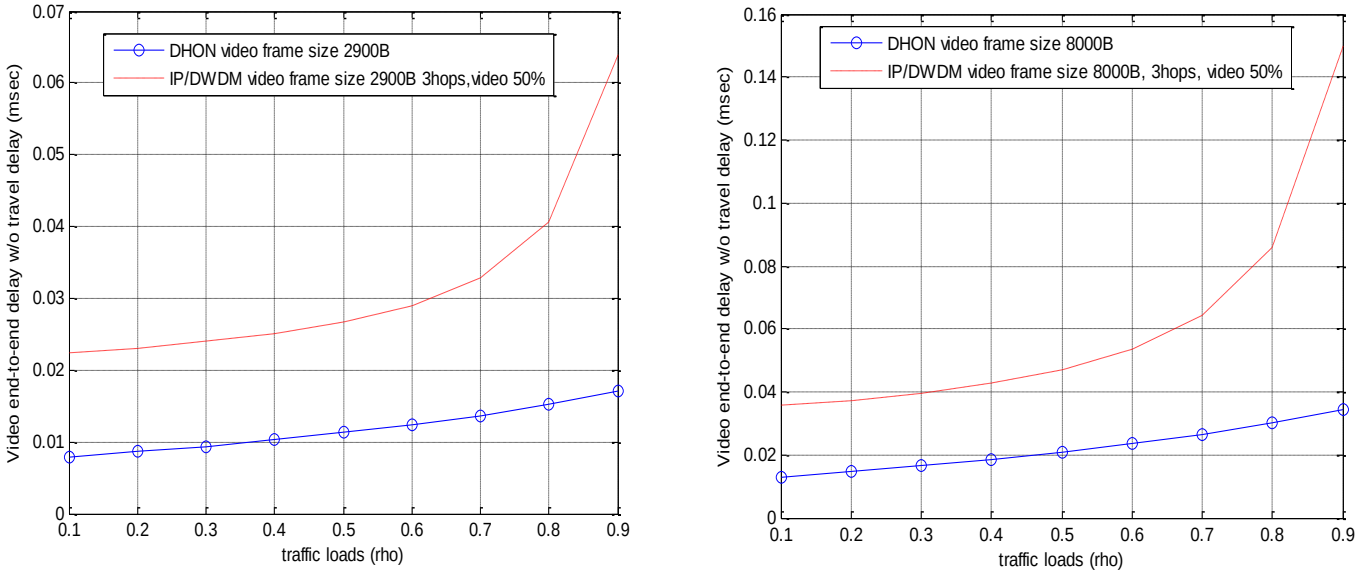

Figure 56. End-to-end delay comparison for each frame size

Figure 56 depicts end-to-end delay comparison when the video traffic is based on 2900B (left plot) vs. 8000B (right plot). Essentially, the end-to-end delay of DHON is lower than IP/DWDM for the entire range of traffic loads, which applies to both cases of frame sizes. One can observe that in the left plot (shorter frame size), the delay difference between both networks is around 0.015 millisecond. In the right plot where the frame size is larger, the delay difference is greater (i.e., 0.03 millisecond).

In addition, we will evaluate effect of video frame size toward end-to-end delay in each type of network. This experiment uses the same parameters for traffic arrivals as the previous one. However, we also investigate a variation of video frame sizes based on particular network. In order to keep traffic load the same for all frame sizes, the arrival rates have to vary, which is associated with particular video frame size.

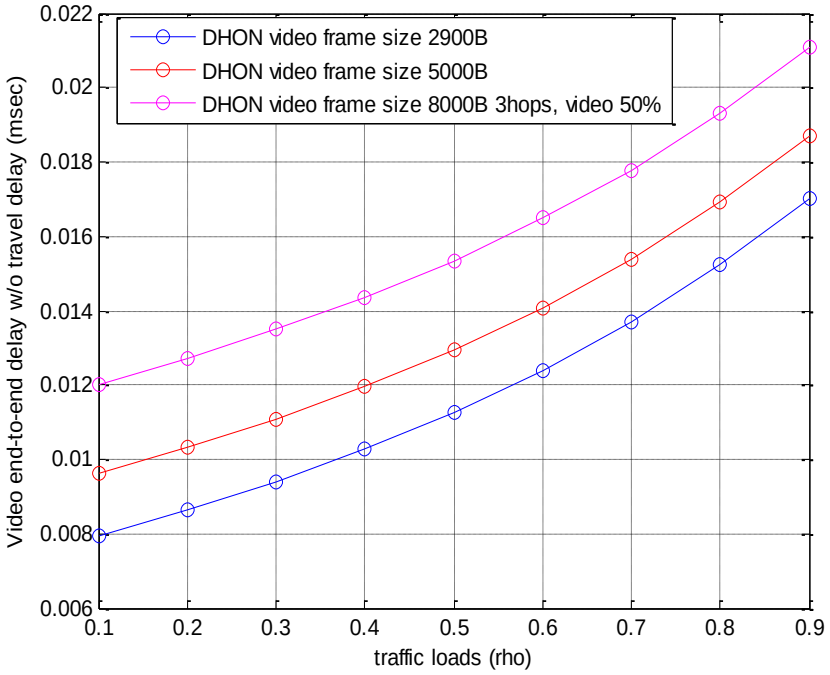

Figure 57. Effect of frame sizes to frame delay in DHON

Figure 57 shows that larger frame size will cause higher delay in DHON based on video prioritized scheduling; although the arrival rate is lower in the case of larger frame size. One can see that those gaps between plots are consistent throughout all range of traffic loads. In addition, we also investigate the effect of frame size in the IP/DWDM network as shown in Figure 58. The

results illustrate that the larger frame size, the higher delay in the channel. Thus, frame size has direct affect to the end-to-end delay for both networks. However, the gaps between plots do not remain the same as the DHON. One can notice that the gaps get smaller during high traffic loads. This is resulted from non-prioritized scheduling.

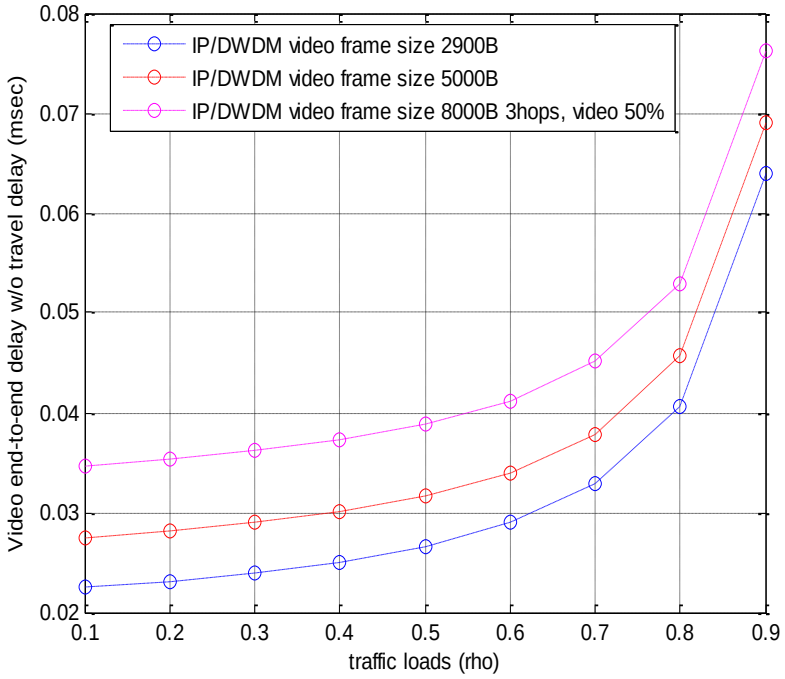

Figure 58. Effect of frame sizes toward frame delay in IP/DWDM

6.5.4 Effect of Traffic Ratio Toward Video Traffic Delay

This section will investigate how video ratio of the traffic demands affects the video frame end-to-end delay with respect to DHON and IP/DWDM. In the experiment, we plot the delay versus

traffic load based on several ratios of video traffic: 50%, 70%, and 90% (medium to high load). The experiment is based on 3 hops link with the following traffic parameters: video frame size=2900B with *CoV*= 0.62, and data packet size=760B with *CoV*=1.5. The results are bellows:

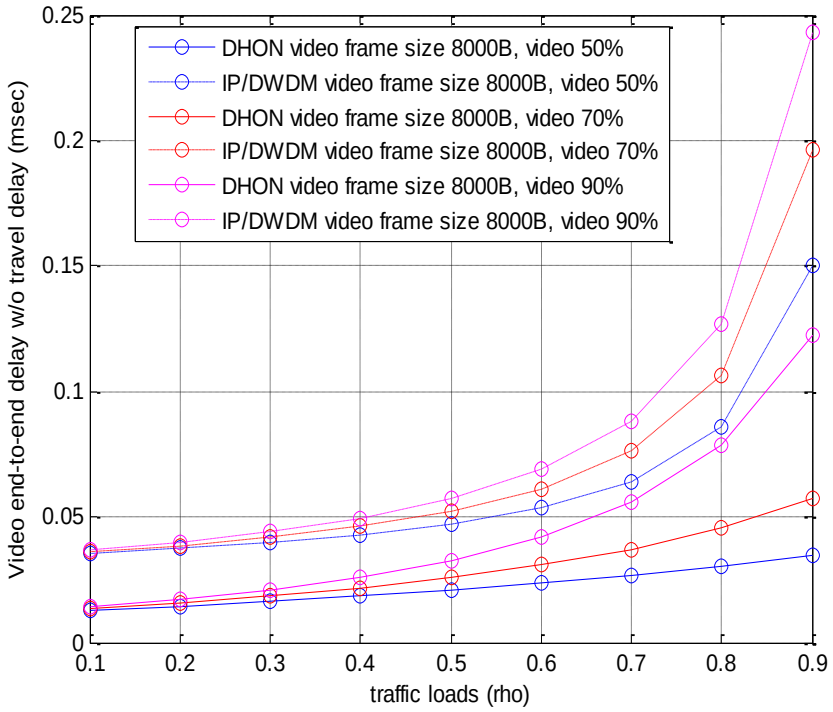

Figure 59. Effect of video ratio toward DHON v.s IP/DWDM

Figure 59 illustrates two groups of results. The first group (i.e., dotted lines) represents end-to-end delay of IP/DWDM network, and the second group (i.e., solid lines) refers end-to-end delay of DHON. Obviously, DHON is able to provide better performance channel (i.e., lower delay) than IP/DWDM for all cases. One can notice that under high video ratio in DHON (i.e., solid

pink) still superior than relatively low ratio (50%) in IP/DWDM due to the video prioritized and no O/E/O at intermediate nodes. However, high video ratio (90%) will be a significant effect on delay in DHON as well.

7.0 CONCLUSION AND FUTURE WORK

Both rapid growth of high bandwidth applications (e.g., HD video, Internet TV) and cloud-based applications, which generate enormous traffic between data centers, will have a great impact on existing backbone networks. The optical switching system plays a major role of massive traffic delivery. However, telecom operators need such a powerful, dynamic, and efficient O-O-O optical switching infrastructure.

In this dissertation, we proposed a promising DHON based on fully optical switches, which are able to perform bottleneck removal, protocol-transparency, and efficient wavelength utilization. The DHON can provide certain levels of channel granularities, which can support several classes of traffic. We have shown that the hybrid switches are able to provide a particular optical switching fabric and infrastructure that is appropriate for any traffic type regarding to QoS constraints of the traffic demand. The framework of switching nodes is proposed, including architectures, traffic classification, and optical channel assignment. In addition, we walked through each step to investigate performance analysis of particular optical channel, which later can solve for numerical results associated with certain traffic environments.

In premium channel, the traffic is transmitted as fast lanes (i.e., real-time reserved channels) which have infinitesimal end-to-end delay. With overflow channel employment we proposed, the network enables to decrease blocking probability and increase utilization in

Premium channel. In other words, number of reserved wavelength channels can reduce with regard to the same QoS constraint. Regarding the overflow traffic, we proposed the mathematic model obtaining 3 moments of method and IPP parameter approximation to forecast irregular traffic blocked from the premium channel. The G/G/1 queueing model based on PH/PH/1 matrix approach is proposed to investigate the overflow channel. Thanks to the overflow system, the proposed network enhances utilization in the wavelength channels allowing the decrease of wavelength channel deployed in the core layer.

Secondary channel supports packet-based traffic over wavelength channel, which classifies into two CoS buffers. We separate HD video traffic as an example of delay sensitive traffic in Class I. The arrival is bundles of encoded video frames, which satisfies less end-to-end delay channel than short packets regarding best effort traffic in CoS II. We proposed M/G/1 as representations for both cases. However, the video frame size is random variable with larger mean than the one regarding data packet in CoS II (i.e., finer granularity). In addition, the distribution of the frame/packet sizes would be different. We have done numbers of experiments to study effects of particular parameters toward performance of the wavelength channels. In addition, mixture of traffic in wavelength channels is also studied. We compare end-to-end delay based on DHON and IP/DWDM in certain network circumstances. Finally, the results showed that DHON based on O-O-O switching paradigm is superior to the IP/DWDM with O-E-O switches in most cases.

7.1 FUTURE WORK

7.1.1 Improving Accuracy for System Representation

All queueing models we have proposed to represent the systems of particular optical channels are based on only queues located at ingress switches. If we desire to improve the accuracy of the model in term of end-to-end user experiences, we should include additional queue located at the egress switch as well. This will cover the case that several ingress nodes request for traffic demands to the same destination server in the same duration, which requires multiplexing at the destination's server. In this case, we have to perform network of queue theory to represent the system for the channel.

7.1.2 Performance Analysis of Traffic Mixture in Multiple Channels

In early chapters, we performed system analyses for multiple wavelength channels when an arrival is either video or data. In addition, we also proposed the system representation for mixture of traffic in a single wavelength channel. However, we skipped the system analysis for a mixture of traffic in multiple channels. The details are bellows:

In Figure 60, $\lambda_{i,j}^{v}$ represents video traffic arrivals to the *CoS* I buffer which delivers transfers to the egress nodes j. Assume the video traffic is generated by video cache server based on Content Delivery Network (CDN) located in region 1, transmitting to the egress node 2

associated with particular allocated channel *c*. Since $\lambda_{i,j}^{d}$ is the video data created by a group of video servers, the times between arriving packets perceived by the *CoS* I queue can be assumed as exponential distributed. We represent the traffic mixture in multiple wavelength channels as a M/G/c queuing system shown below.

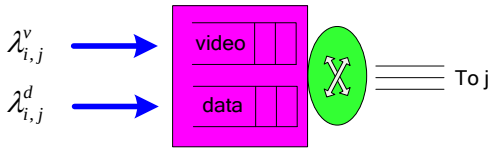

Figure 60. Queueing model for traffic maxture in multiple channels

Moreover, additional research study of non-homogenous traffic in premium channel is another challenge, especially when the allocated traffic fluctuates to an overflow channel.

7.1.3 Number of DHON Channels Based on Realistic Traffic

In our dissertation, we mostly calculate performance parameters with respect to given number of channels, traffic demand characteristics, and channel data rate. It is quite interesting in terms of real implementation, if we can identify numbers of channel deployment for all channel types (i.e., primary, secondary CoS I and II, and overflow) based on real traffic in the United States. Then how much overflow traffic would be in the channel? In fact, the total US Internet traffic comprises several traffic types based on percentage. Finally, a comparison between total numbers of DHON channels and those of single type channel employed in IP/DWDM network

based on similar QoS parameters. We could simplify the problem with the following assumptions and methodologies:

1. Find a value for total US internet traffic
2. Divide the traffic into specific traffic types according to the percentages.
3. Choose a path on the previous NSF topology map
    - assume a given path is typical for all US traffic,
    - assume each edge node supports same numbers of customers
4. Based on 15-node NSF topology, total end-to-end channel is found by 15x14 = 210
5. Divide each traffic type by 210, which will be traffic demands for the given link.
6. Calculate numbers from our plots based on queueing analysis
7. Compare the results with number of channels in IP/DWDM based on similar QoS

APPENDIX

DHON CORE NODE FRAMEWORK

In fact, we proposed DHON under the philosophy of "Dump core with the intelligent edge node." The core node employs less complex switch, in which there is no O/E/O conversion or packet header processing, resulting in cost saving architecture. In fact, processing delay will be a serious factor for large-scale networks, consisting of many intermediate hops between ingress and egress nodes. In order to eliminate processing delay and queuing delay at the intermediate core nodes, the DHON core node should employ OCS and OBS paradigm in which, both switching paradigms do not require any O/E/O conversion and optical buffer in the core layer. Therefore, the aggregation delay at the edge node is the most significant contribution to overall end-to-end delay. In other words, the overall network performance can be simply controlled at the edge node.

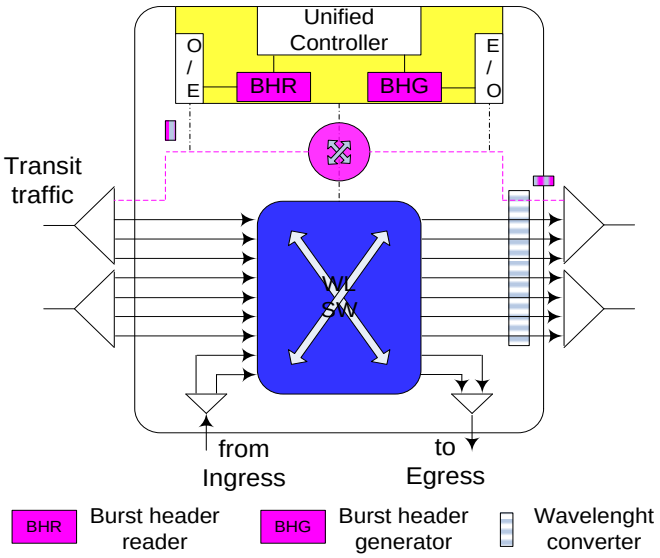

Figure 61. DHON core node (O-O-O)

Considering the core node in Figure 61, the core node employs two types of switching paradigms: reconfigurable OXC (slow switch) and OBS (fast switch). The reconfigurable OXC is responsible to convey the premium and secondary channels; while, the OBS carries only the overflow traffic that is relatively small amount described in 4.0 . In our DHON core node, the data part of all types of traffic transmitted through the DHON core node is absolutely performed in optical domain (O-O-O); no O/E converter or electronic buffer except for the control part.

Both switches (OXC, OBS) share the same controller and transmission system (i.e., optical multiplexers, amplifiers, and fibers); however, each type of switch operates independently. In practice, the cost of reconfigurable OXC is relatively much lower than the OBS, which is still in the research stage. Consequently, the core node is aimed to employ the circuit channel in the first preference rather than using the overflow channel.

Core Node Control Signaling

Considering the circuit channels, the OXC fabric is configured based on the traffic demand requested from several ingress nodes. According to the core node's controller, GMPLS protocol can be deployed for dynamic wavelength assignment regarding OXC. The control broadcast setup probe from ingress to egress nodes along intermediate nodes. All candidates light path channels, associated with routing policy (i.e., shortest path, or routing constraint based routing), would be replied back from the egress to the ingress node via intermediate nodes. Then, the controller selects specific wavelengths, regarding the numbers of requested wavelengths for the demand pair, and the wavelength routing assignment algorithm (explained in section **Error! Reference source not found.**)

On the other hand, the OBS fabric associated with the overflow channel is setup and torn down based on the burst header of each burst packet. Additionally, the switching holding time is significantly shorter than the reconfigurable OXC. It is the matter of fact that the faster switch definitely required higher capability than the slower one, leading to high switching cost.

Wavelength Assignment in core nodes

Regarding the wavelength assignment at the edge node as described in 4.0 . Once each ingress node determines an appropriate number of wavelengths which needs to be assigned to a particular traffic demand, the edge node's control unit will send the signaling to the core layer's controller associated with GMPLS to setup/tear down the connections. Based on the routing assignment (WRA) algorithm deployed in the core layer, the core's controller investigate the candidates routing paths for each demand pair. Additionally, it also examines current available

wavelengths on each link, and selects an appropriate wavelength along the routing path so that the same wavelength cannot be assigned to more than one demand pair on the same fiber link. Figure 62 illustrates the wavelength assignment on the DHON. In this specific network, there are totally four edge nodes on the network. Each edge node requires one wavelength for each destination egress node. Since the edge nodes forms fully mesh connection to the other edge nodes, the minimum number of light paths required for this DHON is N*(N-1) = 4*3 =12 wavelengths (full duplex communication). One can notice that each edge node has three incoming and outgoing wavelengths from/to the other edge nodes, each wavelength can operate simultaneously (full duplex).

For instance, node A has three outgoing wavelengths dedicated to B, C, and D (red, blue, green respectively). In addition, there are three incoming wavelengths to A from B, C, and D (black, pink, yellow respectively). In practice, each wavelength (color) represents each wavelength channel in DWDM system (i.e. 1, 2.5 Gb/s depending on the capacity of transponder line card), and each color in the figure could be multiple wavelengths (not only one for each direction) if the traffic demand to that destination is higher than the capacity of a single transponder line card. Noted that in reality, the multiple wavelengths can be setup for each demand pair.

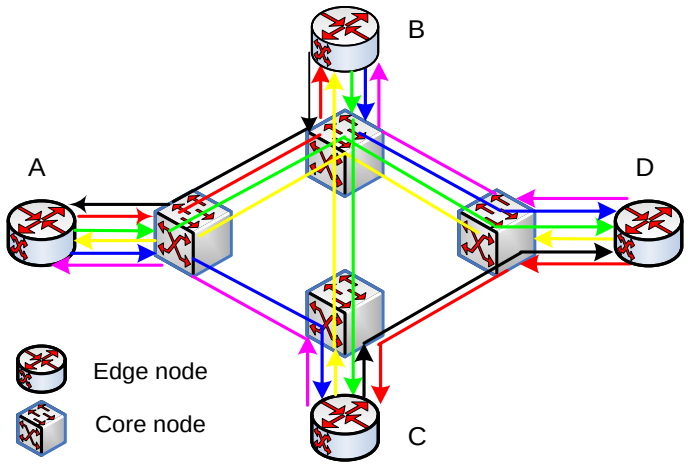

Figure 62. Wavelength routing assignment associated with core network

In this dissertation, we assume that the core switch is reconfigurable, non-blocking to ensure that the switching fabric always has the connection for the entire demand pairs. In addition, a wavelength converter is deployed at each transponder in order to ensure that there is always an available wavelength associated with a particular output port toward the destination. The possibilities of the architecture for the core switch, associated with the reconfigurable OXC (primary and secondary channels) could be wide-sense clos network or reconfigurable, in which the detail of the switching fabric architectures are extensively explained in Thompson's book [32].

BIBLIOGRAPHY

1. *Index, Cisco Visual Networking Index: Forecast and Methodology, 2012-2017*, in *Cisco White Paper*. May 29, 2013.

2. G. Li, D.W., J. Yates, R. Doverspike, and C. Kalmanek, *IP over Optical Cross-connect Architecture.* IEEE Communication Magazine, Feb. 2007.

3. S. Sengupta et al., *Switched optical backbone for cost-effective scalable core IP networks.* IEEE Communication Magazine, Jun. 2003. 41(6): p. 60-70.

4. G. Ellinas et al., *Network control and management challenges in opaque networks utilizing transparent optical switches.* IEEE Communication Magazine, Feb. 2004. 42(2): p. S16- S24.

5. C. Qiao, M.Y., *Optical burst switching (OBS) - a new paradigm for an optical Internet.* J. of High Speed Networks, 1999. 8(1): p. 69-84.

6. J. S. Turner, *Terabit burst switching.* Journal of High Speed Networks, Mar. 1999. 8(1): p. 3-16.

7. M. Yoo et al., *Optical burst switching for service differentiation in the next-generation optical internet.* IEEE Communication Magazine, Feb. 2001. 39(2): p. 98-104.

8. Y. Chen, C.Q., and X. Yu, *Optical Burst Switching (OBS): A New Area in Opitcal Networking Research.* IEEE Network Mag., May-June 2004. 18(3): p. 16- 23.

9. Y. Chi et al., *A novel burst assembly algorithm for OBS networks -- based on data-lenght time-lag product.* IEEE Com., Asia-Pacific Con'05, Oct. 2005.

10. Y. Sun et al., *Design and implementation of an optical burst-switched network testbed.* IEEE Optical Communication, Nov. 2005. 43(11): p. S48- S55.

11. Muhammad Imran, a.K.A., *Performance evaluation of hybrid optical switching with quality of service*, in *Signals and Systems Conference (ISSC)*. 2015, IEEE: Carlow. p. 1 - 6.

12. D.K. Hunter, I.A., *Approaches to optical Internet packet switching.* IEEE Communication Magazine, Sep. 2000. 38(9): p. 116-122.

13. Mahony M., S.D., Hunter K. D., and Tzanakaki A., *The Application of Optical Packet Switching in Future Communication Networks.* IEEE Communication Magazine, Mar. 2001: p. 128-135.

14. S. J. Ben Yoo, *Optical Packet and burst switching technologies for the future photonic internet.* lightwave technology, Dec. 2006. 24(12): p. 4468-4492

15. S. Yao, B.M., and S. Dixit, *Advances in photonic packet switching: an overview.* IEEE Communication Magazine, Feb. 2000. 38(2): p. 84-94.

16. R. V. Caenegem and et al., *The Design of an All-Optical Packet Switching Network.* IEEE Com. Mag., Nov. 2007: p. 52-61.

17. I. d. Miguel et al., *Polymorphic architectures for optical networks and their seamless evolution towards next generation networks.* Photonic Network Communications, 2004. 8(2): p. 177-189.

18. A. K. Garg and R S Kaler, *Performance analysis of optical burst switching high speed network architecture.* IJCSNS, April 2007. 7(4).

19. C. M. Gauger and et al., *Hybrid optical network architectures: bringing packets and circuits together* IEEE Communication Magazine, Aug. 2006. 44(8): p. 36- 42.

20. Mukherjee, B., *Architecture, Control, and Management of Optical Switching Networks.* IEEE Photonics in Switching Conf., Aug. 2007, 2007.

21. C. M. Gauger and B. Mukherjee, *Optical burst transport network (OBTN) - a novel architecture for efficient transport of optical burst data over lambda grids.* High Performance Switching and Routing, 2005., May 2005: p. 58- 62.

22. Fiorani, M., Slavisa Aleksic, and Maurizio Casoni, *Hybrid optical switching for data center networks.* Electrical and Computer Engineering 2014. 2014.

23. Fiorani, M., Maurizio Casoni, and Slavisa Aleksic, *Hybrid optical switching for energy-efficiency and QoS differentiation in core networks.* Optical Communications and Networking May 2013. 5: p. 484-497.

24. Jordi Perelló and et al., *All-optical packet/circuit switching-based data center network for enhanced scalability, latency, and throughput.* IEEE Network Dec 2013. 27(6): p. 14 - 22.

25. K. Christodoulopoulos and et al., *Performance evaluation of a hybrid optical/electrical interconnect.* Optical Communications and Networking, March 2015. **7**(3): p. 193 - 204.

26. Shuping Peng, e.a., *A novel SDN enabled hybrid optical packet/circuit switched data centre network: The LIGHTNESS approach*, in *Networks and Communications (EuCNC), 2014 European Conference on. IEEE*. 2014. p. 1-5.

27. L. Muscariello and et al., *An MMPP-Based Hierarchical Model of Internet Traffic.* Communications, 2004 IEEE International Conference on, June 2004. 4: p. 2143- 2147.

28. A. Banerjee et al., *Generalized multiprotocol label switching: an overview of routing and management enhancement.* IEEE Communication Magazine, Jan. 2001: p. 144-150.

29. S. J. Ben Yoo, *Optical-label switching, MPLS, MPLambdaS, and GMPLS.* Optical Networks Magazine, May/Jun. 2003.

30. E. Mannie, e., *Generalized Multi-protocol Label Switching (GMPLS).* RFC 3945, Oct. 2004.

31. P. Pedroso et al., *Integrating GMPLS in the OBS Networks Control Plane.* ICTON '07, July 2007. 3: p. 1-7.

32. Thompson, R.A., *Telephone Switching Systems*. 2000: Artech House.

33. C. Xin, C.Q., Y. Ye, and S. Dixit, *A Hybrid Optical Switching Approach.* GLOBECOM '03. IEEE, Dec. 2003. **7**: p. 3808- 3812.

34. C. T. Chou and et al., *A hybrid optical network architecture consisting of optical cross connects and optical burst switches.* IEEE Conference on ICCCN 2003, Oct. 2003: p. 53-58.

35. Richard A. Thompson, *Photonic switches in a global ubiquitous networks.* NSF proposal, Dec. 17, 2008.

36. Pratibha, M., *Towards An Optimal Core Optical Networks Using Overflow*. 2009, University of Pittsburgh: Pittsburgh.

37. Pratibha Menon, W.C., and Nicholas Reimer, *Overflow traffic modeling in hybrid optical circuit/burst switching nodes with service differentiation,* in *Optical Fiber Communication (OFC)*. March 2009, IEEE: San Diego, CA. p. 1 - 3.

38. Washington N., P.H., *Performance Analysis of Traffic-Groomed Optical Networks Employing Alternate Routing Techniques*, in *Managing Traffic Performance in Converged Networks*. Sept. 07, Springer Berlin / Heidelberg. p. 1048-1059.

39. Wilkinson, R.I., *The theories for toll traffic engineering in the U.S.A.* Bell Sys. Tech. J., Mar. 1956. 35: p. 421-514.

40. I. Tsirilakis, C.M., and I. Tomkos, *Cost comparison of IP/WDM vs. IP/OTN for European backbone networks.* Transparent Optical Networks, 2005, Proceedings of 2005 7th International Conference, July 2005. 2: p. 46- 49.

41. Mukherjee, B., *WDM Optical Communication Networks: Progress and Challenges.* IEEE Journal On Selected ares in communications, Oct. 2000. 18(10): p. 1810-1824.

42. F. Xue and S. J. Ben Yoo, *High-capacity multiservice optical label switching for the next-generation Internet.* IEEE Communication Magazine, May 2004. 42(5): p. S16-S22.

43. C. Qiao, *Labeled Optical Burst Switching for IP-over-WDM Integration.* IEEE Communication Magazine, Sep. 2000. 38(9): p. 104-114.

44. V. Vokkarane et al., *Generalized burst assembly and scheduling techniques for QoS support in optical burst-switched networks.* GLOBECOM, IEEE, Nov. 2002. 3: p. 2747-2751.

45. J. Y. Wei, J.R.I.M., *Just-in-time signaling for WDM optical burst switching networks.* Journal of Lightwave Technology, Dec. 2000. 18(12): p. 2019-2037.

46. G. M. Lee and et al., *Performance evaluation of an optical hybrid switching system.* GLOBECOM '03, IEEE, 2003. 5: p. 2508 - 2512.

47. Riordan, R.I.W.a.J., *Theories for Toll Traffic Engineering in the U.S.A* Bell Sys. Tech. J., 1955. 35(514).

48. Kuczura, A., *The Interrupted Poisson process as an overflow process.* Bell Syst. Tech. J., Mar. 1973. 52: p. 437-448.

49. Kuczura, A., *A method of moments for the analysis of a switch communication network's performance.* IEEE transcations on communications, Feb. 1977. Com-25(No.2): p. 185-193.

50. Gunter Bolch and et.al., *Queueing Networks and Markov chains*. second ed. Modeling and Performance Evalutation with Computer Science Applications. 2006, New Jersey: A John Wiley & sons Inc.

51. Schehrer, R., *On the Calculation of Overflow Systems with a Finite Number of Sources and Full Available groups.* IEEE Transcations on communications, Jan. 1978. com-26.